

MODELING AND DYNAMICS OF PANTOGRAPH/CATENARY  
SYSTEMS FOR HIGH SPEED TRAINS

by

KURT ARMBRUSTER

SUBMITTED TO THE DEPARTMENT OF  
MECHANICAL ENGINEERING IN  
PARTIAL FULFILLMENT OF THE  
REQUIREMENTS FOR THE DEGREE OF

MASTERS OF SCIENCE IN MECHANICAL ENGINEERING

at the

MASSACHUSETTS INSTITUTE OF TECHNOLOGY

May 1983

Copyright 1983, Massachusetts Institute of Technology

Author \_\_\_\_\_  
Department of Mechanical Engineering  
March 11, 1983

Certified by \_\_\_\_\_  
David . Wormley  
Thesis Supervisor

Accepted by \_\_\_\_\_  
Warren M. Rosenhow  
Chairman, Mechanical Engineering Graduate Committee

MASSACHUSETTS INSTITUTE  
OF TECHNOLOGY

JUN 23 1983

Archives  
LIBRARIES

MODELING AND DYNAMICS OF PANTOGRAPH/CATENARY  
SYSTEMS FOR HIGH SPEED TRAINS

by

KURT ARMBRUSTER

Submitted to the Department of Mechanical Engineering on  
March 11, 1983 in partial fulfillment of the requirements  
for the Degree of Master of Science in Mechanical Engineering

A coupled pantograph and catenary model is developed to investigate the dynamic performance of a catenary and pantograph. The catenary model represents a simple style or two wire catenary incorporating the behavior of the towers and droppers, and the tension, mass and bending stiffness of the wires. The catenary model can be coupled with any pantograph model; a two mass model incorporating non-linear suspension elements is used for these simulations.

The shape of the catenary wires is described by a Fourier sine expansion, and the equations of motion and natural modes of vibration are obtained using Lagrange's method. The dynamic interaction of the pantograph and catenary are solved by decoupling the motions into the natural modes of vibration and using modal analysis.

Performance is evaluated using a computer simulation of the model. The results show the performance of the catenary is strongly influenced by a higher wave speed in the wires. Improvements to the pantograph are also investigated. Lowering the mass, lowering the stiffness of the suspension, and adding moderate damping all improve pantograph performance.

Thesis Supervisor: David N. Wormley  
Professor of Mechanical Engineering

## ACKNOWLEDGEMENTS

I would like to express my deep appreciation to those who assisted in this research: The US DOT Office of University Research who sponsored this work under contract number DTRS-5681-C-00020; Professors Dave Wormley and Warren Seering who supervised the research; Mark Nagurka who proofread the text many times and offered many valuable suggestions; Cal Vesely who did research on pantograph dynamics; Leslie Regan and Joan Gillis typists extraordinaire who helped in the preparation of the final document.

In the words of one of my best ones, "Friends are what make it all worthwhile." While there are many I would like to thank, listing them all seems almost self-indulgent. From my heart comes a genuine thank you to all: The fellow students in the Vehicle Dynamics Lab, the many friends and brothers of Kappa Sigma, and the ladies of Burton Third. But most of all, I thank Roy Mathieu and Mark McMillen -- may these friendships never end.

-- Kurt Armbruster  
March 11, 1983

For my Mother, who gave me the  
patience and understanding; and for  
my Father, who gave me the challenge.

## TABLE OF CONTENTS

	Page
Abstract . . . . .	ii
Acknowledgements . . . . .	iii
Table of Contents . . . . .	v
List of Figures . . . . .	vi
Chapter 1 Introduction . . . . .	1
Chapter 2 Literature Review . . . . .	6
Chapter 3 Model Development and Solution Technique . . . . .	14
3.1 Model Development	14
3.2 Solution Technique	18
Chapter 4 Results . . . . .	26
4.1 Catenary Description and Natural Mode Shapes	26
4.2 Typical System Response	32
4.3 Comparative Performance of Selected Pantographs	40
4.4 Parameter Influence on Performance	45
4.5 Alternate Catenary Configurations	53
Chapter 5 Discussion and Conclusions . . . . .	58
References . . . . .	60
Appendix A Catenary Model Development . . . . .	62
A.1 Modal Analysis Review	62
A.2 Catenary Model Development	64
A.3 Catenary Equation Development	65
Appendix B Pantograph/Catenary Interaction . . . . .	84
B.1 Pantograph Model	84
B.2 Coupling Between the Models	87
B.3 Simulation Technique	89
Appendix C Computer Programs . . . . .	91
C.1 Program MODES.FOR	92
C.2 Program PCAT.FOR	108

## LIST OF FIGURES

Figure Number	Figure Title	Page
1.1	Common Catenary Configurations . . . . .	4
3.1	Catenary Model . . . . .	15
3.2	Pantograph Model . . . . .	17
3.3	Coupling of the Pantograph and Catenary Model . . .	19
4.1	Natural Mode Shapes for Mode 1 Through 6 . . . . .	27
4.2	Natural Mode Shapes for Mode 7 Through 12 . . . . .	28
4.3	Natural Mode Shapes for Mode 13 Through 18 . . . . .	29
4.4	Natural Mode Shapes for Mode 19 Through 20 . . . . .	30
4.5	Catenary Shape Between 0.0 and 0.5 Seconds . . . . .	34
4.6	Catenary Shape Between 0.6 and 1.0 Seconds . . . . .	34
4.7	Catenary Shape Between 1.1 and 1.5 Seconds . . . . .	35
4.8	Catenary Shape Between 1.6 and 2.0 Seconds . . . . .	35
4.9	Catenary Shape Between 2.1 and 2.5 Seconds . . . . .	36
4.10	Catenary Shape Between 2.6 and 3.0 Seconds . . . . .	36
4.11	Displacement of the Catenary and Pantograph . . . . . Prototype 1 Pantograph at 200 km/h	39
4.12	Contact Force History . . . . . Prototype 1 Pantograph at 200 km/h	39
4.13	Displacement of the Catenary and Pantograph . . . . . Prototype 1 Pantograph at 225 km/h	41
4.14	Contact Force History . . . . . Prototype 1 Pantograph at 225 km/h	41

Figure Number	Figure Title	Page
4.15	Comparison of the Variations in Contact Force for the Two Pantographs . . . . .	44
4.16	Influence of Variations in Head Stiffness . . . . .	46
4.17	Zero Stiffness vs, Standard Configuration . . . . .	47
	Prototype 2 Pantograph at 200 km/h	
4.18	Influence of Simultaneous Variation in Head and Frame Damping . . . . .	48
4.19	Influence of Variations in Head Damping . . . . .	49
4.20	Influence of Variations in Frame Damping . . . . .	50
4.21	Head and Frame Damping = .26, .19 vs. Standard . . . . .	51
	Prototype 2 Pantograph at 200 km/h	
4.22	Low Wave Speed Catenary vs. Baseline Catenary . . . . .	54
	Prototype 2 Pantograph at 200 km/h	
4.23	Aluminum Catenary vs. Baseline Copper Catenary . . . . .	54
	Prototype 2 Pantograph at 200 km/h	
A.1	Catenary Model . . . . .	66
B.1	Pantograph Model . . . . .	85
B.2	Flow Chart for the Dynamic Simulations . . . . .	90

## CHAPTER 1

### INTRODUCTION

High speed electric trains are very effective for passenger travel in high density areas. They are widely used throughout Europe and Japan, and in this country they are used in the heavily traveled routes in the Northeast -- principally from Boston to Washington D.C. (the Northeast Corridor). The two best known systems, the TGV in France and the Shinkansen in Japan, often run at speeds as high as of 300 and 250 km/h (186 and 155 mph), respectively. In the U.S., the northeast corridor improvement project for track between Boston and New Haven is directed at increasing the maximum speed to 240 km/h (150 mph). These increased speeds pose a number of developmental problems needing both technically and economically sound solutions. One of these is the problem of electric power collection.

Subway and urban transit applications can use both overhead, 'catenary,' and on the track, 'third rail,' systems for electric power. Above ground trains must use catenaries because of the safety hazard of an exposed third rail. Throughout the world the majority, if not all, intercity trains use catenaries.

The overhead power carried in the catenary is transferred to the train via a mechanical arm known as a pantograph. The pantograph must provide continuous power to the engine, and therefore it must exert a steady force to its collection shoe; a force large enough to ensure continuous power collection, but light enough to prevent excessive wear



of the catenary.

Modern pantograph designs apply a relatively constant uplift force over a wide range of heights. Typically the uplift force is approximately 90 N (20 lbs) and the pantograph can provide this force over a wide range of heights from 0.5 m to 2.5 m (20 - 100 inches); over the majority of the track the catenary is about 2 m above the train. When the train enters a tunnel, however, the catenary drops down and is quite close to the train, and to accommodate the large excursions, almost all pantograph designs are of the two stage type<sup>1</sup>. The first stage, or the frame, accommodates the gross motions while the second stage, often called the head or shoe, tracks the small motions and vibrations of the catenary wire.

The problem of continuous power collection depends on the pantograph, the catenary, and their dynamic interaction. Ideally the pantograph should trace the catenary just lightly enough to ensure positive contact but not move the catenary appreciably. The catenary, on the other hand, should be as stiff as possible, and with as uniform a stiffness as possible to ensure minimal movement in the wire.

The motions of both the pantograph and catenary are distinctly coupled and the performance of the system is determined by their interaction. Increasing the uplift force may increase the contact but it also increases the catenary motions, especially between towers. Large catenary motions are a problem for the pantograph to follow and

---

1. The wide variation in catenary height is not universal. The French SNCF high speed lines have a variation in catenary height of less than 40 cm (16 in) [Ref 1] and the variation of the Japanese Shinkansen lines is even less than that.

the pantograph may lose contact totally interrupting the power. Making the uplift force too small, on the other hand, also degrades the performance because a small disturbance can cause the pantograph to lose contact.

There are many styles of catenaries and the complexity of the catenary depends upon the application. For low speed trolley or transit trains a single tensioned wire is often used. This style catenary is shown in Figure 1.1a. The power wire is supported by towers but the wire sags in between. This is the most economical type of catenary but the sag between towers becomes a problem for the pantograph to track at speeds higher than 50 km/h (30mph).

A more advanced configuration is the simple catenary, and it is shown in Figure 1.1b. It consists of two wires connected together by droppers or hangers. The top wire, called the messenger, is connected to the support towers and the lower wire, or contact wire, is hung from the messenger wire via the droppers. The droppers are of different lengths and are designed to remove the sag from the contact wire. The simple catenary is common for uses up to 160 km/h (100 mph). Although there is little sag in the contact wire there is a large variation in the effective vertical stiffness of the catenary. Near the middle of a span the catenary is compliant and soft. But near the support towers, the catenary is stiff and firm. Even though the contact wire is not connected to the tower it is much stiffer in this region as the presence of the tower acts through the droppers. At speeds higher than 160 km/h this variation in stiffness can become a problem and cause the pantograph to lose contact.

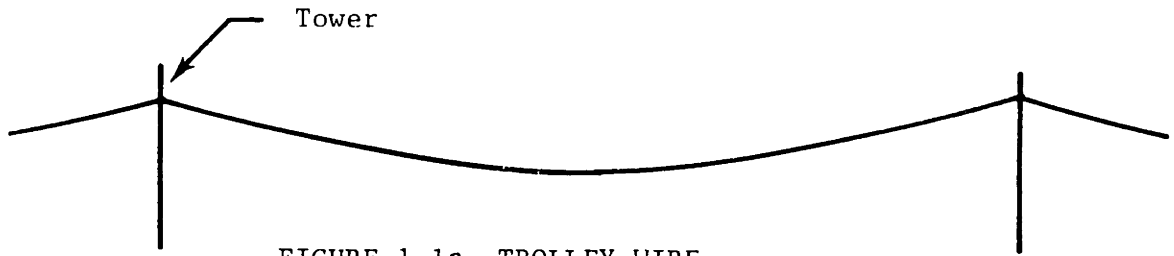


FIGURE 1.1a TROLLEY WIRE

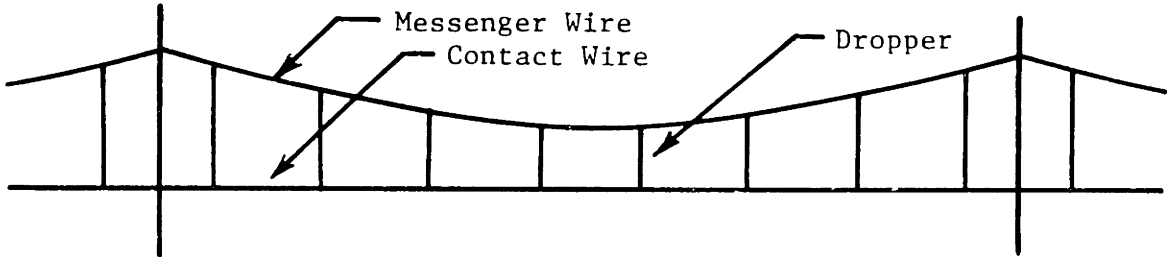


FIGURE 1.1b SIMPLE CATENARY

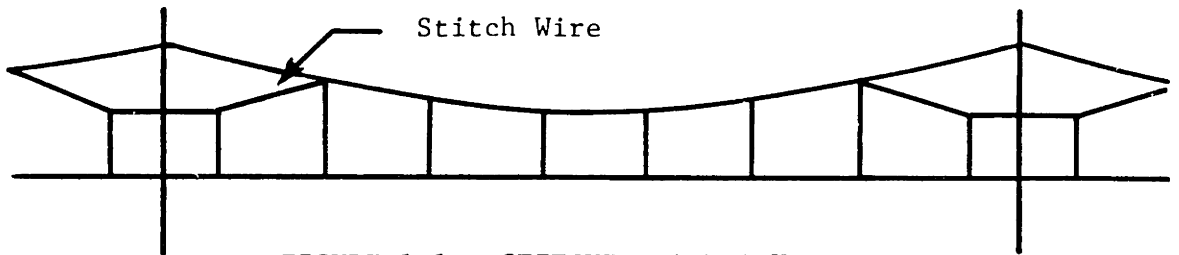


FIGURE 1.1c STITCHED CATENARY

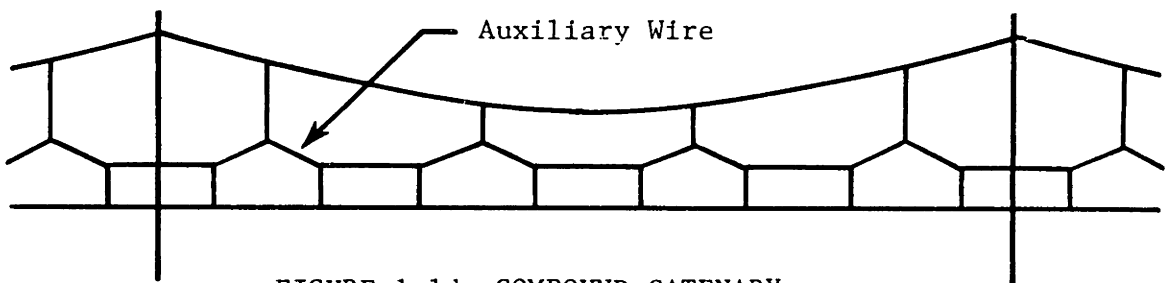


FIGURE 1.1d COMPOUND CATENARY

FIGURE 1.1 COMMON CATENARY CONFIGURATIONS

One design to overcome this problem is the inclusion of a stitch wire at every support tower; this is logically called a stitched catenary and is shown in Figure 1.1c. This catenary is similar to the simple catenary but it also includes an intermediate wire hung from the messenger wire at the supports. The extra wire makes the catenary more compliant near the towers and makes the stiffness of the entire catenary more uniform. The French SNCF 25 kV lines use a stitched catenary designed for speeds of 300 km/h (186 mph).<sup>2</sup>

A second approach for a uniform stiffness is the compound catenary, shown in Figure 1.1d. In this configuration, a third cable known as the auxiliary is hung between the messenger and the contact wire. There are two sets of droppers, one connecting the contact wire to the auxiliary and a second connecting the auxiliary to the messenger. The auxiliary wire and the two sets of droppers help isolate the contact wire from the towers and minimize the variation in stiffness. The Japanese use a compound catenary on the Tokiado line and run trains up to speeds of 250 km/h (they restrict train speeds to 160 km/h during high winds). The Japanese's latest installation, the new Sanyo line, uses a combination of the two designs: a compound catenary with stitching at the towers.

---

2. See Reference [2] p 216/12

## CHAPTER 2

### LITERATURE REVIEW

In the past two decades research on pantograph and catenary dynamics has been actively pursued. A brief review of some of the more significant works is given here, as well as a discussion of some of the technical factors.

One widely accepted suggestion for improving the pantograph is to reduce the mass of the pantograph head. In order to successfully track the wire the head must be responsive to all motions of the wire -- both large and small. High frequency vibration in the catenary is the most difficult motion to track and the force required to maintain contact is proportional to the mass trying to track it. Therefore, reducing the head mass avoids large inertial forces and the pantograph can trace the catenary easier and without losing contact as often.

Many authors fully agree and mention it as the most important factor in improving pantograph performance. See References [2,3,4,5,6]. Gostling and Hobbs [5] support this and further suggest that the head suspension be kept soft. In a study conducted in the USSR by Belyaev, et al. [7] two types of Soviet pantographs were tested. The lighter of the two performed better at higher speeds, although the authors were concerned with its sturdiness. Viscous head damping was added to the pantographs and in both cases resulted in greater uniformity of the contact force. Boissonade [2] tested the Faively high speed pantograph at speeds up to 250 km/h on the French SNCF lines and he also reported

that minimizing the head mass is important. In addition, he advocated the inclusion of extra damping in the pantograph head for all pantographs (They used 36 Ns/m). As a further suggestion, he mentioned the use of one-way damping, a non-linear damper which provides resistance only to downward motion of the head. This was offered only as a suggestion and was not tested.

The Faively pantograph has been evaluated by a number of authors. In addition to those mentioned above, Grey [8] measured aerodynamic lifting forces on the members and links of the pantograph, spring constants for the shoe support, and the damping between the frame and base.

Peters [9] evaluated the performance of both single and dual stage Faively pantographs using loss of contact, rather than contact force variation, as the measure of performance. He reported that during short duration contact losses, those of less than 5 ms, small electrical arcs *are drawn which cause no pantograph or contact wire damage and which easily maintain the primary current.* The most damaging to both wire and collector shoe are medium duration contact losses (5 ms to 20 ms). During separations of more than 20 ms, the forward velocity of the train extinguishes the arc; this causes loss of power but no additional damage. These tests were run with a contact force of 90 N and a pantograph head mass of 15 kg (33 lbm). A significant improvement in performance was achieved by increasing the contact force to 125 N (28 lbs) and reducing the head mass from 15 to 13 kg. Peters reported that 45% of the separations were from 2 to 5 ms in duration. He concluded that unacceptable contact behavior occurred when the standard deviation

of the contact force equaled 1/3 of the mean force.

Vesely at MIT [10] tested an August Stemman pantograph and developed a general pantograph model which incorporates geometric nonlinearities in the frame as well as nonlinearities in the head suspension. The equations of motion for the general pantograph were linearized for use in a two mass model and the effective values for the masses, stiffnesses and damping were determined. This is a valuable addition to the literature since the model can accommodate any pantograph. His model and experimental data matched very closely from 0 - 13 Hz. Above this frequency, structural effects of the links -- which were not modeled -- became important. It was concluded the two mass model provides a very accurate description of the actual pantograph and a full model incorporating the geometric motion of the links is not necessary unless the excursions are greater than 20 cm. The nonlinear head effects, however, are very important and cannot be ignored.

The other key element in the system is the catenary. Several studies have discussed wave speed as an important parameter in the catenary. The wave speed dictates the speed of propagation of a displacement or a force through the catenary. The wave speed in a tensioned wire is determined by a simple equation as the square root of the tension divided by the lineal density.

$$c = \sqrt{T / \rho} \quad (2.1)$$

The density of the wire is dictated by its current carrying capability but the tension is variable and can be as high as the strength of the material will allow. The wave speed is a function of the square root of the tension. Although the studies agree on its importance and its influence on the critical speed (the maximum speed before serious degradation in performance or loss of contact occurs), there is wide discrepancy as to when the critical speed actually occurs. Specialists from O.R.E. [6] state the maximum velocity is the full wave speed. They recommend as high a tension as possible to increase the wave speed to a maximum. Thomet [11] recommends the upper limit for pantograph velocity is one-third the wave speed. He reached this conclusion because at this speed a wave initiated at a tower will reach the next tower and reflect back reaching the the center of the span -- the most compliant section of the catenary -- just as the pantograph reaches the center of the span.

These are somewhat qualitative suggestions but in either case the tension in the catenary should be maximized. This increases the critical speed and also stiffens the catenary. Stiffening is more important for high voltage lines (25 - 50 kV) because the cables are lighter (since they carry less current), displace more for a given pantograph force, and are more susceptible to wind loads. A maximum tension keeps these motions to a minimum.

Cable tension should not only be high, it should also be maintained at a constant level. Most high performance catenaries are kept at a constant tension through the use of pulleys and counterweights at the end of a spool length of cable (typically 1200 - 1500 meters). This



arrangement eliminates many of the problems associated with fixed span catenaries which are sensitive to temperature variations. Fixed span catenaries sag with heat, 'hog' with the cold, and can suffer fatigue damage. The constant tension catenary is generally more expensive but lasts longer. Thomet claims constant tension catenaries can also be kept at a higher tension. He concluded that a cadmium copper catenary can be kept at 70% of the yield stress for life if tension is never relieved.

Other novel approaches for improving performance have been tried. Sell, et al. [12], in an attempt to detune the system, substituted springs for rigid droppers, varied dropped spacing, and supplied droppers with both pneumatic and hydraulic dampers. Several configurations were tried, but the improvement did not justify the expense in any of the cases.

In order to better understand the dynamics and interaction of a catenary-pantograph system several combined models have been developed. Most of the pantograph and catenary models have been developed together, with the majority of the development work focused upon the catenary model. The pantograph models have been for the most part two mass linear models.

There have been several noteworthy attempts to develop a theoretical solution to the catenary dynamics problem. Morris [13] in 1964 developed an analog computer simulation for a system composed of a simple two mass pantograph and a catenary consisting of a series of lumped masses each suspended from a spring and connected together with massless tensioned strings. This simplification was necessary to reduce

the problem to a size easily handled by an analog computer. The simplifications were severe enough to make this model of limited usefulness.

A second analytic solution for catenary motion was presented by Gilbert and Davies [14]. They considered the catenary as a massless tensioned string embedded in an elastic medium whose stiffness varied periodically. This may be an unacceptable simplification, especially considering the lack of any mass in the catenary model, but it was an analytic solution and allowed preliminary prediction of the critical speeds.

Abbot [15] modelled a trolley wire style catenary by replacing the differential equations of motion with finite difference equations and used numerical methods to solve the problem.

Levy, Bain and Leclerc [16] produced a model for a simple catenary by representing it in terms of the undamped, normal mode generalized coordinates. This decoupled the equations for solution of the dynamic response. The response was simulated on a digital computer with the accuracy controlled by the number of modes considered. The usual two mass pantograph model was used.

Scott and Rothman [17] produced several computer programs to evaluate various catenary systems. They were able to compare their results of the simple catenary with earlier experimental work performed by Willets and Edwards [18]. Predictions of the critical speed agreed well but predictions of the percentage of time in separation did not agree as well.

Hobbs [19] developed a finite element model and conducted experiments to verify it. He concluded the wire bending stiffness can be ignored but the wire mass cannot be ignored. The test catenary was shaken by a hydraulic ram and accelerometers mounted on the wire were monitored. They describe a theoretical model which considers the first fifteen modes of vibration, and compared favorably with the experimental measurements.

Recently there has been a growing interest in aluminum catenaries. This is primarily motivated by the increasing price of copper, but there may be additional advantages to an aluminum catenary. For an equivalent current carrying capability an aluminum catenary is approximately one-half the weight and can hold the same tension as a copper one. The decrease in weight yields a wave speed approximately 1.41 times higher than the wave speed in a copper catenary, and the decrease in weight also permits longer distances between spans and/or lighter support towers.

Wear has been a factor considered in aluminum catenaries. Thomas [20] in 1966 examined a French composite catenary used in Bordeaux with an aluminum cable and a steel core. He stated that after 500,000 passages of the pantograph shoe (which is the limit life for a copper catenary) the wire showed little wear and had the possibility of an additional 100,000 passages. More recently Carlson and Griggs [21]

---

3. Aluminum is not as good a conductor and has a resistivity 1.65 times that of copper; therefore an aluminum wire must have a cross sectional area 1.65 times a copper wire's. However, aluminum has a density 0.302 times copper's, resulting in an equivalent wire of about half the weight. The yield stress of aluminum is 0.60 times copper's, but with the required increase in cross sectional area, the two wires can handle the same tension.

reported that after an initial break-in period the wear rates between copper and aluminum are not significantly different.

## CHAPTER 3

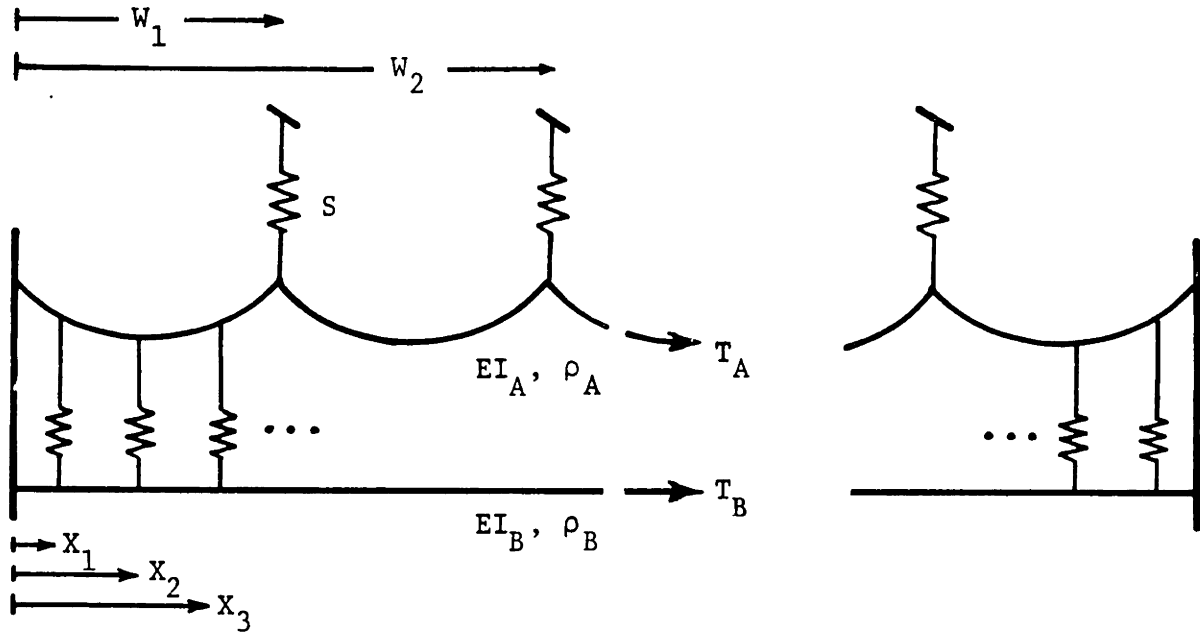
### MODEL DEVELOPMENT AND SOLUTION TECHNIQUE

This chapter highlights the development of the model and solution technique for the pantograph/catenary system. The models of the catenary and pantograph are developed to investigate dynamic phenomenon and to evaluate pantograph performance. The two models are developed separately here, but in the simulation the two are directly coupled to form a complete system model. The solution technique is summarized here outlining the methodology involved, while an in depth analysis is covered in Appendices A and B.

#### 3.1 Model Development

To simulate the dynamics of the catenary a model of the two wire, simple style catenary was chosen. The simple catenary configuration contains all the characteristic dynamic effects present in the advanced designs without the excessive complexity required to model the stitched or compound catenary. The single cable or trolley wire catenary, on the other hand, is significantly different than the advanced designs and a model based on this catenary would have only limited use in predicting pantograph performance.

A schematic of the catenary model is shown in Figure 3.1. The model represents a finite length of the simple catenary style, and incorporates the following features:



Tower Stiffness:  $S$   
 Dropper Stiffness:  $K$   
 Distance to the  $j$ th Tower:  $W_j$   
 Distance to the  $i$ th Dropper:  $X_i$   
 Stiffness of the Two Wires:  $EI_A, EI_B$   
 Density of the Two Wires:  $\rho_A, \rho_B$   
 Tension in the Two Wires:  $T_A, T_B$

FIGURE 3.1: CATENARY MODEL

- o Simple catenary with a contact wire and a messenger wire
- o Variable spacing between the droppers and between the towers
- o Contact and messenger wires are each modeled with a bending stiffness, constant tension, and a uniform density
- o Damping is distributed proportional to the mass of the wires to ensure orthogonality of the natural modes
- o The two wires are connected by droppers modeled as massless elastic springs
- o The messenger wire is connected to the towers modeled as massless elastic springs

To represent the pantograph a two mass model incorporating suspension nonlinearities was chosen. The two mass model, as shown by Vesely [10], is accurate for pantograph displacements up to 20 cm (The pantograph motions in the simulations never exceeded 10 cm). The pantograph model, shown in Figure 3.2, incorporates the following features:

- o The motion of the pantograph is modeled by two masses: a frame mass and a head mass
- o The applied uplift force is modeled as a constant,  $F_0$
- o Stiffness of the contact strips is modeled by a linear spring,  $K_s$
- o Stiffness between the head and the frame is modeled by a linear spring,  $K_h$
- o A mechanical stop is included limiting the relative motion between the head and the frame
- o Two types of damping elements between the head and the frame are modeled: linear damping and one-way damping.
- o Stiffness between the frame and the base is modeled by a linear spring,  $K_f$
- o Two types of damping elements between the frame and the base are modeled: linear damping and one-way damping

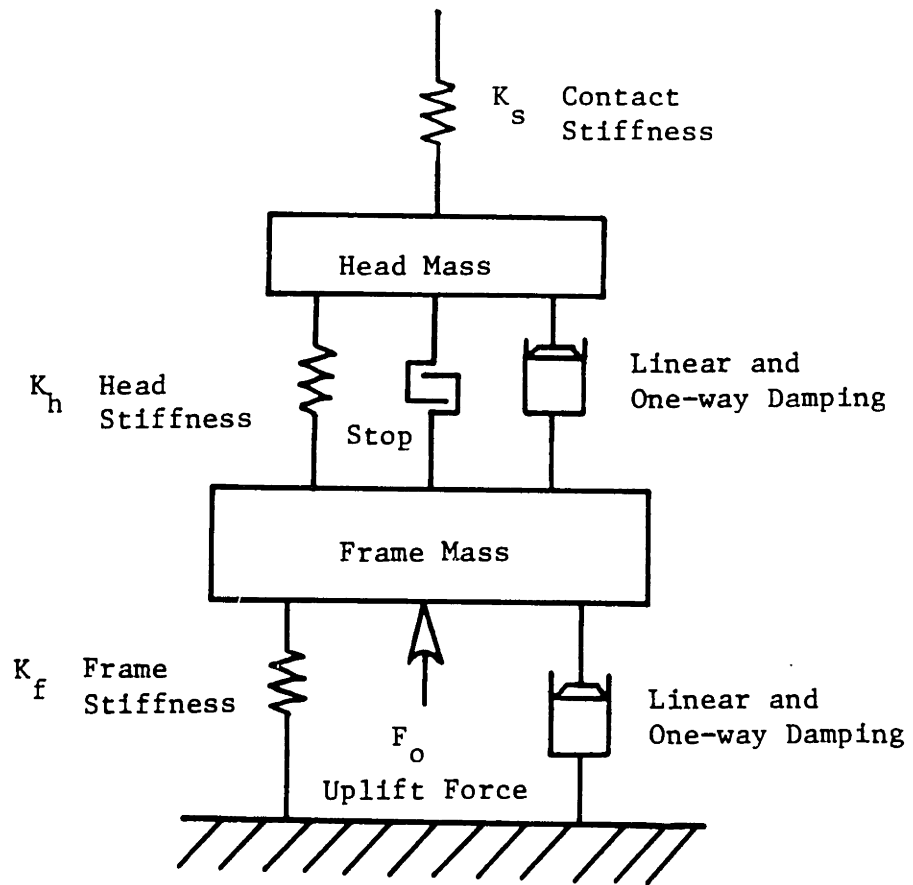


FIGURE 3.2: PANTOGRAPH MODEL



The pantograph and catenary models are coupled due to contact constraints. During contact, the force acting on the pantograph head is equal and opposite to the force on the lower catenary wire. Further, the vertical displacements of the pantograph head and the lower wire at the contact point are identical. The pantograph and catenary are shown in contact in Figure 3.3.

The pantograph traces the varying shape of the lower catenary wire and develops a varying contact force. The force displaces the catenary wire and produces the shape the pantograph must follow. If the contact force is less than the applied constant uplift force the pantograph and catenary wire rise together deflecting the catenary wire vertically; if the contact force is greater than the applied uplift force the pantograph and catenary wire fall together. Except during brief losses of contact when the two are considered independently, the pantograph and catenary form a coupled system.

### 3.2 Solution Technique

The dynamic response problem of the catenary and pantograph is solved using Fourier, Lagrange and modal analysis techniques. Simple Fourier analysis is used to describe the dynamic displacements of the catenary wires as a sine-series expansion and to describe the natural mode shapes of the catenary. The equations of motion are derived using a Lagrange formulation, and modal analysis is used to express the equations of motion in a standard form and, most importantly, allows the catenary model to be easily coupled with any pantograph model. The solution technique is presented briefly here and is developed in detail in Appendices A and B.

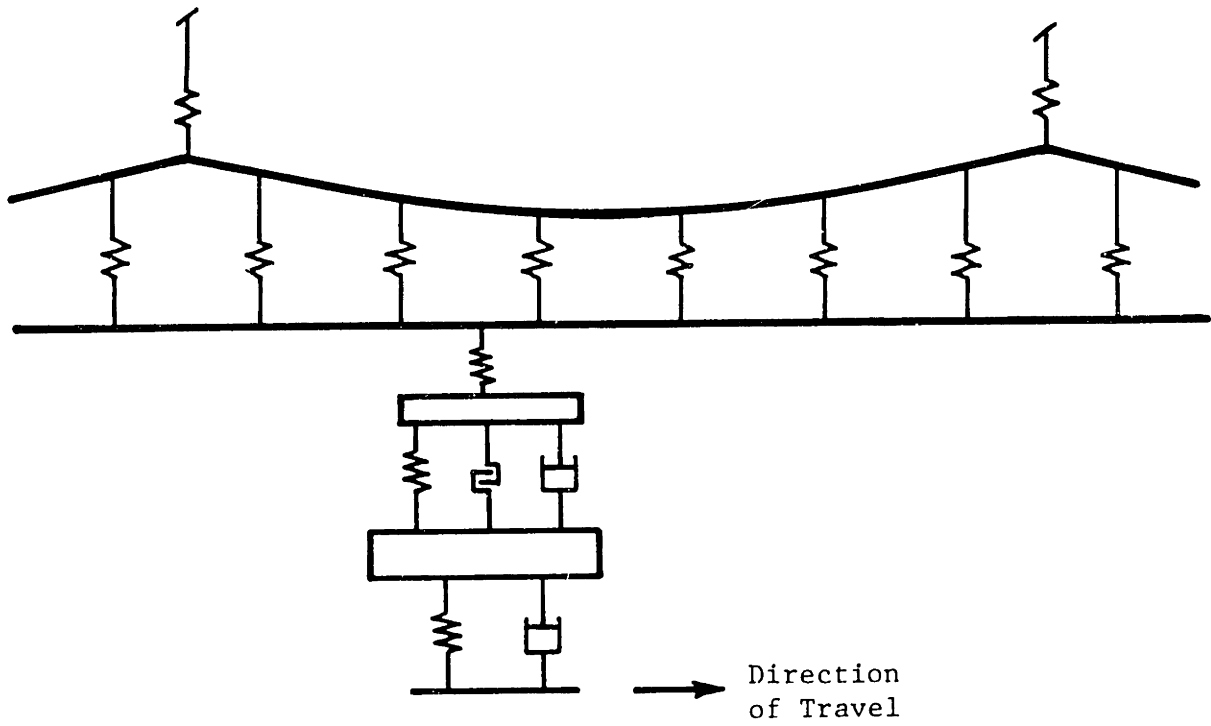


FIGURE 3.3: COUPLING OF THE PANTOGRAPH AND CATENARY MODELS

First, to describe the dynamic displacement of each wire from its equilibrium position, the displacement shape of each catenary wire is described by a sine-series expansion. A simple result of Fourier analysis is any shape with fixed ends can be mathematically described by superposing an infinite set of sine functions, each with an appropriate amplitude. A close approximation of the shape can be made with a finite number of sine terms. Considering a finite number of sine terms transforms the shape of the catenary wires from an infinite number of degrees of freedom into a finite number of degrees of freedom. Therefore the displacements are described by a finite term sine-series expansion: one series representing the shape of the contact (lower) wire, a second series representing the shape of the messenger (upper) wire.

$$y(x,t) = \sum A_m(t) \sin\left(\frac{m\pi x}{L}\right) \quad \text{upper wire} \quad (3.1)$$

$$y(x,t) = \sum B_m(t) \sin\left(\frac{m\pi x}{L}\right) \quad \text{lower wire}$$

where:

$y$  = The displacement of the upper wire

$A_m$  = The amplitude of the  $m$ th sine term, upper wire

$B_m$  = The amplitude of the  $m$ th sine term, lower wire

$x$  = The distance along the catenary

$L$  = The total length of the catenary

$m$  = An integer, designates the harmonic number

The shape of the wires and the displacement of any point on the wires is expressed as a function of the amplitude terms  $A_m$  and  $B_m$ .

Further, the shape of the wires as a function of time is expressed as a function of the time varying amplitude terms  $A_m(t)$  and  $B_m(t)$ . Therefore the amplitude terms  $A_m(t)$  and  $B_m(t)$  provide a sufficient and convenient set of generalized coordinates for deriving the equations of motion of the catenary.

The amplitude terms are used to derive expressions for the kinetic and potential energy. The kinetic energy results from the motion of the mass of the wire, and the potential energy results from displacements of the restoring elements: the tension in the wires, the bending stiffness in the wires, the dropper springs and the tower springs.

Lagrange's equation is applied to the expressions of kinetic and potential energy to obtain the equations of motion of the catenary. The equations of motion represent the unforced homogeneous case. The homogeneous equations contain only  $A$ ,  $\ddot{A}$ ,  $B$ , and  $\ddot{B}$  terms (displacement and acceleration terms) because all the elements of the catenary model are linear elements and because the damping terms and forcing function are neglected. The equations are arranged with the second derivative terms on the left and the amplitude terms on the right.

Since the catenary model is a linear system the catenary will always vibrate in a natural mode or a combination of its natural modes. The system will, in general, have as many natural modes as degrees of freedom, and when the system is excited in a natural mode the motion must be harmonic and the acceleration terms are defined by:

$$\ddot{A}_m = -\omega^2 A_m \tag{3.2}$$

$$\ddot{B}_m = -\omega^2 B_m$$

where:

$\omega$  = The frequency of vibration

To identify the natural modes the second derivative terms in the equations of motion are replaced with equation (3.2). This substitution expresses each equation of motion solely as a function of the amplitude terms and the frequency of vibration.

The equations of motion for both the upper and lower wires are then arranged in matrix-vector form, with the amplitude terms  $A_m$  and  $B_m$  written as a single vector  $\Gamma$ . The left hand side of the matrix equation is the frequency squared times the identity matrix,  $I$ , multiplied by the vector of amplitude terms,  $\Gamma$ . The right hand side of the equation is a square matrix of coefficients,  $H$ , multiplied by the vector of amplitude terms,  $\Gamma$ .

$$\omega^2 I \Gamma = H \Gamma \quad (3.3)$$

where:

$\omega$  = the frequency of vibration

$I$  = the identity matrix

$\Gamma$  = vector of the amplitude terms  
( $A_m$  s and  $B_m$  s)

$H$  = the dynamic matrix

The natural modes are easily evaluated from the matrix  $H$ . The equations of the system are decoupled into the natural modes by an eigenvalue analysis. The eigenvalues of the matrix  $H$  give the square of the natural frequencies and the eigenvectors give the set of amplitude terms describing the natural mode shapes. Each natural mode shape is

determined by using equation (3.1) and inserting the amplitude terms from each eigenvector.

The advantage of using modal analysis is two-fold: 1) it provides a convenient method of expressing the dynamics of the catenary, and 2) it allows the catenary model to be easily coupled with any pantograph model.

Using modal analysis for the catenary model allows it to be matched with any pantograph model (linear, nonlinear, or active controlled pantograph). The equations of motion of the pantograph model can be written with the natural modes of the catenary in standard modal form. The natural modes of the catenary are orthogonal and can be considered independently, and each modal equation is influenced by the pantograph. The resulting equations are second order linear differential equations of the form:

$$M_i \ddot{z}_i + 2\zeta_i \omega_i M_i \dot{z}_i + \omega_i^2 M_i z_i = Q_i \quad (3.4)$$

where:

$z_i(t)$  = The  $i$ th modal response function

$M_i$  = The  $i$ th modal mass

$\zeta_i$  = The damping ratio

$\omega_i$  = The  $i$ th natural frequency

$Q_i$  = The  $i$ th modal forcing function

The influence of the pantograph is represented in the modal forcing function,  $Q_i$

$$Q_i = \int f(x,t) \phi_i(x) dx \quad (3.5)$$

where:

$f(x,t)$  = The applied force distribution

$\phi_i$  = The  $i$ th natural mode shape

There is a modal equation for each natural mode of the catenary, each mode has an individual modal forcing function,  $Q_i$ , and each mode has an individual response. The dynamics of the catenary are determined by the set of modes and the shape is calculated by superposing the modes by equation (3.6)

$$y(x,t) = \sum z_i(t) \phi_i(x) \quad (3.6)$$

where:

$z_i(t)$  = the  $i$ th modal forcing function

$\phi_i(x)$  = the  $i$ th natural mode shape described by equation (3.1) and the amplitudes from the  $i$ th eigenvector

The modal equations for the catenary and the equations of motion for the pantograph model described above have been coded into a Fortran program and their interaction simulated on a digital computer. The pantograph and catenary are considered as a single coupled system in simulation; the pantograph head and the lower catenary wire share the same position and the coupling comes from the contact force between them. Only during momentary losses of contact are the two considered independently; in this case the contact force is zero until the pantograph regains contact with the catenary.

This chapter presents an overview of the model and solution technique. Technical details have been omitted to avoid obscuring the overall methodology. They are presented in Appendicies A and B for

further reference. The next chapter presents the natural modes and many of the results obtained using this model.



## CHAPTER 4

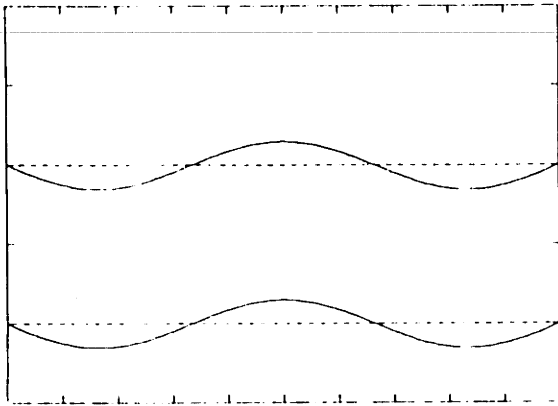
### RESULTS

The model developed in Chapter 3 has been implemented into a computer simulation and used for a variety of investigations: (1) Determining the natural modes of the catenary, (2) Dynamic simulations of both pantograph and catenary, (3) Evaluation of different pantograph designs, (4) Sensitivity studies of the parameters in the pantograph model, and (5) Evaluation of different catenary designs. The results are presented here and illustrate the behavior and dynamics of the pantograph and catenary.

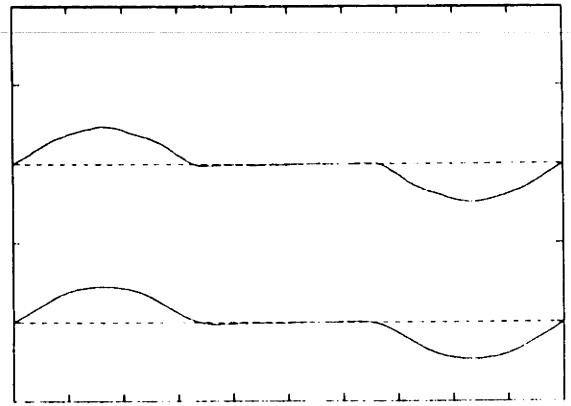
#### 4.1 Catenary Description and Natural Mode Shapes

Determining the natural mode shapes and natural frequencies of a specific catenary configuration is the first part of the simulation. The majority of the simulations have been run with three spans of a typical copper catenary and the parameters are given in Table 4.1. Figures 4.1 through 4.4 show the first 20 natural mode shapes. Each plot shows the modal displacements (dimensionless) versus the distance along the catenary. The upper curve is the mode shape of the upper wire (messenger wire); the lower curve is the mode shape of the lower wire (contact wire).

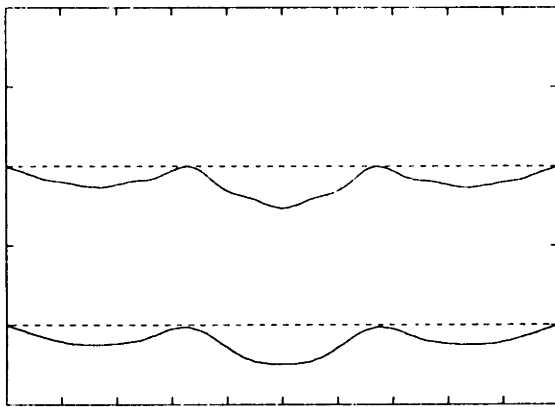
The stiffness of the support towers and the stiffness of the droppers has a strong influence on the natural modes. The towers are stiff and move very little with catenary vibration. The small



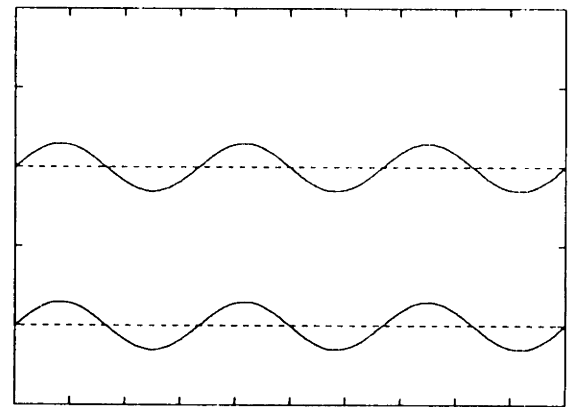
Mode 1 0.73 Hz



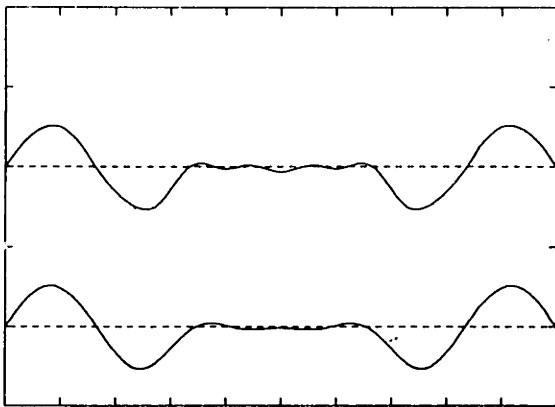
Mode 2 0.74 Hz



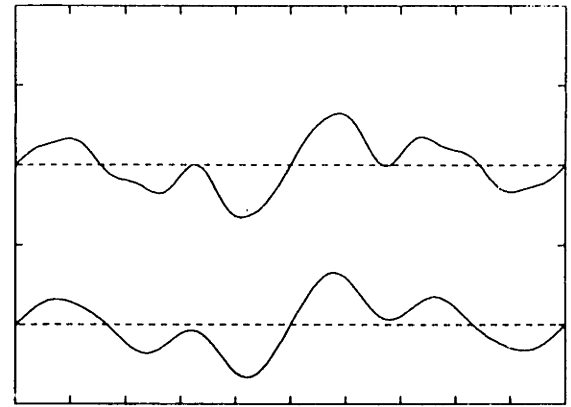
Mode 3 0.75 Hz



Mode 4 1.47 Hz

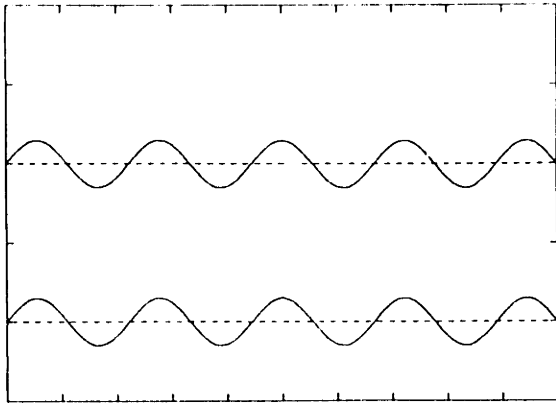


Mode 5 1.48

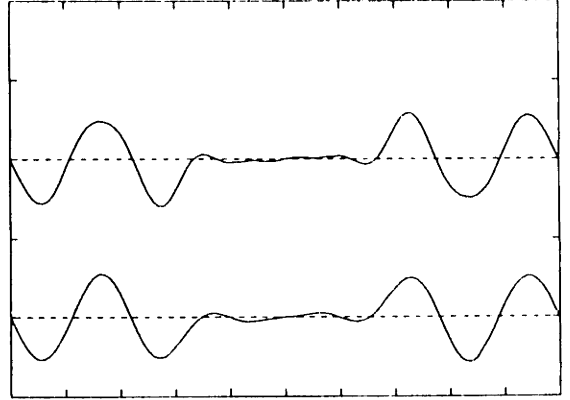


Mode 6 1.50 Hz

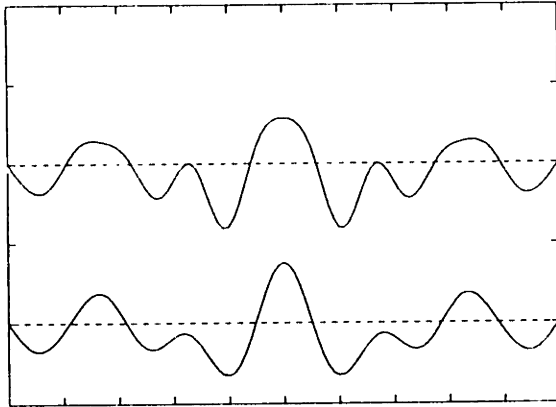
FIGURE 4.1: NATURAL MODES SHAPES FOR MODE 1 THROUGH 6



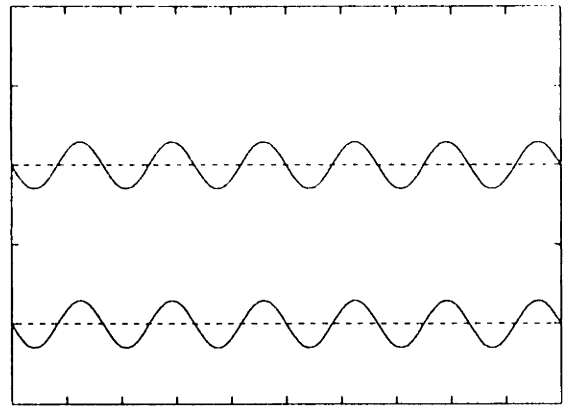
Mode 7 2.20 Hz



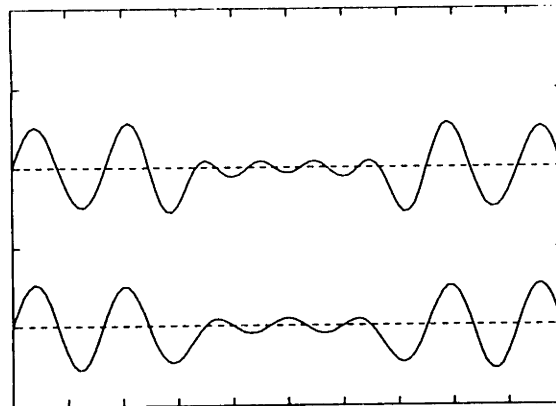
Mode 8 2.22 Hz



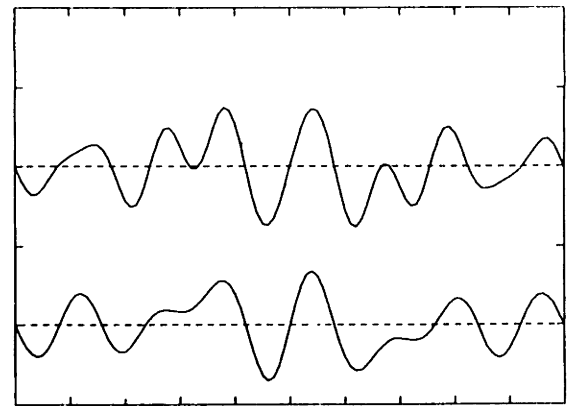
Mode 9 2.25 Hz



Mode 10 2.94 Hz

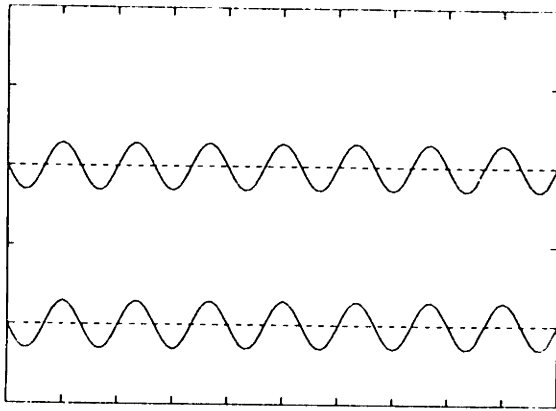


Mode 11 2.95 Hz

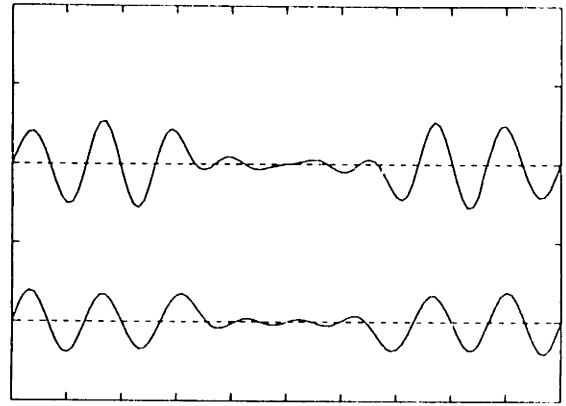


Mode 12 2.99 Hz

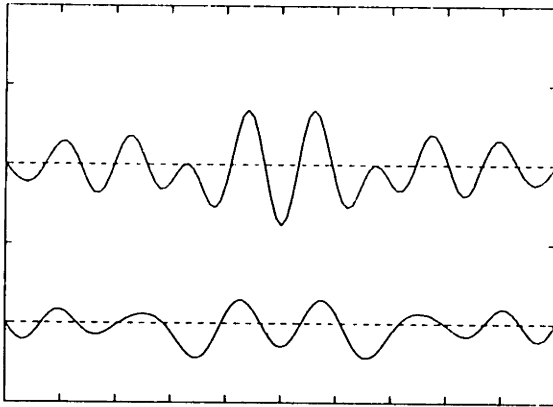
FIGURE 4.2: NATURAL MODE SHAPES FOR MODE 7 THROUGH 12



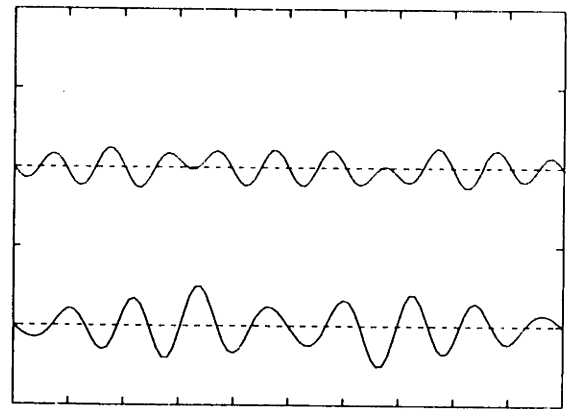
Mode 13 3.67 Hz



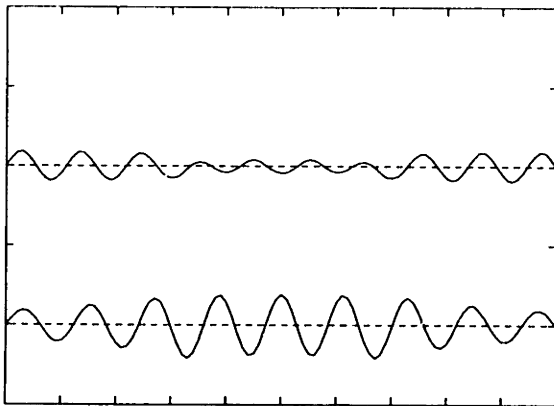
Mode 14 3.70 Hz



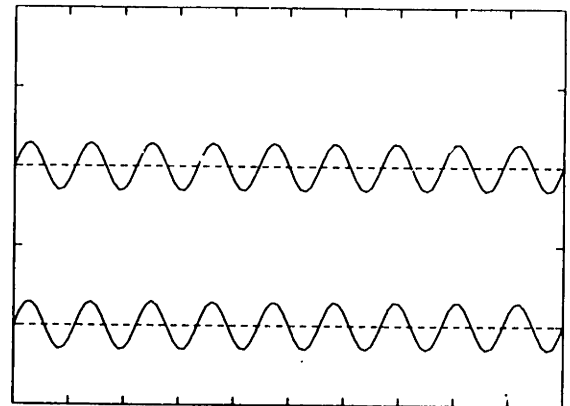
Mode 15 3.70 Hz



Mode 16 4.03 Hz

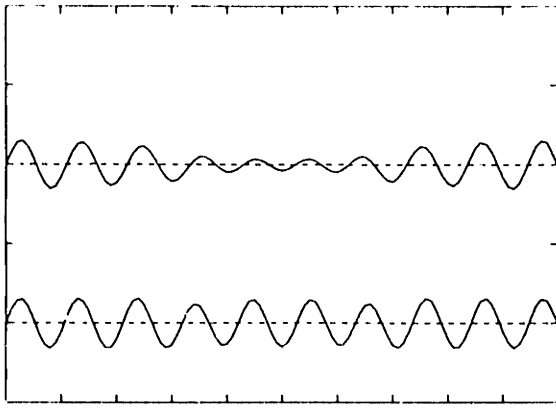


Mode 17 4.17 Hz

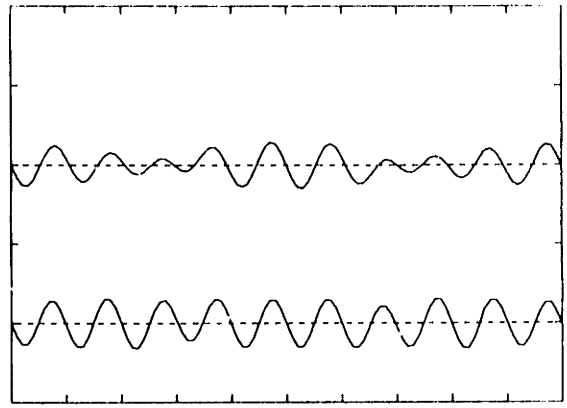


Mode 18 4.41 Hz

FIGURE 4.3: NATURAL MODE SHAPES FOR MODE 13 THROUGH 18



Mode 19 4.55 Hz



Mode 20 4.74 Hz

FIGURE 4.4: NATURAL MODE SHAPES FOR MODE 19 THROUGH 20

TABLE 4.1  
 BASELINE CATENARY PARAMETERS

Wire:	Copper	
Length:	228.6 m	750 ft
Tower Spacing:	3 Spans 76.2 m	250 ft
Dropper Spacing:	6 per span 12.8 m	42 ft
Tower Stiffness:	17,510 kN/m	100,000 lb/in
Dropper Stiffness:	43,775 kN/m	250,000 lb/in
Tension: Upper Wire	24 kN	5,400 lb
Lower Wire	28 kN	6,300 lb
Density: Upper Wire	1.786 kg/m	1.2 lbm/ft
Lower Wire	2.378 kg/m	1.6 lbm/ft
Stiffness: Upper Wire	861.2 N m <sup>2</sup>	.125 lb in <sup>2</sup>
Lower Wire	2584. N m <sup>2</sup>	.375 lb in <sup>2</sup>
Catenary Damping Ratio:	0.02	
Number of Modes Considered:	20	
Average Wave Speed:	112 m/s	250 mph

\* A 20 term sine expansion is used for each wire, giving 40 natural mode shapes. Inspection of the results shows approximately half of the modes from 0 to 5 Hz and the other half 100 to 500 Hz. The high frequency modes do not represent the true natural modes of the catenary, but result from the shape description using a finite number of sine terms. Therefore, these modes do not represent the true natural modes of the system and are ignored in the simulation.

displacement at the towers distinguishes each of the three spans; and this is especially noticeable in the first several modes. Even the shape of the lower catenary wire is dominated by the towers. Although the wire is not directly connected to the towers, the presence of the towers acts through the droppers, limiting the motion at these points.

The droppers are even stiffer than the towers and also move very little with catenary vibration. At low frequencies the behavior of the upper and lower wires is almost indistinguishable and at higher frequencies the shape of the two wires differs only between dropper locations.

The bending stiffness of the catenary wires, however, has little influence on the mode shapes, and this is best demonstrated in the first several mode shapes. At the towers, the mode shapes have shape discontinuities in shape, indicative of compliant bending. Further, each span can vibrate independent of the neighboring span, and the frequencies are almost identical whether or not they vibrate together. If the bending stiffness of the catenary wires were important the motion of each span would strongly influence the others and the behavior would be more closely coupled.

#### 4.2 Typical System Response

The baseline catenary has been simulated with several pantograph designs, and this section presents typical performance results using a standard industrial pantograph. The prototype #1 pantograph is run at 200 km/h (124 mph) and the parameters appear in Table 4.2.

Figures 4.5 through 4.10 represent the time history of the catenary shape, with the shape of the lower catenary wire plotted at 0.1 second intervals. The shape plots are separated five per figure for clarity, and the six figures span a total of 3.0 seconds. A vertical line on each plot shows the horizontal position of the pantograph at the time of the plot.

In the early part of the simulation (0.0 - 0.9 sec) the lower wire displaces upwards as the pantograph moves down the wire, and the displacement grows monotonically and linearly. Between 0.9 and 1.0 sec, the displacement of the catenary reaches a maximum, and then begins to fall. The wire will not move much at the towers due to the towers' stiffness, and the wire drops to meet this constraint.

From 1.0 to 1.4 sec, the pantograph approaches the first tower, and the shape of the wire is very steep. The pantograph moves down to accommodate the catenary but the pantograph's inertia and the rapid descent of the wire briefly raises the contact force.

At 1.37 sec the pantograph passes the first tower and the catenary begins rising again. The shape changes direction at the tower -- from a steep descent to a moderate incline -- and the pantograph attempts to trace this change. It is a difficult motion to follow and can often cause loss of contact at higher speeds.

The motion of the pantograph displaces the catenary, and causes the catenary wires to vibrate once the pantograph has passed. Between 1.7 and 2.4 sec the catenary makes a full excursion -- from full negative displacement to full positive ( $\pm 4$  cm) -- vibrating in the first natural mode (0.7 Hz). This vibration is very lightly damped and may



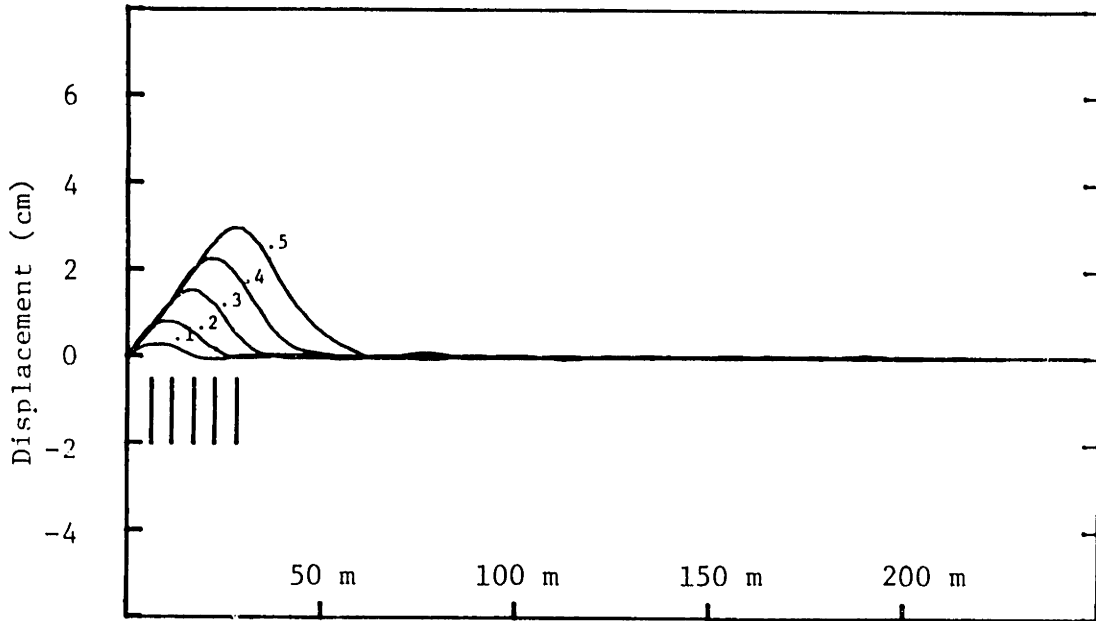


FIGURE 4.5: CATENARY SHAPE BETWEEN 0.0 AND 0.5 SECONDS

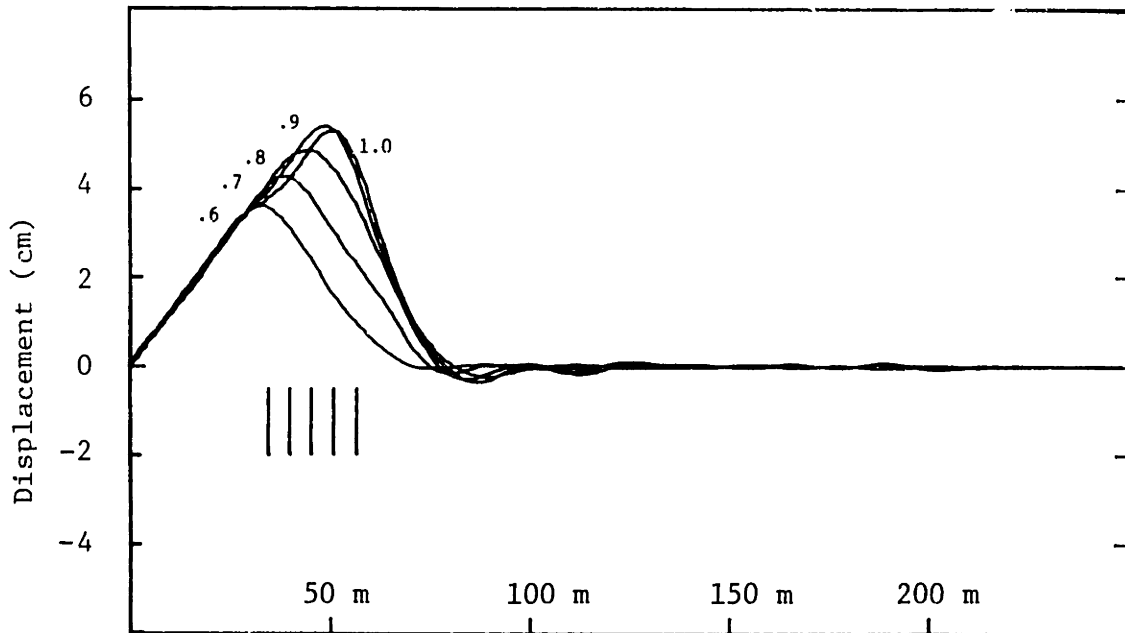


FIGURE 4.6: CATENARY SHAPE BETWEEN 0.6 AND 1.0 SECONDS

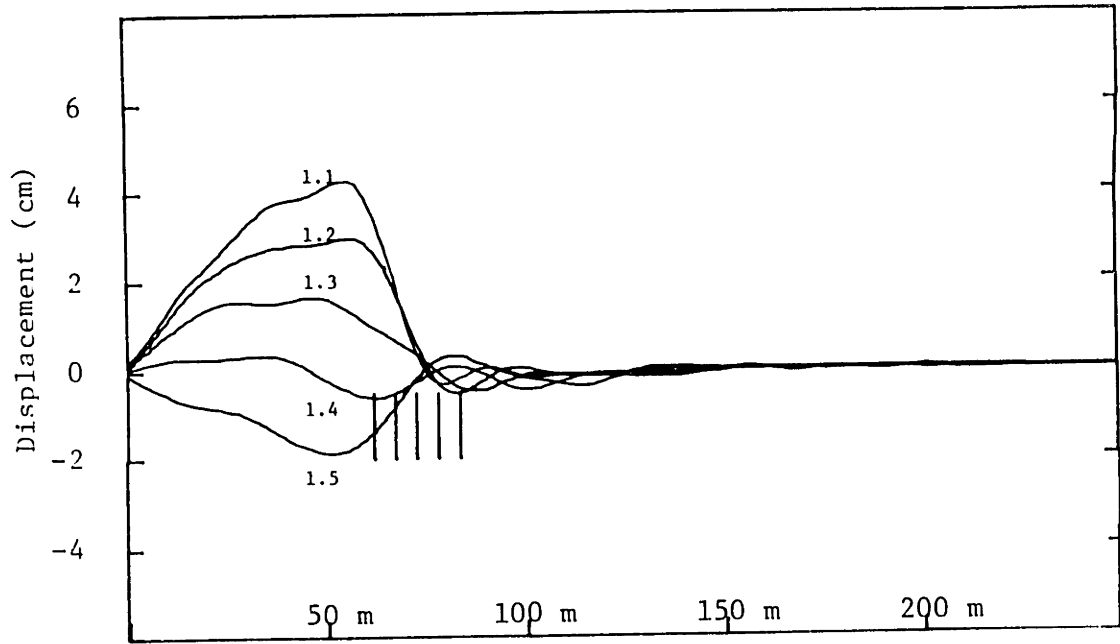


FIGURE 4.7: CATENARY SHAPE BETWEEN 1.1 AND 1.5 SECONDS

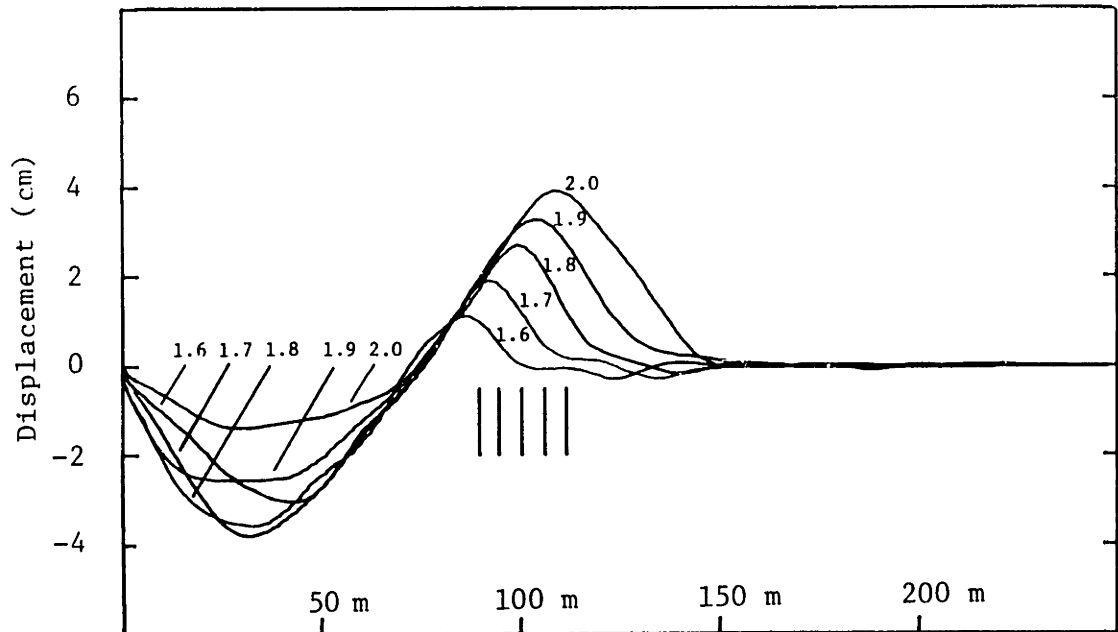


FIGURE 4.8: CATENARY SHAPE BETWEEN 1.6 AND 2.0 SECONDS

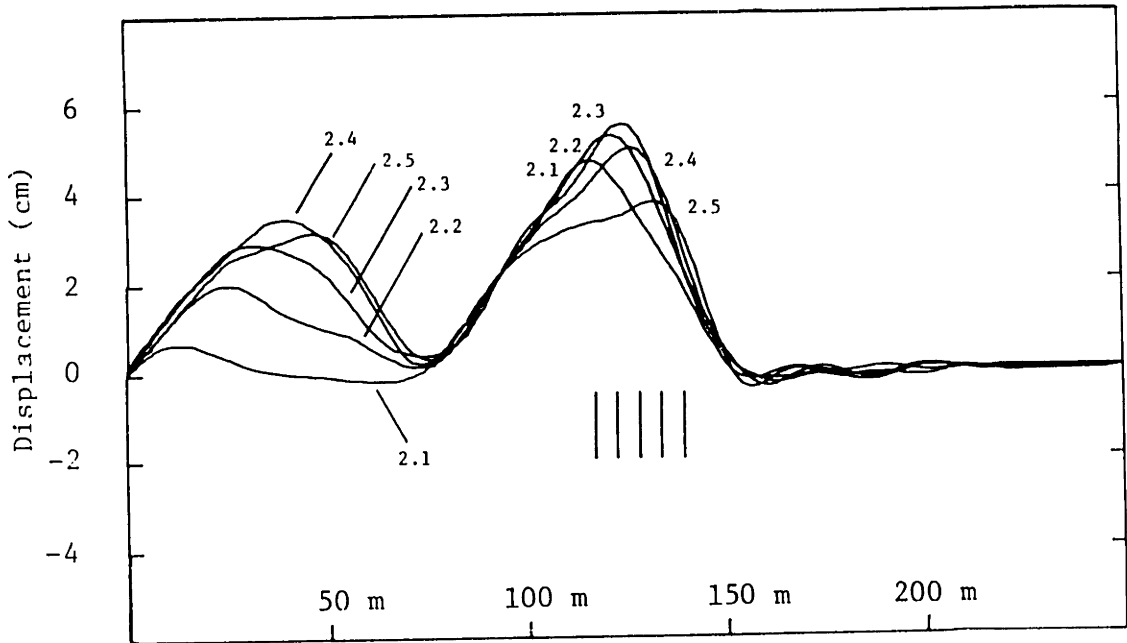


FIGURE 4.9: CATENARY SHAPE BETWEEN 2.1 AND 2.5 SECONDS

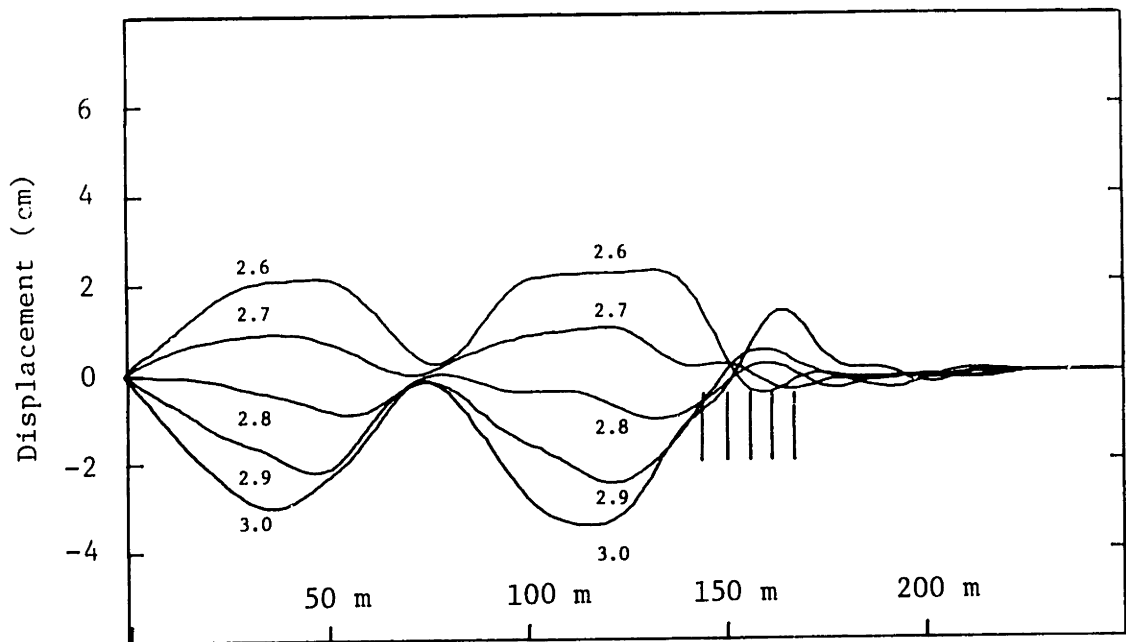


FIGURE 4.10: CATENARY SHAPE BETWEEN 2.6 AND 3.0 SECONDS

TABLE 4.2  
 PROTOTYPE #1 PANTOGRAPH PARAMETERS

Head Mass:	13.1 kg	28.8 lbm
Frame Mass:	25.0 kg	55.1 lbm
Stiffness of the Pantograph Shoe:	82.3 kN/m	470 lb/in
Stiffness Between the Head and Frame:	9.58 kN/m	54.72 lb/in
Stiffness Between the Frame and Base:	0.0 kN/m	0.0 lb/in
Damping Between the Head and Frame:	300 Ns/m	1.714 lb sec/in
Damping Between the Frame and Base:	1.0 Ns/m	.006 lb sec/in
Uplift Force:	90 N	20.2 lb

o Data represents an August Stemman Pantograph, See Reference [10]

cause tracking problems for trains using multiple pantographs.

The behavior described above reoccurs when the pantograph crosses the second span. After the pantograph passes the first tower, the displacement of the catenary wire increases linearly and monotonically; once the pantograph exits the second span, free vibration is excited in the catenary; and as before, it is dominated by the first mode. The consistent behavior of the spans emphasizes the validity of the model and the validity of considering a finite length of catenary.

The displacements of the catenary, pantograph head, and pantograph frame for the above system are all shown in Figure 4.11. The plots are the displacements from the datum at the moving point of contact, and are superposed one above another.

The displacements of the catenary and pantograph grow almost linearly until the peak is reached, and then decrease rapidly as the support tower is approached. The maximum displacement occurs at 0.91 sec, significantly past the middle of the span. The shift of the peak is due to the forward momentum of the pantograph and the displacement wave of the catenary, and becomes dramatic at a higher train speed or a lower catenary wave speed. The shift and the constraint of the stiff support towers cause the steep descent of the wire, and the further past the center the peak displacement occurs the steeper the descent will be.

The change in catenary shape at the towers, from a descent to an incline, effects pantograph performance. At 200 km/h the pantograph head maintains contact but the pantograph frame, which is heavier and slower to respond than the head, undershoots when the pantograph passes the tower. The relative displacement between the head and frame is

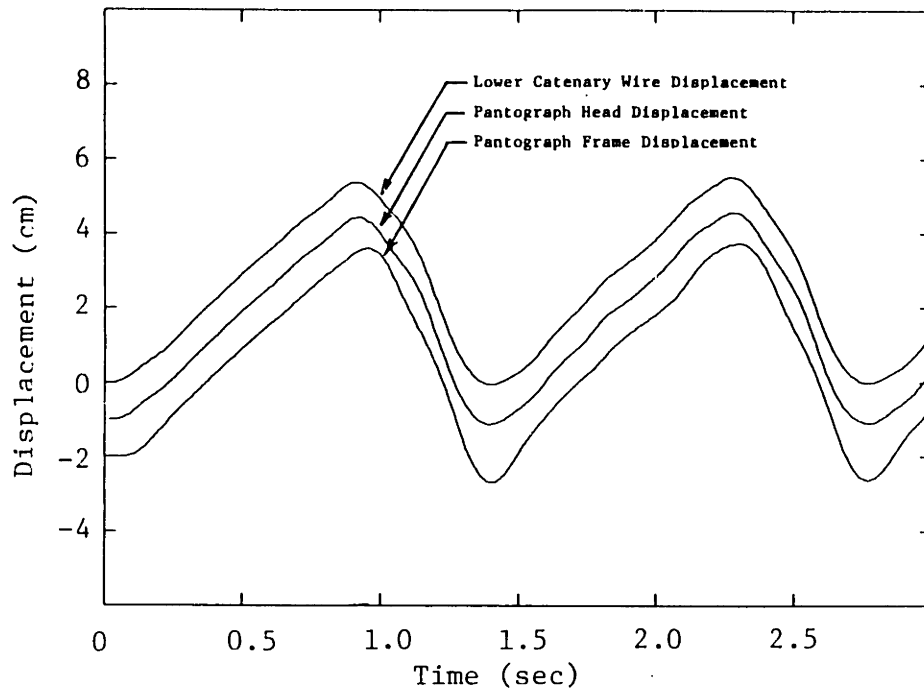


FIGURE 4.11: DISPLACEMENT OF THE CATENARY AND PANTOGRAPH  
 PROTOTYPE 1 PANTOGRAPH AT 200 km/h

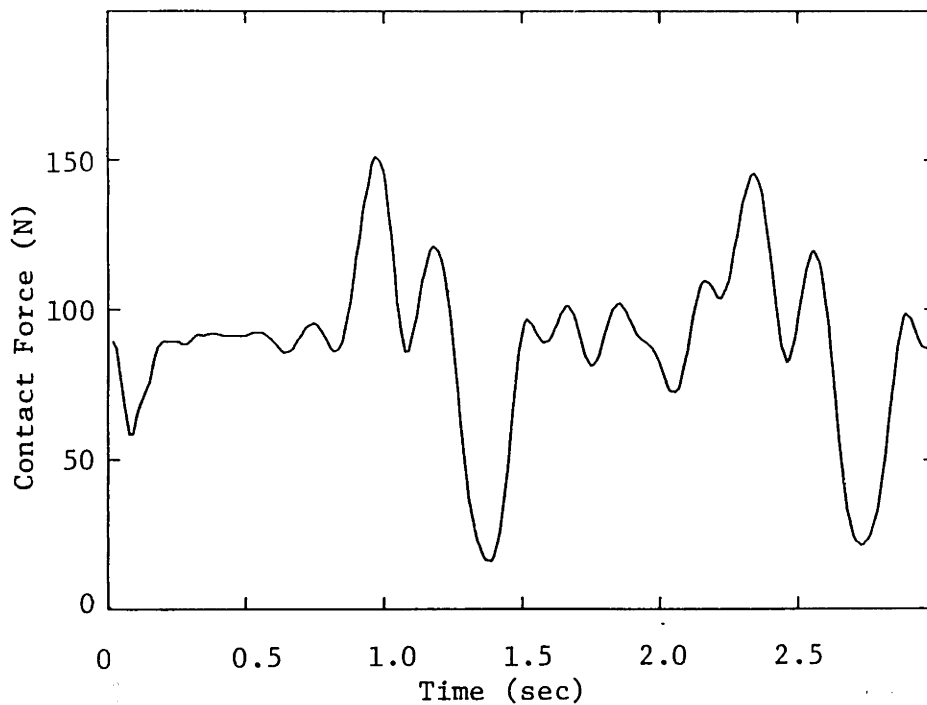


FIGURE 4.12: CONTACT FORCE HISTORY  
 PROTOTYPE 1 PANTOGRAPH AT 200 km/h

accommodated by the suspension, but the slow response of the frame mass results in a lower contact force.

The contact force is shown in Figure 4.12. The contact force is highest just before the pantograph passes the tower. The peak in force occurs when the pantograph is tracking the steep descent of the wire and reaches a maximum of 152 N at 0.96 sec. The contact force reaches a minimum of 44 N just after the pantograph passes each tower ( $t = 1.37, 2.72$  sec), and occurs as the catenary wire begins rising.

#### Effects of Increasing Speed

At 225 km/h the pantograph cannot follow the catenary and loss of contact occurs. The loss of contact occurs just after passage of the towers (1.2 and 2.4 sec) and can be observed in either Figure 4.13 or Figure 4.14. Figure 4.13 shows the displacement of the catenary wire and pantograph, and the separation occurs when the trajectory of the lower wire and pantograph head differ. Figure 4.14 shows the contact force and the force vanishes when the pantograph loses contact.

#### 4.3 Comparative Performance of Selected Pantographs

Two pantograph designs have been compared using the baseline catenary. The two pantographs represent commercial designs: Prototype #1 is discussed above (parameters given in Table 4.2) and Prototype #2 has the parameters given in Table 4.3. The two pantographs are run at speeds from 150 km/h to 250 km/h (124 to 156 mph), and data similar to that shown above are obtained for each pantograph at each speed.

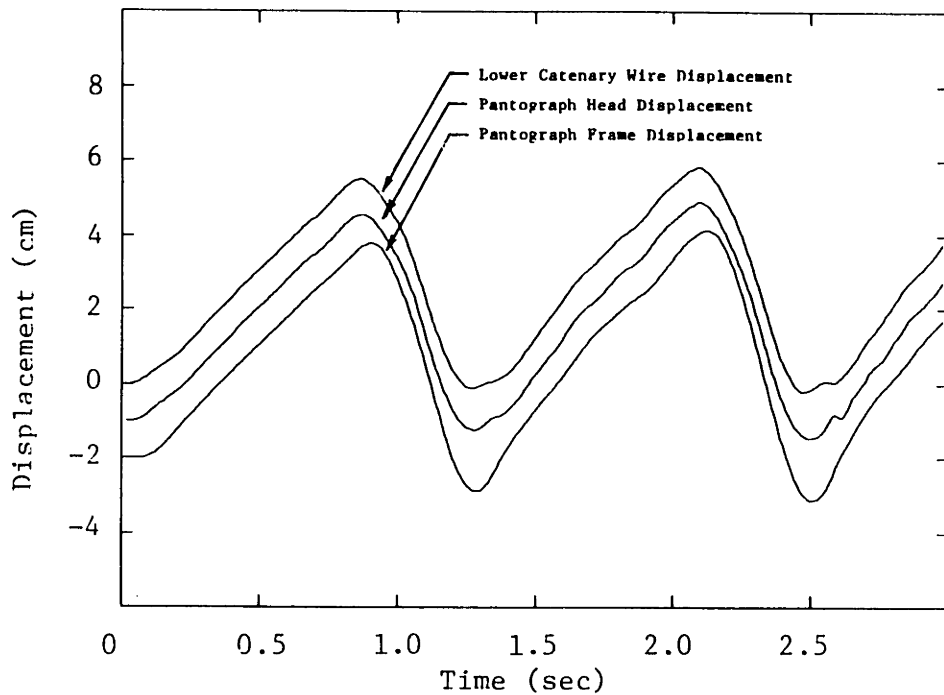


FIGURE 4.13: DISPLACEMENT OF THE CATENARY AND PANTOGRAPH PROTOTYPE 1 PANTOGRAPH AT 225 km/h

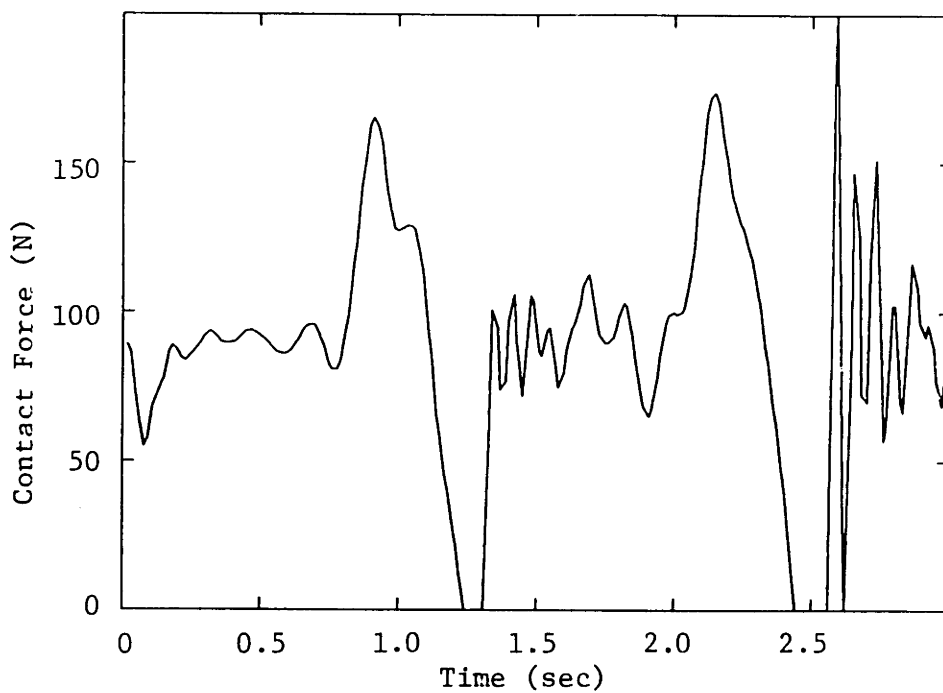


FIGURE 4.14: CONTACT FORCE HISTORY PROTOTYPE 1 PANTOGRAPH AT 225 km/h



TABLE 4.3

## PROTOTYPE #2 PANTOGRAPH PARAMETERS

Head Mass:	9.1 kg	20 lbm
Frame Mass:	17.2 kg	38 lbm
Stiffness of the Pantograph Shoe:	82.3 kN/m	470 lb/in
Stiffness Between the Head and Frame:	7.0 kN/m	40 lb/in
Stiffness Between the Frame and Base:	0.0 kN/m	0.0 lb/in
Damping Between the Head and Frame:	130 Ns/m	.743 lb sec/in
Damping Between the Frame and Base:	30 Ns/m	.171 lb sec/in
Uplift Force:	90 N	20.2 lb

o Data represents a Faively Pantograph, See Reference [19]

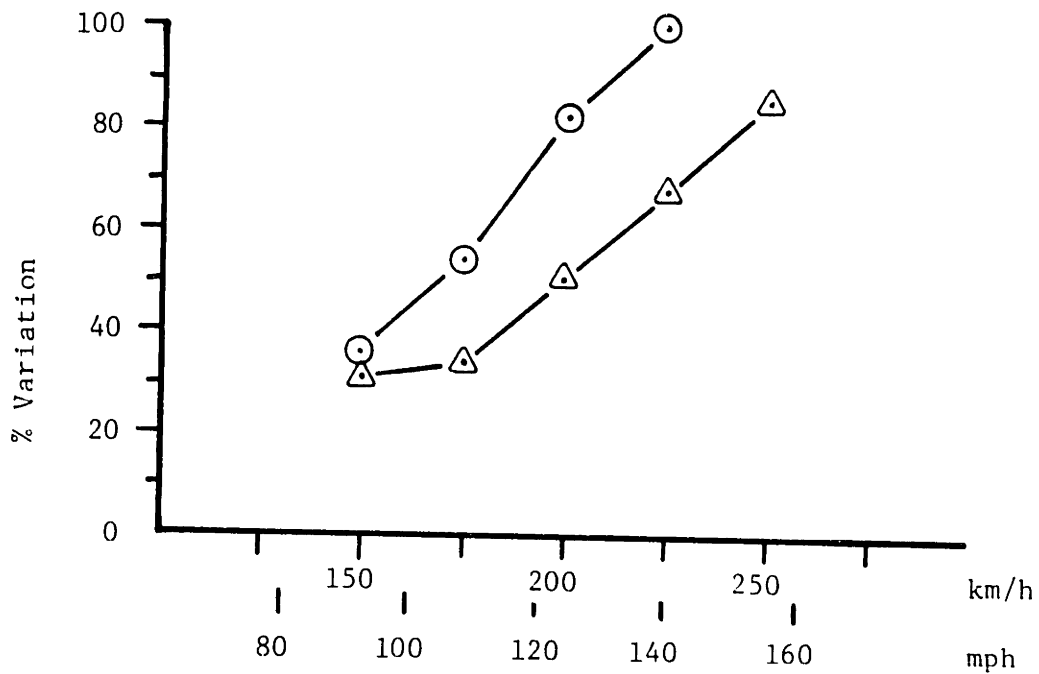
The variation in contact force is selected as the performance index for the two designs and the force variation of both pantographs is presented in Figure 4.15. The variation in contact force is of interest for two reasons: a low variation means a lower uplift force can be used, and the variation shows the safety margin before loss of contact occurs.

Comparison of the two designs shows prototype #2 performs better than prototype #1 at all the speeds tested. Prototype #1 starts to lose contact with the catenary at 225 km/h (140 mph), while prototype #2 maintains contact at this speed and does not lose contact until above 250 km/h. The support tower is the critical area for both pantographs, and the minimum contact force occurs just after passing a tower.

The superior performance of the prototype #2 pantograph is mainly due to the reduced mass of the pantograph. The head and frame masses of prototype #2 are, respectively, 9.1 kg and 17.2 kg (20.0 and 38.0 lbm); prototype #1 has masses of 13.1 kg and 25.0 kg (28.8 and 55.1 lbm), respectively. A lighter mass, especially in the head, has less inertial resistance to motions of the catenary, and is desirable for tracking the quick variations and high-frequency vibrations in the wires. The prototype #1 pantograph represents a fairly rugged design, whereas prototype #2 pantograph is a very lightweight design, and was created with the goal of designing the lightest possible pantograph.<sup>4</sup>

---

4. See Reference 19 pp 341-342



CONTACT FORCE VARIATION

Pantograph and Speed (km/h)	Contact Force High/Low (N)	Percent Variation
Prototype #1 150	122/58	35.6 %
Prototype #1 175	125/41	54.4
Prototype #1 200	152/16	82.2
Prototype #1 225	LOC	LOC
Prototype #1 250	LOC	LOC
Prototype #2 150	113/61	32.2
Prototype #2 175	114/60	33.3
Prototype #2 200	133/44	51.1
Prototype #2 225	143/28	68.9
Prototype #2 250	166/13	85.6

- o All runs were made with a nominal uplift of 90 N
- o LOC = Loss of Contact

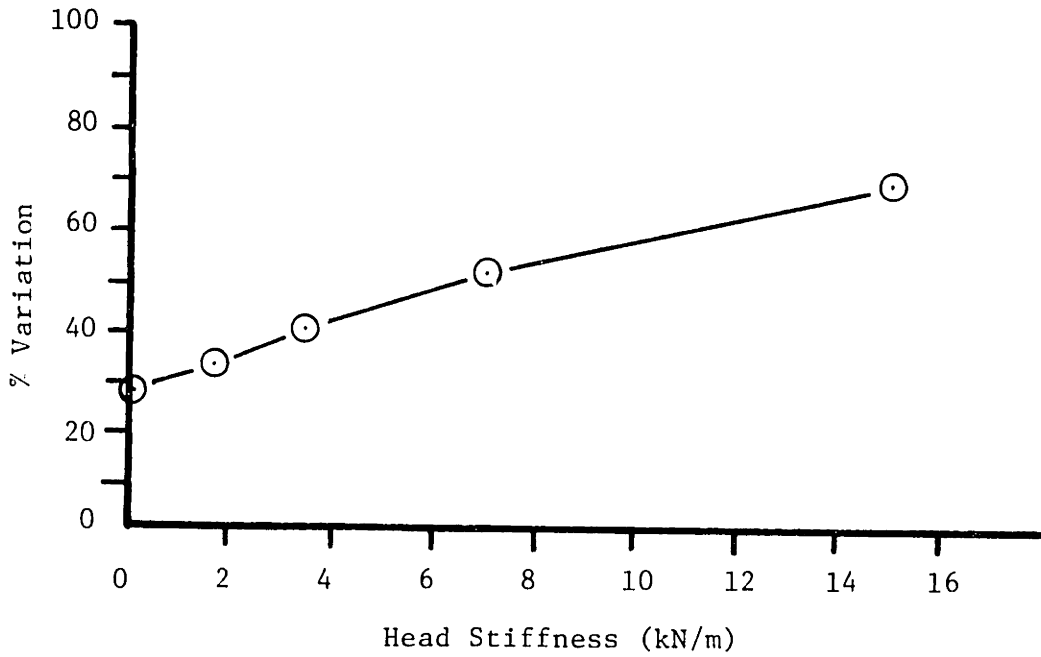
FIGURE 4.15: COMPARISON OF THE VARIATION IN CONTACT FORCE FOR THE TWO PANTOGRAPHS

#### 4.4 Parameter Influence on Performance

The pantograph model has been used as a design tool to investigate possible improvements to pantograph design. Variations in the damping and stiffness elements are investigated. Minimizing the head and frame mass to improve performance is not readressed here, but is discussed briefly above and in depth in References [2,3,4,5,6]. The essential result is the lower the mass the better -- limited only by the structural integrity and rigidity of the pantograph.

The prototype #2 pantograph is typical of a well-designed lightweight pantograph and is used as a baseline in this investigation. The effect of varying only the stiffness of the head suspension is shown in Figure 4.16. As before, variation in contact force is the performance index and all the runs are at 200 km/h. The results show the head stiffness should be as low as possible, the best performance is achieved with zero stiffness. A plot of the contact force for the case of zero head stiffness appears in Figure 4.17. The performance is clearly superior to the standard configuration; the contact force is more uniform, and occurs without the large maxima and minima near the towers. With zero stiffness the variation in contact force is 28%, which is significantly less than the 51% variation of the standard configuration.

The performance of the pantograph due to changes in damping is investigated in Figures 4.18 through 4.21<sup>5</sup>. The head and frame damping ratios in the prototype #2 pantograph initially are 0.26 and 0.04, respectively. Figure 4.18 illustrates the effect of varying the damping of the head and frame together, i.e. with the same damping ratio for each. The best performance in this case results from moderate damping,



Head Stiffness (Newtons/meter)	Contact Force High/Low (N)	Percent Variation
0 N/m	115/72	28 %
1,750	119/60	30
3,500	126/54	40
7,000	133/44	51
15,000	144/28	69

o All runs were made with the Prototype #2 pantograph at 200 km/h with a nominal uplift of 90 N

FIGURE 4.16: INFLUENCE OF VARIATIONS IN HEAD STIFFNESS

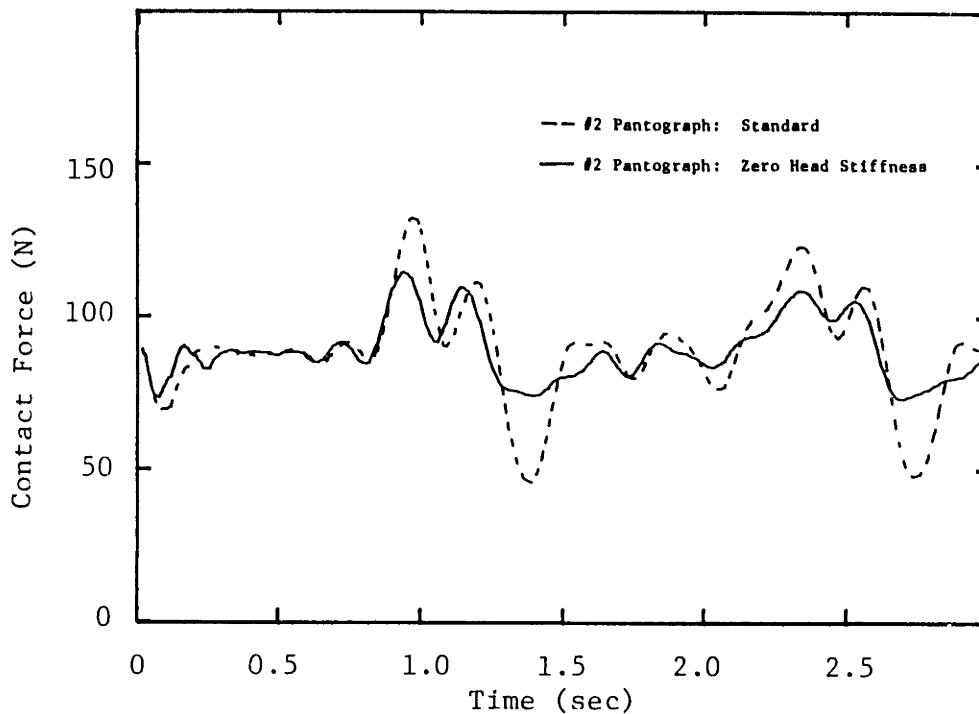


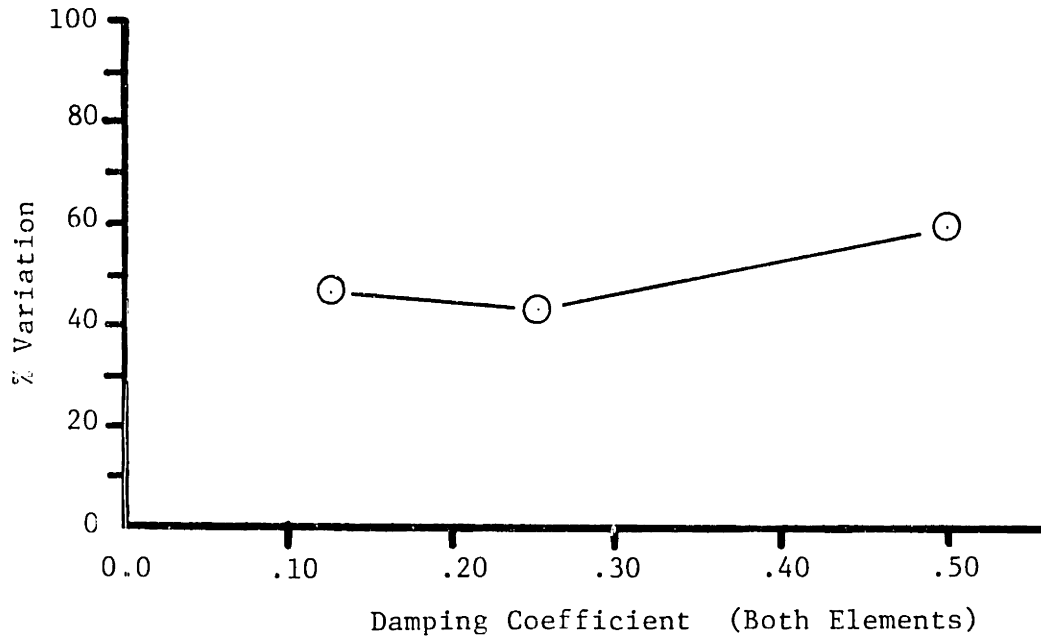
FIGURE 4.17: ZERO HEAD STIFFNESS VS. STANDARD CONFIGURATION  
 PROTOTYPE 2 PANTOGRAPH AT 200 km/h

head and frame damping ratios equal 0.25, 0.25 respectively, giving a contact force variation of 44%.

Varying the damping in each element separately is also considered. In Figure 4.19 the head damping alone is varied, and it shows that this improves the performance only slightly. The variation in contact force is 52% using a damping ratio of 0.5, 0.0, a small improvement over the 63% variation obtained with a damping ratio of 0.125, 0.0. Varying the

---

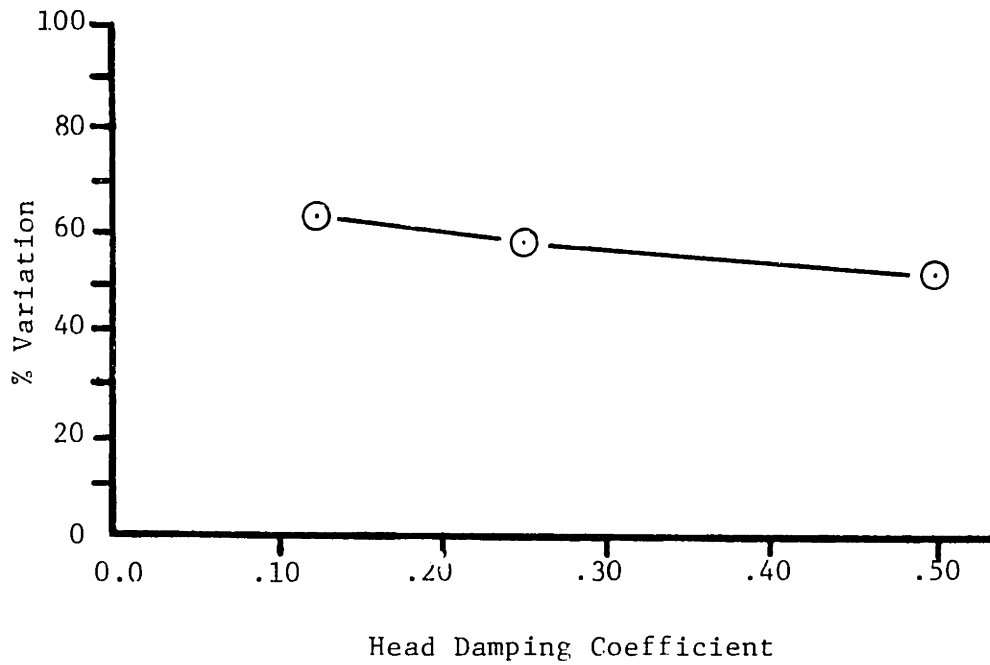
5. The damping is defined by the effective damping ratio, zeta. The two damping ratios define 1) the ratio of critical damping of the head mass vibrating on the head to frame spring and head to frame damper 2) the ratio of critical damping of the frame mass vibrating on the head to frame spring and frame to base damper. The damping ratio is not a perfect index. For a system with a very low stiffness using the same damping ratios presented here would result in insufficient damping. The ratio of damping to mass may be a better index.



Head and Frame Damping Ratios		Damping Values $B_1$ (Ns/m) $B_2$		Contact Force High/Low (N)	Percent Variation
.125	.125	63	87	130/49	46 %
.25	.25	126	174	130/62	44
.5	.5	252	347	144/63	60

- o All runs were made with the Prototype #2 pantograph at 200km/h with a nominal uplift of 90 N

FIGURE 4.18: INFLUENCE OF SIMULTANEOUS VARIATION IN HEAD AND FRAME DAMPING

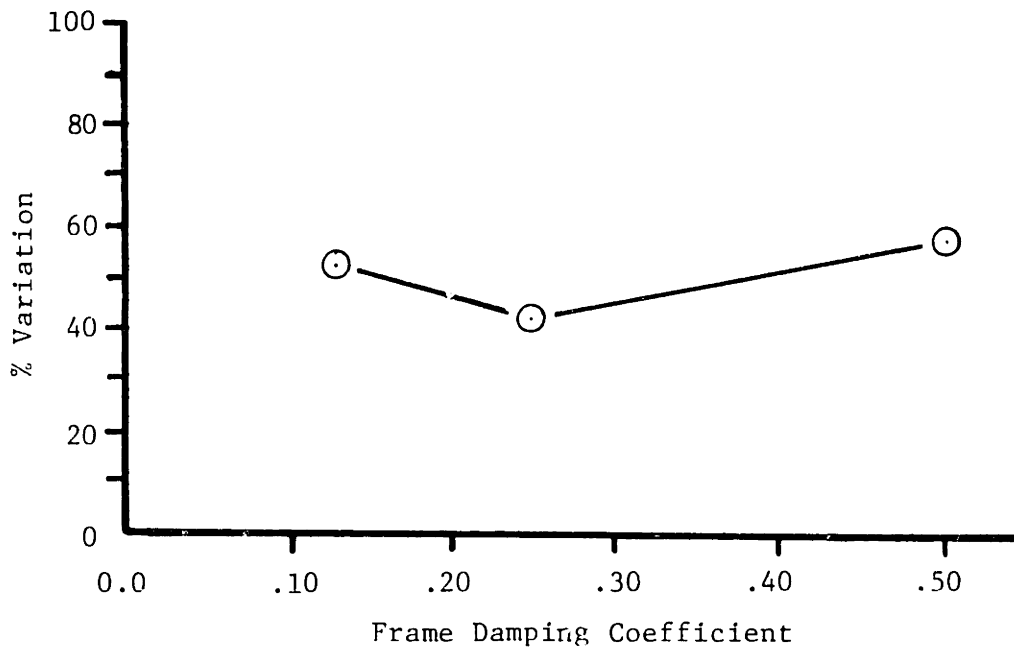


Head and Frame Damping Ratios		Damping Values $B_1$ (Ns/m) $B_2$		Contact Force High/Low (N)	Percent Variation
.125	0.00	63	0	136/33	63 %
.25	0.00	126	0	135/38	58
.5	0.00	252	0	136/43	52

o All runs were made with the Prototype #2 pantograph at 200 km/h with a nominal uplift force of 90 N

FIGURE 4.19: INFLUENCE OF VARIATIONS IN HEAD DAMPING





Head and Frame Damping Ratios		Damping Values		Contact Force	Percent Variation
		$B_1$ (Ns/m)	$B_2$	High/Low (N)	
0.04	.125	20	87	131/42	53 %
0.04	.25	20	174	128/58	42
0.04	.5	20	347	142/64	58

- o All runs were made with the Prototype #2 pantograph at 200 km/h with a nominal uplift force of 90 N
- o A small amount of head damping is required to stabilize the head in the simulations

FIGURE 4.20: INFLUENCE OF VARIATIONS IN FRAME DAMPING

frame damping has more dramatic influence, and is shown in Figure 4.20. In this case the optimum damping occurs at  $\zeta = 0.0, 0.25$  with a contact variation of 42%. Lower and higher frame damping significantly increases the contact force variation.

Several configurations with different damping in both elements are investigated and a list of the results appears in Table 4.4. The best performance for this pantograph was obtained using a damping ratio of 0.26, 0.19, and a plot of the contact force for this configuration is shown in Figure 4.21. The contact force variation for this case is 40%, the least variation of any configuration.

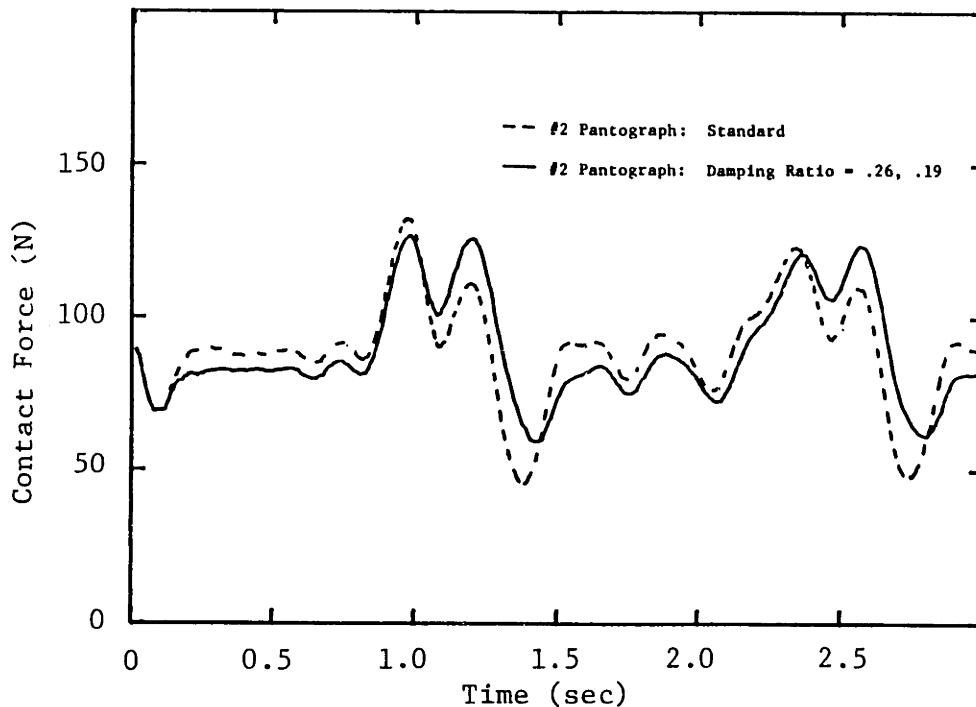


FIGURE 4.21: HEAD AND FRAME DAMPING = .26, .19 VS. STANDARD PROTOTYPE 2 PANTOGRAPH AT 200 km/h

TABLE 4.4  
 INFLUENCE OF INDEPENDENT VARIATIONS  
 IN HEAD AND FRAME DAMPING

Head and Frame Damping Ratios		Damping Values B <sub>1</sub> (Ns/m) B <sub>2</sub>		Contact Force High/Low	Percent Variation
.13	.09	65	65	131/46	49 %
.25	.125	126	87	129/53	43
.26	.19	130	130	126/59	40
.50	.125	252	87	130/58	44
.51	.37	260	260	139/66	54

Several simulations were run incorporating one-way damping. In general, the use of this damping increases the lowest force but does not reduce the highest force. These advantages reduce the risk of loss of contact and allow lower uplift forces to be used. Moderate damping ratios from 0.125 to 0.250 work well but a quantitative comparison has not been established.

#### 4.5 Alternate Catenary Configurations

The baseline catenary, used in the majority of the simulations, has been compared with alternate catenary configurations. One design is a low wave speed copper catenary. This catenary has parameters identical to the baseline except for lower tension in the wires (required to lower the wave speed), and the parameters are given in Table 4.5. The low wave speed catenary has a wave speed of 69 m/s or 250 km/h in comparison to the base line catenary with a wave speed of 112 m/s or 403 km/h. The performance of the catenary with the prototype #2 pantograph at 200 km/h is shown in Figure 4.22.

The performance of this catenary is not acceptable. The small oscillations in contact force at the start of the simulation do not subside, but grow. The contact force exceeds 200 N and then reaches zero with loss of contact at the tower ( $t = 1.37$  sec). The pantograph bounces off the catenary several times and does not maintain steady contact. The performance is unsatisfactory and emphasizes the importance of wave speed as a parameter in catenary design.

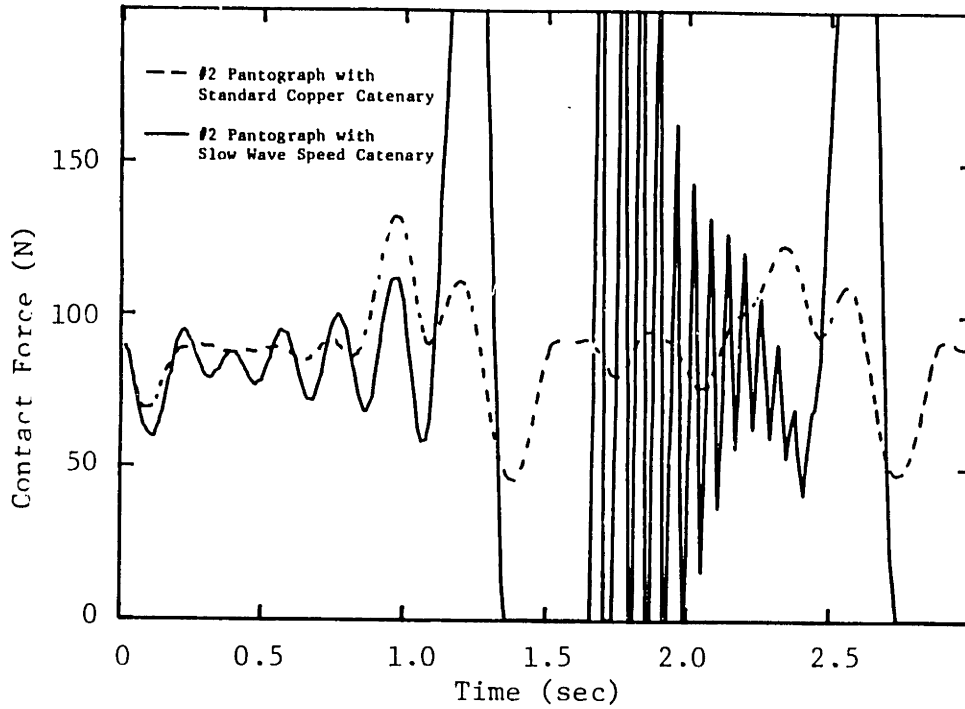


FIGURE 4.22: LOW WAVE SPEED CATENARY VS. BASELINE CATENARY  
 PROTOTYPE 2 PANTOGRAPH AT 200 km/h

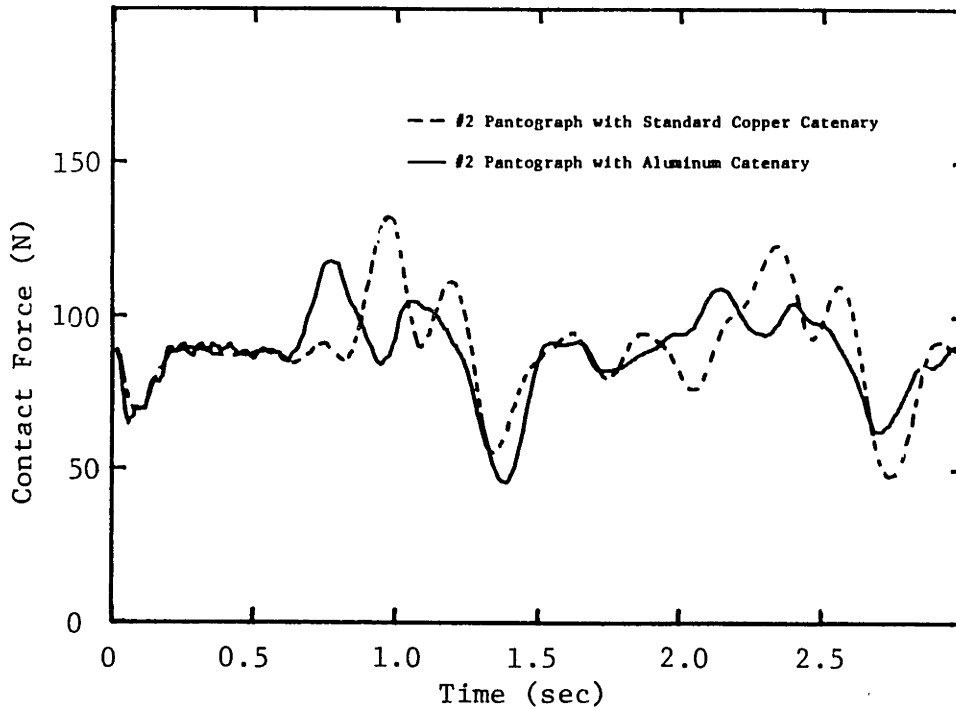


FIGURE 4.23: ALUMINUM CATENARY VS. BASELINE COPPER CATENARY  
 PROTOTYPE 2 PANTOGRAPH AT 200 km/h

TABLE 4.5

LOW WAVE SPEED CATENARY PARAMETERS

Wire:	Copper	
Length:	228.6 m	750 ft
Tower Spacing:	3 Spans 76.2 m	250 ft
Dropper Spacing:	6 per span 12.8 m	42 ft
Tower Stiffness:	17,510 kN/m	100,000 lb/in
Dropper Stiffness:	43,775 kN/m	250,000 lb/in
Tension: Upper Wire	9.83 kN	2,210 lb
Lower Wire	11.47 kN	2,580 lb
Density: Upper Wire	1.786 kg/m	1.2 lbm/ft
Lower Wire	2.378 kg/m	1.6 lbm/ft
Stiffness: Upper Wire	861.2 N m <sup>2</sup>	.125 lb in <sup>2</sup>
Lower Wire	2584. N m <sup>2</sup>	.375 lb in <sup>2</sup>
Catenary Damping Ratio:	0.02	
Number of Modes Considered:	20	
Average Wave Speed:	69 m/s	154 mph

An aluminum catenary has also been investigated. An equivalent aluminum catenary has the same tension and approximately half the lineal density. These two factors increase the wave speed significantly and generally improve performance. The parameters of the aluminum catenary are shown in Table 4.6, and the aluminum catenary is simulated with the prototype #2 pantograph at 200 km/h in Figure 4.23. The equivalent aluminum catenary is superior to the baseline copper catenary in dynamic performance; the variation in contact force is lower (38% vs. 51%) and the peaks in force appear earlier due to the faster dynamic response of the aluminum catenary.

This chapter illustrates many of the possible performance evaluations and the major results are highlighted in Chapter 5.

TABLE 4.6  
ALUMINUM CATENARY PARAMETERS

Wire:	Aluminum	
Length:	228.6 m	750 ft
Tower Spacing:	3 Spans 76.2 m	250 ft
Dropper Spacing:	6 per span 12.8 m	42 ft
Tower Stiffness:	17,510 kN/m	100,000 lb/in
Dropper Stiffness:	43,775 kN/m	250,000 lb/in
Tension: Upper Wire	24 kN	5,400 lb
Lower Wire	28 kN	6,300 lb
Density: Upper Wire	0.90 kg/m	0.6 lbm/ft
Lower Wire	1.19 kg/m	0.8 lbm/ft
Stiffness: Upper Wire	1,604 N m <sup>2</sup>	.233 lb in <sup>2</sup>
Lower Wire	4,743 N m <sup>2</sup>	.688 lb in <sup>2</sup>
Catenary Damping Ratio:	0.02	
Number of Sine Terms:	20	
Number of Modes Considered:	20	
Average Wave Speed:	158 m/s	350 mph



## CHAPTER 5

### DISCUSSION AND CONCLUSIONS

The major contributions of this thesis are the development of an analytic model to describe the dynamics of a pantograph/catenary system, and the application of this model to predict, compare and improve the performance of different pantograph designs.

Simulation studies conducted with the model show that the mass and tension in the wires are very important since they determine the wave speed, while bending stiffness has a negligible effect. To improve the performance, the wave speed should be as high as possible (tension at a maximum, lineal density at a minimum). Increasing the wave speed allows displacements created by the pantograph to propagate faster and allows the wire to adopt a more uniform shape, avoiding the steep descent of the wires near the support towers. In addition, the dynamic performance of an equivalent copper and aluminum catenary were compared. The aluminum catenary showed a performance improvement with a 25% reduction in contact force variation (38% variation for aluminum vs. 51% for copper).

Pantograph design is also strongly influenced by mass; lighter pantographs perform better. Pantograph performance can also be improved by variations in the stiffness and damping elements. Using an industrial pantograph as a baseline, a performance improvement of 45% was obtained by incorporating zero stiffness in the pantograph head.

The performance of the baseline also improved with variation in the damping. A 21% improvement was obtained by increasing the damping ratio in the frame and head to 0.26 and 0.19, respectively.

This study provides several benefits to the field pantograph/catenary dynamics. It provides an accurate representation of a catenary and a good dynamic model which can be extended to analyze higher frequency vibration, and/or extended to investigate actively controlled pantographs. It provides an illustration and descriptive understanding of catenary dynamics and their influence on pantograph performance. Finally, it provides suggestions for future pantograph designs which will improve performance.

## REFERENCES

1. Boissonnade, Pierre, and Dupont, "SNCF Tests Collection Systems for Highspeeds," International Railway Journal, October, 1975
2. Boissonnade and Pierre, "Catenary Design for High Speeds," Rail International, March, 1975, pp 205-217
3. Boissonnade, Pierre, and Dupont, "Current Collection with Two-Stage Pantographs on the New Paris-Lyon Line," Railway Gazette International, October 1977
4. Gostling, R.J. and Hobbs, A.E.W., "The Interaction of Pantographs and Overhead Equipment: Practical Applications of a New Theoretical Method," paper presented at Institute of Mechanical Engineers, Derby Branch, February 1981
5. Coxen, D.J., Gostling, R.J. and Whitehead, K.M., "Evolution of a Simple High-Performance Pantograph," Railway Gazette, January 1980
6. Communications of the O.R.E., "Behavior of Pantographs and Overhead Equipment at Speeds Above 160 km/h," Rail International, January 1972
7. Belyaev, I.A., Vologine, V.A. and Freifeld, A.V., "Improvement of Pantographs and Catenaries and Method of Calculating Their Mutual Interactions at High Speeds," Rail International, June 1977, pp 309-328
8. Grey, R.T., "Test Results of General Electric-Faiveley Pantograph for High Speed Operation," Report prepared for U.S. Department of Transportation, Office of High Speed Ground Transportation, December 1967
9. Peters, John, "Dead Line Testing of the Faiveley Single and Dual Stage Pantographs on the RTT Catenary System," U.S. Department of Transportation Technical Report FRA/TCC-81/01
10. Vesely, G.C., "Modeling and Experimentation of Pantograph Dynamics," S.M. Thesis, Massachusetts Institute of Technology, 1983
11. Thomet, Michael, "Catenary and High Speed Power Collection," Joint ASME, IEEE Railroad Technical Conference, Conference Paper C76 458-5 IA, 1976
12. Sell, R.G., Prince, G.E. and Twine, D., "An Experimental Study of the Overhead Contact System for Electric Traction at 25 kV," Proceeding of the Institute of Mechanical Engineers, Britain, 1964-65

13. Morris, R.B., "Application of an Analogue Computer to a Problem of Pantograph and Overhead Line Dynamics," Proceedings of the Institute of Mechanical Engineers, Britain, 1964-65
14. Gilbert, G. and Davies, H.E.H., "Pantograph Motion on a Nearly Uniform Railway Overhead Line," Proceedings of the IEEE, Volume 113, pp 485, 1966
15. Abbott, M.R., "A Numerical Method for Calculating the Dynamic Behavior of a Simple Catenary Overhead Contact System for Electric Railway Traction," Royal Aircraft Establishment, Technical Report 67156, 1967
16. Levy, S., Bain, J.A. and Leclerc, E.J., "Railway Overhead Contact Systems, Catenary-Pantograph Dynamics for Power Collection at High Speeds," Journal of Engineering for Industry, ASME Paper 68-RR2, November 1968
17. Scott, P.R. and Rothman, M., "Computer Evaluation of Overhead Equipment for Electric Railroad Traction," IEEE Transactions on Industry Applications, Volume 1A-10, No. 5, September/October 1974
18. Willets, T.A. and Edwards, D.R., "Dynamic-Model Studies of Overhead Equipment for Electric Railway Traction - Part 1, Simple Catenary Equipment," Proceedings of the Institute of Electrical Engineers, Volume 113, April 1966, p. 690
19. Hobbs, A.E.W., "Accurate Prediction of Overhead Line Behavior," Railway Gazette International, September 1977, pp 3339-343
20. Thomas, A.G., "Aluminum Conductors in Transport Systems," Electrical Times, June 16, 1966, pp 889-891
21. Carlson, L.E. and Griggs, G.E., "Aluminum Catenary Quarterly Report," Prepared for the D.O.T., Contract Number DOT-FR-9154, February 1981
22. Biggs, J.M., "Introduction to Structural Dynamics," McGraw-Hill Book Company, New York, 1964
23. Clough, R.W. and Penzien, J., "Dynamics of Structures," McGraw-Hill Book Company, New York, 1975

## APPENDIX A

### CATENARY MODEL DEVELOPMENT

This appendix develops the equations of motion and the natural modes for a simple style, two wire catenary.

#### A.1 Modal Analysis Review

A system of  $n$  degrees of freedom has  $n$  natural modes. Associated with each mode is a natural frequency,  $\omega$ , and a natural mode shape,  $\phi$ . The mode shapes of a dynamic linear system are orthogonal and therefore system displacements can be expressed as a sum of the natural modes multiplied by appropriate, time-varying modal amplitudes, or modal response functions, a technique known as modal decomposition. [Ref. 22, 23]

$$y(x,t) = \sum \phi_i(x) z_i(t) \quad (A.1)$$

where

$y(x,t)$  = the time varying displacement of the system

$\phi_i(x)$  = the  $i$ th natural mode shape

$z_i(t)$  = the modal amplitude of the  $i$ th mode

$i$  = the mode number

The mode shape,  $\phi$ , depends only upon position; and the modal amplitude,  $z$ , depends only upon time. When a system is excited in a natural mode, the system and all the system elements, maintain the same relative displacements to each other, and the mode shape describes this relation. Once the mode shapes are known, the dynamics of the system are determined by the amplitudes,  $z(t)$ .

The benefit of separating the motion into modal components is the modes may be considered independently and the equations reduce to simple, linear, second order, differential equations of the form:

$$M_i \ddot{z}_i(t) + C_i \dot{z}_i(t) + K_i z_i = Q_i \quad (\text{A.2})$$

where

- $z_i$  = the  $i$ th modal amplitude
- $M_i$  = the modal mass of the  $i$ th mode
- $C_i$  = the modal damping of the  $i$ th mode
- $K_i$  = the modal stiffness of the  $i$ th mode
- $Q_i$  = the forcing function of the  $i$ th mode

The modal mass,  $M_i$ , is defined by

$$M_i = \int_0^{\ell} \rho \phi_i^2 dx \quad (\text{A.3})$$

where  $\rho$  is the the lineal density.

The modal damping is defined by equation (A.4) and must be distributed proportional to the mass to ensure orthogonality of the modes.

$$C_i = \int_0^{\ell} c(x) \phi_i^2 dx \quad (\text{A.4})$$

where  $c(x)$  is the damping (distributed proportional to mass)

The modal stiffness,  $K_i$ , is given by

$$K_i = \int_0^{\ell} k(x) \phi_i^2 dx \quad (\text{A.5})$$

where  $k(x)$  represents the spring constants and effective stiffnesses along the length.

The forcing function,  $Q_i$  is:

$$Q_i(t) = \int_0^l f(x,t) \phi_i dx \quad (A.6)$$

where  $f(x,t)$  is the applied force (time and position varying). The natural frequency of the system when vibrating in the  $i$ th mode is given by equation and follows from the natural frequency of a simple system as:

$$\omega_i = \sqrt{K_i/M_i} \quad (A.7)$$

An efficient way to express equation (A.2) is in terms of the natural frequency, the damping ratio and the modal mass as:

$$M_i \ddot{z}_i(t) + 2M_i \xi_i \omega_i \dot{z}_i(t) + M_i \omega_i^2 z_i(t) = Q_i \quad (A.8)$$

Once the mode shapes and frequencies are known, the time response of each mode is determined by equation (A.8) and the total system response is determined by applying equation (A.1) and summing up the individual responses.

## A.2 Catenary Model Description

The response of the catenary is determined by writing the displacement of each wire as a Fourier sine-series expansion. The equations of motion are derived using the amplitudes of the sine terms and Lagrange's method, and are used to obtain the natural frequencies and natural mode shapes of the catenary. Using these modes the equations for the catenary are written in modal form along with the equation for a pantograph model. These equations are solved

using a fourth-order Runge-Kutta numerical integration routine.

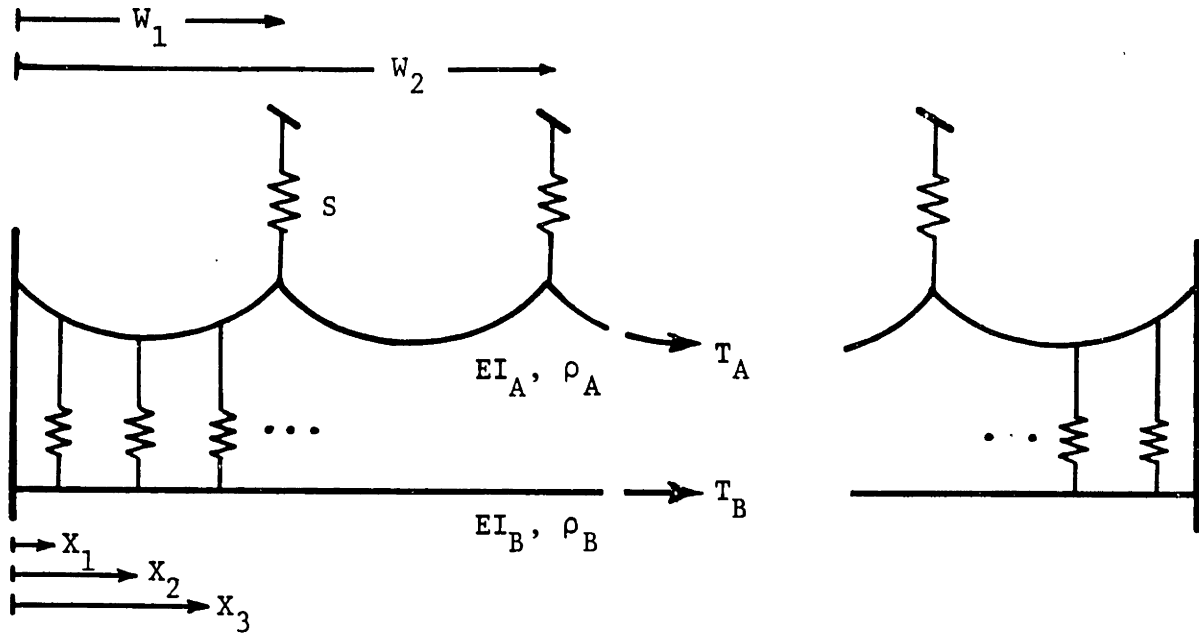
The model of the catenary is shown in Figure A.1, and incorporates the following features:

- Simple Catenary with a contact wire and a messenger wire.
- Variable spacing allowed between the towers and between the droppers.
- Contact and support wires are each modeled with a bending stiffness, constant tension, and a uniform density.
- Damping distributed proportional to the mass of the wires to ensure orthogonality of the modes.
- The two wires are connected by droppers. These are modeled as massless springs  $K_1$  through  $K_p$ .
- The mass of the droppers is not directly included but is modeled by distributing it evenly along, and equally between the two wires.
- The top wire is connected to flexible towers modeled as springs  $S_1$  through  $S_Q$ .
- The ends of both wires must have zero displacement but are allowed to have any angle

### A.3 Catenary Equation Development

Using Fourier analysis the shape of a finite length,  $L$ , can be represented in terms of a sum of both sine and cosine terms, each term with an appropriate amplitude. For the catenary, let  $y(x,t)$  describe the displacement of the catenary wire, both as a function of position,  $x$ , and of time,  $t$ . The boundary conditions require zero displacements of the two ends ( $x=0$  and  $x=L$ ); therefore no cosine terms may exist. The two wires, the contact and the support wire, are written separately and as functions of sine terms only as:





Tower Stiffness:  $S$   
 Dropper Stiffness:  $K$   
 Distance to the  $j$ th Tower:  $W_j$   
 Distance to the  $i$ th Dropper:  $X_i$   
 Stiffness of the Two Wires:  $EI_A, EI_B$   
 Density of the Two Wires:  $\rho_A, \rho_B$   
 Tension in the Two Wires:  $T_A, T_B$

FIGURE A.1: CATENARY MODEL

$$y_A(x,t) = \sum_m A_m(t) \sin\left(\frac{m\pi x}{L}\right) \quad \text{Upper Wire} \quad (\text{A.9a})$$

$$y_B(x,t) = \sum_m B_m(t) \sin\left(\frac{m\pi x}{L}\right) \quad \text{Lower Wire} \quad (\text{A.9b})$$

where

- $y_A$  = the displacement of the upper wire
- $y_B$  = the displacement of the lower wire
- $A_m$  = the amplitude of the mth sine term for the upper wire
- $B_m$  = the amplitude of the mth sine term for the lower wire
- $x$  = the distance along the catenary
- $L$  = the total length of the catenary
- $m$  = an integer. Designates the harmonic number.

The shape of these wires is time varying, therefore the amplitudes  $A_m$  and  $B_m$  are time varying and can be written  $A_m(t)$  and  $B_m(t)$ . Since they describe the shape of the whole catenary at all times the amplitudes can be used to write the equations of motion for the catenary, and obtain the natural modes of the catenary.

The catenary equations are developed using a Lagrange formulation. Each sine wave is an admissible motion, and the amplitudes provide a sufficient and convenient set of generalized coordinates.

To use Lagrange's method the expression for the kinetic coenergy<sup>+</sup> and the potential energy are written in terms of the generalized coordinates. The kinetic coenergy,  $T^*$ , for a lumped system is:

---

<sup>+</sup> For a linear system the kinetic coenergy equals the kinetic energy.

$$T^* = 1/2 Mv^2 \quad (A.10)$$

Or, for a continuous system

$$T^* = 1/2 \int_{x=0}^{\ell} \rho \dot{y}^2 dx \quad (A.11)$$

and for the two wires of the catenary:

$$T^* = 1/2 \int_0^{\ell} \rho_A \dot{y}_A^2 + \rho_B \dot{y}_B^2 dx \quad (A.12)$$

Differentiating equation (A.9) with respect to time yields:

$$\dot{y}_A = \sum_m \dot{A}_m \sin\left(\frac{m\pi x}{L}\right) \quad (A.13a)$$

$$\dot{y}_B = \sum_m \dot{B}_m \sin\left(\frac{m\pi x}{L}\right) \quad (A.13b)$$

Inserting these equations into Equation (A.12):

$$T^* = 1/2 \int_0^{\ell} \rho_A \left[ \sum_m \dot{A}_m \sin\left(\frac{m\pi x}{L}\right) \right]^2 + \rho_B \left[ \sum_m \dot{B}_m \sin\left(\frac{m\pi x}{L}\right) \right]^2 dx \quad (A.14)$$

Evaluating the integral gives the final result for the kinetic energy:

$$T^* = \frac{\rho_A L}{4} \sum \dot{A}_m^2 + \frac{\rho_B L}{4} \sum \dot{B}_m^2 \quad (A.15)$$

The potential energy of the system equals the sum of all the potential energies. They are: the tension in the wires, the bending of the wires, the displacement of the dropper springs, and the displacement

of the tower springs:

$$V = V_{\text{TEN}} + V_{\text{BEND}} + V_{\text{DROP}} + V_{\text{TOW}} \quad (\text{A.16})$$

where

$V$  = the total potential energy

$V_{\text{TEN}}$  = the potential energy due to the tension in wires

$V_{\text{BEND}}$  = the potential energy due to the bending stiffness

$V_{\text{DROP}}$  = the potential energy due to the dropper springs

$V_{\text{TOW}}$  = the potential energy due to the tower springs

In general the potential energy is the integral of force,  $f$ , and displacement,  $r$ .

$$V = \int_0^r f \cdot dr \quad (\text{A.17})$$

For the potential energy due to tension,  $V_{\text{TEN}}$  is the integral along the length of the cable of the incremental potential energy,

$$\delta V_{\text{TEN}}: \quad V_{\text{TEN}} = \int_0^l \delta V_{\text{TEN}} \quad (\text{A.18})$$

where

$$\delta V = \int_0^r f \cdot dr \quad (\text{A.19})$$

with the force in the same direction as the displacement. This force can be determined by investigating a free body diagram of an incremental length of cable,  $\delta x$ . Figure A.2 shows such a diagram. Looking at the free body diagram the tension is the same throughout, but the

direction of the vectors is different. The two vectors are:

$$T_1 = \frac{-T}{\sqrt{1 + \left(\frac{dy}{dx}\right)^2}} \left\{ \hat{i} + \frac{dy}{dx} \hat{j} \right\} \quad (\text{A.20})$$

$$T_2 = \frac{T}{\sqrt{1 + \left(\frac{dy}{dx} + \frac{d^2y}{dx^2} \delta x\right)^2}} \left\{ \hat{i} + \left(\frac{dy}{dx} + \frac{d^2y}{dx^2} \delta x\right) \hat{j} \right\} \quad (\text{A.21})$$

When the two vectors are summed the component in the y direction is:

$$f = T \frac{d^2y}{dx^2} \delta x + \text{higher order terms} \quad (\text{A.22})$$

The force,  $f$ , is the component of  $T_3$  in the y direction

$$f = T \frac{d^2y}{dx^2} \delta x \quad (\text{A.23})$$

Equating equation (A.19) becomes

$$V = \int_0^y T \frac{d^2y}{dx^2} \delta x \, dy \quad (\text{A.24})$$

$d$  and  $\delta$  are linear operators and commute, and

$$dy = \frac{dy}{dx} dx$$

Therefore equation (A.24) can be written:

$$\delta V = T \delta x \int_0^y \frac{d^2 y}{dx^2} \frac{dy}{dx} dx$$

Letting

$$u = \frac{dy}{dx} \quad du = \frac{d^2 y}{dx^2} dx \quad (A.25)$$

And then integrating leads to:

$$\delta V = T \frac{1}{2} \left( \frac{dy}{dx} \right)^2 \delta x \quad (A.26)$$

Plugging into equation (A.18) gives the desired expression for tension.

$$V_{TEN} = \frac{1}{2} T \int_0^L \left( \frac{dy}{dx} \right)^2 \delta x \quad (A.27)$$

The potential energy may now be evaluated using equation (A.9) for the displacement. Evaluating  $\frac{dy}{dx}$  and substituting for the top wire gives:

$$V_{TEN,A} = \frac{1}{2} T_A \int_0^L \left[ \sum_m \frac{m\pi}{L} A_m \cos\left(\frac{m\pi x}{L}\right) \right]^2 \delta x \quad (A.28)$$

Evaluating this integral

$$V_{TEN,A} = \frac{T_A \pi^2}{4L} \sum_m m^2 A_m^2 \quad (A.29)$$

Adding in the effect of the lower wire B, the final expression for the potential energy due to tension effects is obtained:

$$V_{TENS} = \frac{T_A \pi^2}{4L} \sum_m m^2 A_m^2 + \frac{T_B \pi^2}{4L} \sum_m m^2 B_m^2 \quad (A.30)$$

An expression for the potential energy due to the bending stiffness of the cable may be derived as:

$$V_{BEND} = \int_0^l \frac{M_b^2}{2EI} dx \quad (A.31)$$

where

- $M_b$  is the bending moment
- $E$  Young's Modular
- $I$  Area moment of inertia

From the mechanics of solids

$$M_b \approx \frac{\partial^2 y}{\partial x^2} EI \quad (A.32)$$

Plugging into equation (A.31) yields:

$$V_{BEND} = \int_0^l \frac{EI}{2} \left( \frac{\partial^2 y}{\partial x^2} \right)^2 dx \quad (A.33)$$

The second derivative of displacement is obtained from equation (A.9)

as:

$$\frac{d^2 y}{dx^2} = \sum_m -A_m \frac{m^2 \pi^2}{L^2} \sin\left(\frac{m\pi x}{L}\right) \quad (A.34)$$

Substituting equation (A.34) yields (for upper wire)

$$V_{\text{BEND},A} = \int_0^L \sum_m A_m \frac{m^2 \pi^2}{L^2} \sin\left(\frac{m\pi x}{L}\right) dx \quad (\text{A.35})$$

Evaluating the integral gives

$$V_{\text{BEND},A} = \frac{EI_A \pi^4}{4L^3} \sum_m m^4 A_m^2 \quad (\text{A.36})$$

Adding in the effect of the other wire, the final expression for the potential energy due to bending effects is obtained:

$$V_{\text{BEND}} = \frac{EI_A \pi^4}{4L^3} \sum_m m^4 A_m^2 + \frac{EI_B \pi^4}{4L^3} \sum_m m^4 B_m^2 \quad (\text{A.37})$$

The potential energy in the droppers and the towers must be evaluated. These elements are both modeled as linear springs. The potential energy for a linear spring is

$$V_{\text{SPR}} = 1/2 K \Delta^2 \quad (\text{A.38})$$

For the dropper springs  $\Delta$  represents the difference between the upper and lower wires.

$$\Delta = y_A - y_B \quad (\text{A.39})$$

The potential energy for the droppers must be evaluated at each dropper location  $x = X_1, X_2, \dots, X_p$

$$V_{\text{DROP}} = 1/2 \sum_{j=1}^P K_j (y_A - y_B)^2 \Big|_{x=X_j} \quad (\text{A.40})$$



Using equation (A.9) for the displacement, the potential energy for the dropper springs is

$$V_{\text{DROP}} = 1/2 \sum_{j=1}^P K_j \left[ \sum_m (A_m - B_m) \sin\left(\frac{m\pi X_j}{L}\right) \right]^2 \quad (\text{A.41})$$

The potential energy for the support springs is now evaluated, and must be done at each tower location  $x = W_1, W_2, \dots, W_Q$

$$V_{\text{TOW}} = 1/2 \sum_{j=1}^Q S_j y_A^2 \Big|_{x=W_j} \quad (\text{A.42})$$

where  $S_j$  = the stiffness of the  $j$ th tower

Substituting equation (A.9) for the displacement the potential energy of the support tower springs may be derived

$$V_{\text{TOW}} = 1/2 \sum_{j=1}^Q S_j \left[ \sum_m A_m \sin\left(\frac{m\pi W_j}{L}\right) \right]^2 \quad (\text{A.43})$$

Substituting equation (A.30), (A.37), (A.41), and (A.43) into equation (A.16) yields an expression for the total potential energy:

$$\begin{aligned} V_{\text{TOTAL}} = & \frac{T_A \pi^2}{4L} \sum_m m^2 A_m^2 + \frac{T_B \pi^2}{4L} \sum_m m^2 B_m^2 \\ & + \frac{EI_A}{4L^3} \pi^4 \sum_m m^4 A_m^2 + \frac{EI_B}{4L^3} \pi^4 \sum_m m^4 B_m^2 \\ & + 1/2 \sum_{j=1}^P K_j \left[ \sum_m (A_m - B_m) \sin\left(\frac{m\pi X_j}{L}\right) \right]^2 \\ & + 1/2 \sum_{j=1}^Q S_j \left[ \sum_m A_m \sin\left(\frac{m\pi W_j}{L}\right) \right]^2 \end{aligned} \quad (\text{A.44})$$

With the expression for the kinetic coenergy and the potential energy determined, written above in equation (A.15) and (A.44), Lagrange's method can be used to develop the equations of motion for the catenary. In order to determine the natural modes, it is only necessary to investigate the unforced homogeneous case (no input, no damping). For any admissible motion of the catenary Lagrange's equation must be satisfied:

$$\frac{d}{dt} \left( \frac{\partial L}{\partial \dot{\xi}} \right) - \frac{\partial L}{\partial \xi} = 0 \quad (\text{A.45})$$

where

$$L = T^* - V$$

$\xi$  = generalized coordinate

The generalized coordinates are  $A_m$  and  $B_m$ , the amplitude of the sine terms. Each sine wave (or combination of waves) is an admissible motion, therefore for each  $m$  Lagrange's equations must be satisfied.

$$\frac{d}{dt} \left( \frac{\partial L}{\partial \dot{A}_m} \right) - \frac{\partial L}{\partial A_m} = 0 \quad (\text{A.46a})$$

$$\frac{d}{dt} \left( \frac{\partial L}{\partial \dot{B}_m} \right) - \frac{\partial L}{\partial B_m} = 0 \quad (\text{A.46b})$$

Using equation (A.15). The first part of equation (A.46) can be evaluated

$$\frac{\partial L}{\partial \dot{A}_m} = 1/2 \rho_A L \dot{A}_m \quad (\text{A.47a})$$

$$\frac{\partial L}{\partial \dot{B}_m} = 1/2 \rho_B L \dot{B}_m \quad (\text{A.47b})$$

Taking the time derivative gives

$$\frac{d}{dt} \left( \frac{\partial L}{\partial \dot{A}_m} \right) = 1/2 \rho_A L \ddot{A}_m \quad (\text{A.48a})$$

$$\frac{d}{dt} \left( \frac{\partial L}{\partial \dot{B}_m} \right) = 1/2 \rho_B L \ddot{B}_m \quad (\text{A.48b})$$

The second half of equation (A.46) is evaluated using equation (A.44):

$$\begin{aligned} - \frac{\partial L}{\partial A_m} &= \frac{T_A \pi^2}{2L} m^2 A_m + \frac{EI_A \pi^4}{2L^3} m^4 A_m \\ &+ \sum_{j=1}^P K_j \sin\left(\frac{m\pi X_j}{L}\right) \sum_r (A_r - B_r) \sin\left(\frac{r\pi X_j}{L}\right) \\ &+ \sum_{j=1}^Q S_j \sin\left(\frac{m\pi W_j}{L}\right) \sum_r A_r \sin\left(\frac{r\pi W_j}{L}\right) \end{aligned} \quad (\text{A.49})$$

where r sums over the same range as m, i.e.,  $A_r = A_m$  for  $r = m$

Similarly:

$$-\frac{\partial L}{\partial B_m} = \frac{T_B \pi^2}{2L} m^2 B_m + \frac{EI_B \pi^4}{2L^3} m^4 B_m$$

$$- \sum_{j=1}^P K_j \sin\left(\frac{m\pi X_j}{L}\right) \sum_r (A_r - B_r) \sin\left(\frac{r\pi X_j}{L}\right) \quad (\text{A.50})$$

Lagrange's equation, equation (A.46a),

$$\frac{d}{dt} \left( \frac{\partial L}{\partial \dot{A}_m} \right) - \frac{\partial L}{\partial A_m} = 0 \quad (\text{A.46a})$$

can be written for each  $m$  as:

$$\left( \frac{\rho_A L}{2} \right) \ddot{A}_m + \left( \frac{T_A \pi^2 m^2}{2L} + \frac{EI_A \pi^4 m^4}{2L^3} \right) A_m$$

$$+ \sum_{j=1}^P K_j \sin\left(\frac{m\pi X_j}{L}\right) \sum_r (A_r - B_r) \sin\left(\frac{r\pi X_j}{L}\right)$$

$$+ \sum_{j=1}^Q S_j \sin\left(\frac{m\pi W_j}{L}\right) \sum_r A_r \sin\left(\frac{r\pi W_j}{L}\right) = 0 \quad (\text{A.51})$$

With a similar expression for  $B_m$

This equation is a function of the amplitudes and their second derivative and is of the form:

$$\alpha \ddot{A}_m + \beta A_m + \gamma = 0 \quad (\text{A.52})$$

where  $\gamma$  is a function of  $A_m$  and  $B_m$ .

Because the catenary model is a linear system it is free to vibrate in its natural mode(s). And, true for all linear systems, it has as many modes as degrees of freedom. In a natural mode the motion of the system will be harmonic (sinusoidal). Therefore, the amplitudes term  $A_m$  and  $B_m$  must also be harmonic, and:

$$\begin{aligned}\ddot{A}_m &= -\omega^2 A_m \\ \ddot{B}_m &= -\omega^2 B_m\end{aligned}\tag{A.53}$$

where

$\omega$  = the natural frequency of the mode

$m$  = the number of the sine term

Substitution equation (A.53) into equation (A.51) yields:

$$\begin{aligned}\omega^2 A_m &= \left( \frac{T_A \pi^2 m^2}{\rho_A L^2} + \frac{EI_A \pi^4 m^4}{\rho_A L^4} \right) A_m \\ &+ \frac{2}{\rho_A L} \sum_{j=1}^P \left[ K_j \sin\left(\frac{m\pi X_j}{L}\right) \sum_r (A_r - B_r) \sin\left(\frac{r\pi X_j}{L}\right) \right] \\ &+ \frac{2}{\rho_A L} \sum_{j=1}^Q \left[ S_j \sin\left(\frac{m\pi W_j}{L}\right) \sum_r A_r \sin\left(\frac{r\pi W_j}{L}\right) \right]\end{aligned}\tag{A.54}$$

$$\omega_{B_m}^2 = \frac{T_B \pi^2 m^2}{\rho_B L^2} + \frac{EI_B \pi^4 m^4}{\rho_B L^4} B_m$$

$$\frac{2}{\rho_B L} \sum_{j=1}^P \left[ K_j \sin\left(\frac{r\pi X_j}{L}\right) \sum_r (A_r - B_r) \sin\left(\frac{4\pi X_j}{L}\right) \right] \quad (A.55)$$

A double sum such as

$$\sum_{i=1}^I [R_i \times \sum_{j=1}^J S_j] \quad (A.56)$$

can be rewritten as

$$\sum_{j=1}^J [S_j \times \sum_{i=1}^I R_i] \quad (A.57)$$

Therefore we can rewrite equation (A.54) as:

$$\begin{aligned} \omega_{A_m}^2 = & \left( \frac{T_A \pi^2 m^2}{\rho_A L^2} + \frac{EI_A \pi^4 m^4}{\rho_A L^4} \right) A_m \\ & + \sum_r \left[ A_r \cdot \frac{2}{\rho_A L} \sum_{j=1}^P K_j \sin\left(\frac{m\pi X_j}{L}\right) \sin\left(\frac{r\pi X_j}{L}\right) \right] \\ & - \sum_r \left[ B_r \cdot \frac{2}{\rho_A L} \sum_{j=1}^P K_j \sin\left(\frac{m\pi X_j}{L}\right) \sin\left(\frac{r\pi X_j}{L}\right) \right] \\ & + \sum_r \left[ A_r \cdot \frac{2}{\rho_A L} \sum_{j=1}^Q S_j \sin\left(\frac{m\pi W_j}{L}\right) \sin\left(\frac{r\pi W_j}{L}\right) \right] \quad (A.58) \end{aligned}$$

which can be reduced further to:

$$\omega^2 A_m = \alpha(m) A_m + \sum_r A_r \sigma_{AA}(m,r) + \sum_r B_r \sigma_{AB}(m,r) \quad (\text{A.59})$$

where:

$$\alpha(m) = \frac{T_A \pi^2 m^2}{\rho_A L^2} + \frac{EI_A m^4}{\rho_A L^4}$$

$$\begin{aligned} \sigma_{AA}(m,r) = & \frac{2}{\rho_A L} \sum_{j=1}^P K_j \sin\left(\frac{m\pi X_j}{L}\right) \sin\left(\frac{r\pi X_j}{L}\right) \\ & + \sum_{j=1}^Q S_j \sin\left(\frac{m\pi W_j}{L}\right) \sin\left(\frac{r\pi W_j}{L}\right) \end{aligned}$$

$$\sigma_{BB}(m,r) = \frac{2}{\rho_B L} \sum_{j=1}^P \sin\left(\frac{m\pi X_j}{L}\right) \sin\left(\frac{r\pi X_j}{L}\right)$$

Similarly equation (A.55) can be written as:

$$\omega^2 B_m = \beta(m) B_m + \sum_r A_r \sigma_{BA}(m,r) + \sum_r B_r \sigma_{BB}(m,r) \quad (\text{A.60})$$

where:

$$\beta(m) = \frac{T_B \pi^2 m^2}{\rho_B L^2} + \frac{EI_B \pi^4 m^4}{\rho_B L^4} \quad (\text{A.61})$$

$$\sigma_{BA}(m,r) = -\frac{2}{\rho_B L} \sum_{j=1}^P K_j \sin\left(\frac{m\pi X_j}{L}\right) \sin\left(\frac{r\pi X_j}{L}\right)$$

$$\sigma_{BB}(m,r) = \frac{2}{\rho_B L} \sum_{j=1}^P K_j \sin\left(\frac{m\pi X_j}{L}\right) \sin\left(\frac{r\pi X_j}{L}\right)$$

Equations (A.59) and (A.60) can be written in matrix form

$$\omega^2 [I] \underbrace{\begin{bmatrix} A_1 \\ \vdots \\ A_m \\ B_1 \\ \vdots \\ B_M \end{bmatrix}}_{\Gamma} + \underbrace{\begin{bmatrix} \alpha(1) & & & & & \\ & \ddots & & & & \\ & & \alpha(m) & & & \\ & & & \beta(1) & & \\ & & & & \ddots & \\ & & & & & \beta(m) \end{bmatrix}}_{\Xi} \underbrace{\begin{bmatrix} A_1 \\ \vdots \\ A_m \\ B_1 \\ \vdots \\ B_m \end{bmatrix}}_{\Gamma} + \underbrace{\begin{bmatrix} & & & & & \\ & & & & & \\ \sigma_{AA} & & & & & \sigma_{AB} \\ & & & & & \\ \sigma_{BA} & & & & & \\ & & & & & \\ & & & & & \sigma_{BB} \end{bmatrix}}_{\Theta} \underbrace{\begin{bmatrix} A_1 \\ \vdots \\ A_m \\ B_1 \\ \vdots \\ B_m \end{bmatrix}}_{\Gamma} \tag{A.61}$$

Or as

$$\omega^2 [I] \Gamma = [\Xi + \Theta] \Gamma \tag{A.62}$$

Letting

$$H = [\Xi + \Theta] \tag{A.63}$$

The final form of the catenary equations is obtained:

$$\omega^2 I \Gamma = H \Gamma \tag{A.64}$$

The eigenvalues of the matrix H give the natural frequencies squared.

The eigenvalues are the same as finding the roots of the characteristic equation:

$$\text{DET}(\lambda I - H) = 0 \tag{A.65}$$

The eigenvector for each eigenvalue gives the set of amplitudes for each mode.



Denoting  $\lambda_i$  as the  $i$ th eigenvalue of the matrix, and  $\Gamma_{ij}$  as the  $j$ th element of the  $i$ th eigenvector we obtain

$$\omega_i = \sqrt{\lambda_i} \quad (\text{A.66})$$

The amplitudes are:

$$\begin{aligned} A_{im} &= \Gamma_{im} \\ B_{im} &= \Gamma_{i(m+M)} \end{aligned} \quad (\text{A.67})$$

The natural mode shapes are:

$$\phi_i = \sum_{m=1}^M A_{im} \sin\left(\frac{m\pi x}{L} A\right) + \sum_{m=1}^M B_{im} \sin\left(\frac{m\pi x}{L} B\right) \quad (\text{A.68})$$

where

$M$  = the maximum number of sine terms considered in the sum

There are  $2M$  natural modes resulting from this technique. Inspection of the modes shows approximately half in the lower frequency range and the other half in a much higher frequency range. The half in the high frequency range are not indicative of the true natural modes, but are a consequence of the solution technique using a finite number of sine terms. These higher modes should not be considered in the system response.

The above method determines the natural mode shapes. With the natural modes known, the response of the system is most effectively calculated using modal analysis. The response of each mode can be

found using equation (A.8)

$$M_i \ddot{z}_i(t) + 2M_i \xi_i \omega_i \dot{z}_i(t) + M_i \omega_i^2 z_i(t) = Q_i \quad (\text{A.8})$$

where

$z_i(t)$  = the  $i$ th modal response function or modal amplitude

$Q_i$  = the  $i$ th modal forcing function

$\omega_i$  = the  $i$ th natural frequency

$M_i$  = the  $i$ th modal mass (a scalar)

$\xi_i$  = the  $i$ th damping ratio

There will be  $N$  modal response equations, where  $N$  is the number of modes considered.

The displacement of the catenary as a function of time is given by the sum of the individual modal responses:

$$y(x,t) = \sum_{i=1}^N \phi_i(x) z_i(t) \quad (\text{A.1})$$

The coupling between the pantograph and the catenary comes from the modal forcing function,  $Q_i$ . The forcing function depends only upon the mode shape and the contact force. Any pantograph model can be used to obtain the contact force as the equations are developed independently of the catenary equations.

## APPENDIX B

### PANTOGRAPH/CATENARY INTERACTION

This appendix develops the equations of motion for the pantograph, shows the coupling of the pantograph equations with the natural modes of the catenary, and discusses the simulation technique for the response of the total system.

#### B.1 Pantograph Model

The pantograph model is shown in Figure B.1. The model is a two mass model with nonlinear suspension elements. It makes no attempt to model geometric nonlinearities or vibration of the pantograph's links. The model does, however, include the following features:

- Two mass pantograph model with a frame mass and a head mass.
- A constant force,  $F_o$ , to model the applied uplift force
- Stiffness of the contact strip is modeled by a linear spring,  $K_s$
- Stiffness of the suspension between the head and frame is modeled by a linear spring,  $K_h$
- A mechanical stop limiting the relative motion between the head and the frame is included
- Two types of damping elements between the head and the frame are modeled: linear damping, and one-way damping
- Stiffness of the suspension between the frame and the base is modeled by a linear spring,  $K_f$
- Two types of damping elements between the frame and the base are modeled: linear damping and one-way damping.

Before developing the full nonlinear equations, the equations for a simple linear model are investigated first. The equations for the linear pantograph may be easily derived, and using the displacement of the head mass and the displacement of the frame mass as coordinates the equations are:

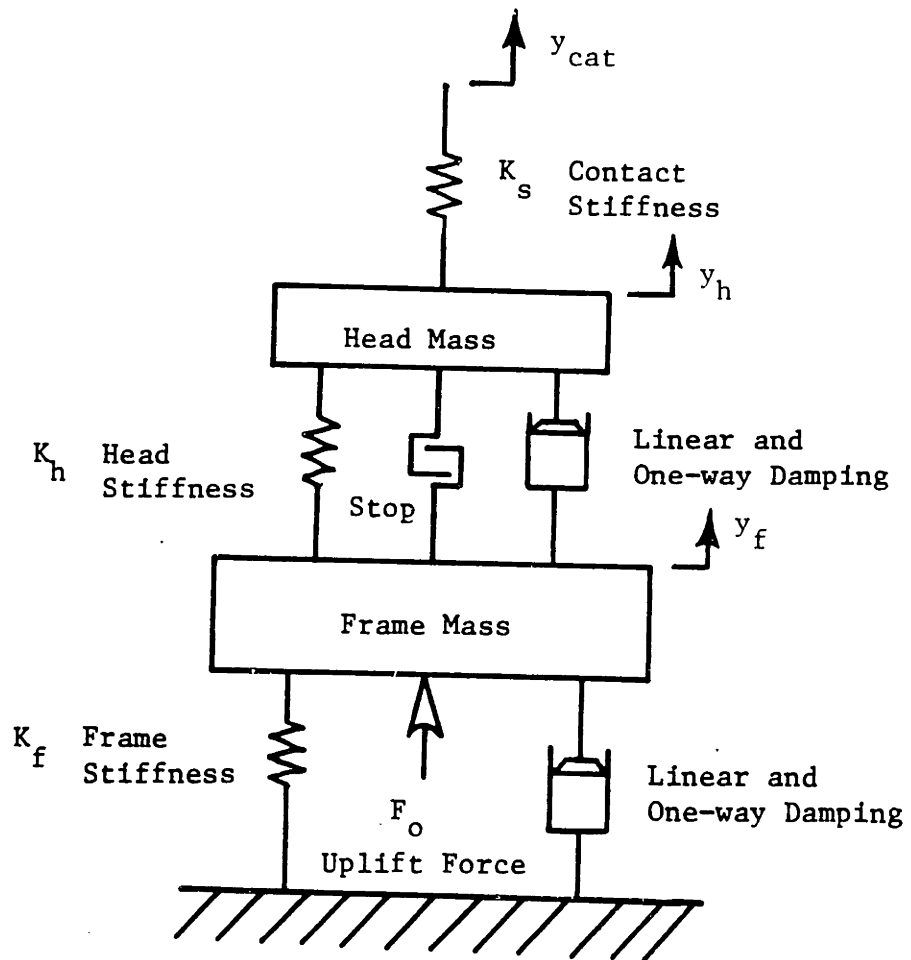


FIGURE B.1: PANTOGRAPH MODEL

$$M_h \ddot{y}_h + B_h (\dot{y}_h - \dot{y}_f) + K_h (y_h - y_f) = F_c \quad (\text{B.1})$$

$$M_f \ddot{y}_f + B_h (\dot{y}_f - \dot{y}_h) + B_f \dot{y}_f + K_h (y_f - y_h) + K_f y_f = 0 \quad (\text{B.2})$$

where

- $F_c$  = the dynamic contact force
- $y_h$  = the displacement of the head mass
- $y_f$  = the displacement of the frame mass
- $M_h$  = the head mass
- $M_f$  = the frame mass
- $B_h$  = the damping between the head and frame
- $B_f$  = the damping between the frame and base
- $K_h$  = the stiffness between the head and frame
- $K_f$  = the stiffness between the frame and base

The contact force,  $F_c$ , is determined from the interaction of the pantograph and catenary. The interaction is modeled by a spring with a stiffness typical of the flexure of the contact strips. Therefore the contact force is:

$$F_c = K_s (y_{\text{cat}} - y_h) + F_o \quad (\text{B.3})$$

where

- $y_{\text{cat}}$  = the displacement of the lower catenary wire
- $y_h$  = the displacement of the pantograph head
- $K_s$  = the stiffness of the contact strip
- $F_o$  = the static applied uplift force

When the pantograph loses contact with the catenary the contact force is set to zero and the two systems are considered separately until the pantograph regains contact.

The above provides the complete set of equations for the linear model; a full model is developed by including the effects of several nonlinear elements. To simulate these nonlinear elements the set of linear equations are augmented with the nonlinearities.

To limit the motion between the head and the frame a mechanical stop is included in the model. At each time step the distance between the head and frame is checked to ensure the stops have not been hit. If they have been the head and frame are constrained to move together until motion is reversed and the stops are freed.

One-way or unidirectional damping is also included in the full nonlinear model. This is not an element of any current pantograph, but it is included to assess its benefit for future pantograph. A one-way damper is a damper which resists motion in only one direction. In the simulation extra damping was added to the model whenever the velocity between the head and frame was negative (the head moving away from the wire). If the velocity was positive no extra damping was applied. The same relationship held for the one-way damper attached between the frame and base.

## B.2 Coupling Between the Models

The coupling between the pantograph and catenary comes exclusively through the contact force. When the pantograph is in contact with the catenary the motion of the pantograph head (more precisely, the top of the spring  $K_s$ ) and the lower catenary wire are identical, and the contact force has a non-zero value which is determined from their mutual interaction. When

the pantograph loses contact, the contact force becomes zero and the position of the pantograph and catenary are independent until the pantograph regains contact. Only during momentary losses of contact are the pantograph and catenary two separate systems. At all other times they are directly coupled: they share the same position and they share the same force.

The contact force enters the pantograph equations in equation B.1 as the variable  $F_c$ . It enters the catenary model equations as part of the modal forcing function. The relationship for the modal forcing function is given in Appendix A as equation A.6

$$Q_i(t) = \int_0^l f(x,t) \phi_i dx \quad (\text{Eqn A.6})$$

where

$Q_i(t)$  = the forcing function of the  $i$ th mode

$\phi_i$  = the mode shape of the  $i$ th mode

$f(x,t)$  = the applied force distribution (units of force/length)

There is a forcing function equation for each mode. Therefore at every time step the forcing function is calculated for each mode, and then using this forcing function each individual modal response is calculated from the second order differential equation in equation A.8.

Since the contact force is applied to the lower wire only the B terms of each mode need be considered. Equation A.6 therefore becomes:

$$Q_i = \int_0^l f(x,t) \sum_m B_{im} \sin\left(\frac{m\pi x}{L}\right) dx \quad (\text{B.4})$$

If the force is applied at a single point and moves with a velocity  $V$  the position of the applied force is  $Vt$ .

$$Q_i = F_c(t) \sum_m B_{im} \sin\left(\frac{m \pi Vt}{L}\right) \quad (\text{B.5})$$

where

$F_c(t)$  = the applied contact force (units of force)

This is easily generalized for multiple pantographs. For two pantographs the forcing function is:

$$Q_i = F_1 \sum_m B_{im} \sin\left(\frac{m \pi Vt}{L}\right) + F_2 \sum_m B_{im} \sin\left(\frac{m \pi (Vt - X_p)}{L}\right) \quad (\text{B.6})$$

where  $F_1$  = the contact force of the first pantograph

$F_2$  = the contact force of the second pantograph

$X_p$  = the distance between the first and second pantograph

### B.3 Simulation Technique

To simulate the dynamic response of the pantograph and catenary the equations of motion for both were solved simultaneously using a fourth order Runge Kutta integration technique. The catenary equations (N equations, where N equals the number of modes), the two pantograph equations (equations B.1 and B.2) and the nonlinear elements were written into Fortran code. The response of each modal amplitude,  $z$ , and the response of the pantograph is calculated at each time step. The position of the catenary wire at each instant is given by equation A.1 and summing up the individual modes. The time is then incremented and the process repeated until the final time of the simulation is reached. Figure B.2 summarizes the technique used in the dynamic simulation.



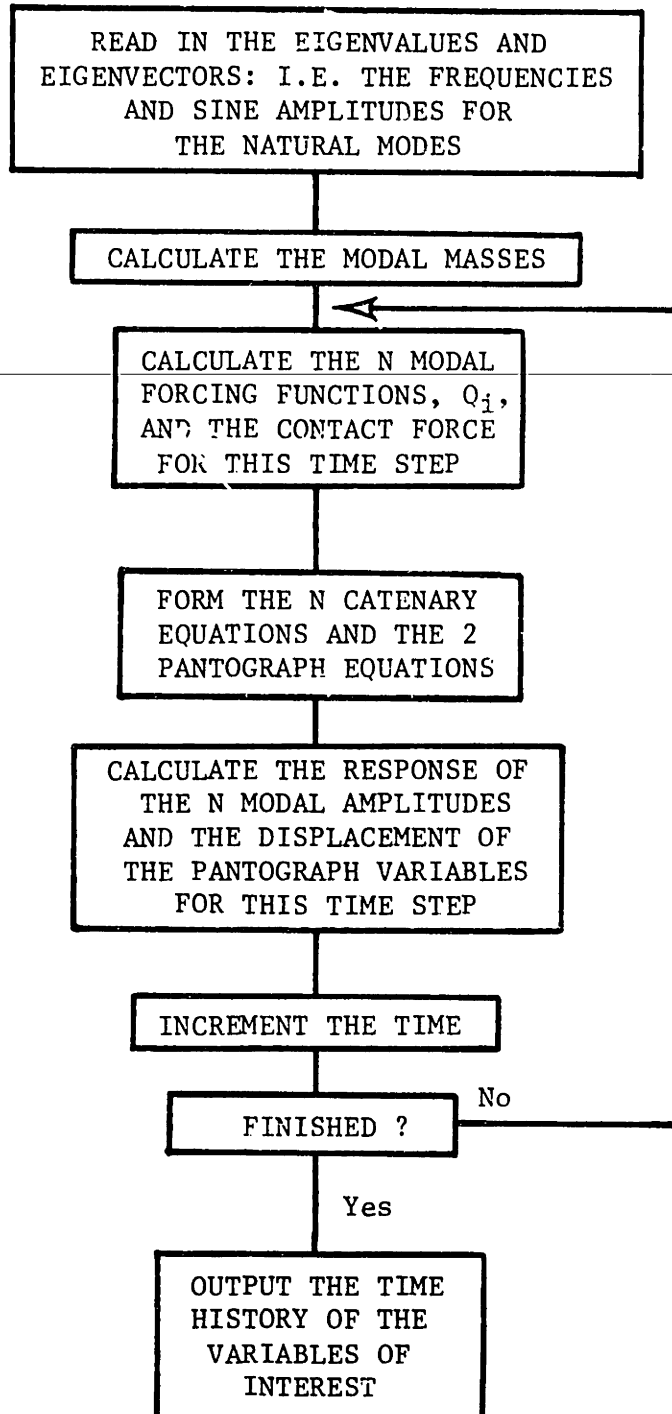


FIGURE B.2: FLOW CHART FOR THE DYNAMIC SIMULATIONS

APPENDIX C

- C.1 FORTRAN PROGRAM MODES.FOR
- C.2 FORTRAN PROGRAM PCAT.FOR

C KURT ARMBRUSTER  
 C MASTERS THESIS PROGRAM  
 C COPYRIGHT 1983, MASSACHUSETTS INSTITUTE OF TECHNOLOGY  
 C PROGRAM TO DETERMINE THE NATURAL MODES OF A SIMPLE STYLE CATENARY  
 C

REAL\*8 WNAT,WR,WI,EVECT  
 REAL\*8 SIGMA(41,42)  
 COMMON ALEN,NSPAN,NTOW,NDROP,TSPRING,DSPRING,TENSA,TENSB,  
 1RHOA,RHOB,EIA,EIB,MTERM,MTERM2,TSPACE(5),DSPACE(30),  
 2WNAT(41),WR(41),WI(41),EVECT(41,42)  
 CHARACTER\*10 NAME  
 PI=3.1415926536

C CCC

C ALEN = THE TOTAL LENGTH OF THE CATENARY  
 C ALPHA = THE DIAGONAL TERM IN THE XI MATRIX FOR  
 C WIRE A. REPRESENTS THE POTENTIAL ENERGY  
 C DUE TO THE TENSION AND THE BENDING STIFFNESS  
 C OF THE UPPER WIRE  
 C BETA = THE DIAGONAL TERM IN THE XI MATRIX FOR  
 C WIRE B. REPRESENTS THE POTENTIAL ENERGY  
 C DUE TO THE TENSION AND THE BENDING STIFFNESS  
 C OF THE LOWER WIRE  
 C DSPACE(J) = THE DISTANCE FROM THE ORIGIN TO THE  
 C J TH DROPPER  
 C DSPRING = THE SPRING CONSTANT OF THE DROPPERS  
 C EIA = THE BENDING STIFFNESS OF WIRE A  
 C EIB = THE BENDING STIFFNESS OF WIRE B  
 C JDROP = THE DROPPER NUMBER  
 C JTOW = THE TOWER NUMBER  
 C MTERM = THE MAXIMUM NUMBER OF SINE TERMS

```

C
C      MTERM2      =      CONSIDERED
C      NDROP       =      TWICE MTERM
C      NSPAN       =      THE TOTAL NUMBER OF DROPPERS
C      NTOW        =      THE NUMBER OF SPANS OF THE CATENARY
C      NTOW + 1    =      EQUALS NTOW + 1
C      NTOW        =      THE TOTAL NUMBER OF TOWERS
C      SIGMA       =      THE EQUATION MATRIX. THE EIGENVALUES
C      OF WHICH ARE WR AND WI, THE EIGENVECTORS
C      OF WHICH ARE THE MATRIX A.
C      RHOA        =      THE LINEAL DENSITY OF THE UPPER WIRE, WIRE A
C      RHOB        =      THE LINEAL DENSITY OF THE LOWER WIRE, WIRE B
C      TENSA       =      THE TENSION IN THE UPPER WIRE, WIRE A
C      TENS        =      THE TENSION IN THE LOWER WIRE, WIRE B
C      TSPACE(J)  =      THE DISTANCE FROM THE ORIGIN TO THE
C      J TH TOWER
C      TSPRING     =      THE SPRING CONSTANT OF THE TOWERS
C      WI(J)       =      THE IMAGINARY PART OF THE J TH
C      EIGENVALUE. SHOULD ALWAYS BE ZERO.
C      WR(J)       =      THE REAL PART OF THE J TH EIGENVALUE
C      WNAT(J)    =      THE NATURAL FREQUENCY OF MODE NUMBER
C      J. EQUALS THE SQUARE ROOT OF THE
C      EIGENVALUE WR(J)
C
CCCCCCCCCCCCCCCCCCCCCCCCCCCCCCCCCCCCCCCCCCCCCCCCCCCCCCCC
WRITE (6,700)
FORMAT('1')
TYPE*, THIS PROGRAM FINDS THE NATURAL FREQUENCIES AND NATURAL
TYPE*, MODES SHAPES FOR AN ARBITRARY CATENARY SYSTEM. IT FIRST
TYPE*, ASKS FOR THE PARAMETERS DESCRIBING THE CATENARY AND THEN
TYPE*, FINDS THE NATURAL FREQUENCIES AND THEN THE MODE SHAPES AS A
TYPE*, SUM OF SINE TERMS THROUGH THE USE OF AN EIGENVALUE SUBROUTINE.
WRITE(6,701)

```

```

700

```

```

701  FORMAT(1X,/)
      TYPE*, COMPUTE THE NATURAL MODES OF A NEW SYSTEM (ENTER 1)
      TYPE*, OR JUST PLOT THE MODES OF A PREVIOUS SYSTEM (ENTER 2)
      ACCEPT*,ANS
      IF (ANS.NE.1) GO TO 100
      CALL PRINT1
      TYPE*, INPUT THE PARAMETERS OF THE CATENATRY SYSTEM
      TYPE*, 1 = USE STANDARD PARAMETERS
      TYPE*, 2 = INPUT FROM THE KEYBOARD
      TYPE*,
      TYPE*, CHOICE ?
      ACCEPT*, ANS
      IF (ANS.EQ.1) THEN
          CALL STDPAR
      ELSEIF (ANS.EQ.2) THEN
          CALL INPUT
      ENDIF
      WRITE(6,701)
      TYPE*, INPUT THE NUMBER OF SIN TERMS FOR THE FOURIER SERIES (MAX = 20)
      ACCEPT*, MTERM
      MTERM2 = 2. * MTERM
C
C  READ IN THE LOCATION OF THE TOWERS AND DROPPERS
      CALL SPACE
C
C  FILL THE UPPER LEFT HAND QUADRANT OF THE SIGMA MATRIX
      DO 201 I=1,MTERM
      DO 202 J=1,MTERM
      IM=I
      JR=J
      SUM = 0.0
      DO 203 JDROP=1,NDROP
      SUM =SUM + DSPRING*SIN((IM*PI*DSPACE(JDROP)))/ALEN)

```

```

203 1 *SIN((JR*PI*DSPACE(JDROP)))/ALEN)
CONTINUE
DO 204 JTOW=1,NTOW
SUM = SUM + TSPRING*SIN((IM*PI*TSPACE(JTOW)))/ALEN)
204 1 *SIN((JR*PI*TSPACE(JTOW)))/ALEN)
CONTINUE
SIGMA(I,J) = (2./((RHOA*ALEN))*SUM
202 CONTINUE
201 CONTINUE
C
C FILL THE UPPER RIGHT HAND QUADRANT OF THE SIGMA MATRIX
DO 205 I=1,MTERM
DO 206 J= (MTERM+1), (2*MTERM)
IM = I
JR = J-MTERM
SUM=0.0
DO 207 JDROP=1,NDROP
SUM = SUM + DSPRING*SIN((IM*PI*DSPACE(JDROP)))/ALEN)
207 1 *SIN((JR*PI*DSPACE(JDROP)))/ALEN)
CONTINUE
SIGMA(I,J)=-2./((RHOA*ALEN))*SUM
206 CONTINUE
205 CONTINUE
C
C FILL THE LOWER LEFT HAND QUADRANT OF THE SIGMA MATRIX
DO 208 I= (MTERM+1), (2*MTERM)
DO 209 J=1,MTERM
IM = I - MTERM
JR = J
SUM = 0.0
DO 210 JDROP = 1,NDROP
SUM =SUM +DSPRING*SIN((IM*PI*DSPACE(JDROP)))/ALEN)
210 1 *SIN((JR*PI*DSPACE(JDROP)))/ALEN)

```

```

WRITE(6,700)
TYPE*, '----- PLOTTING SECTION -----'
WRITE(6,701)
TYPE*, ' THIS SECTION PLOTS THE MODE SHAPES OF THE CATENARY SYSTEM.
TYPE*, ' THE USER MUST BE LOGGED INTO A GRAPHICS TERMINAL, OTHERWISE THE
TYPE*, ' PLOTS WILL NOT APPEAR ON THE SCREEN. THE HARDCOPY PLOTS WILL
TYPE*, ' BE FOUND UNDER THE FILE NAME "HDCOPY.PLT"'
WRITE (6,701)
TYPE*, ' PLEASE INPUT THE FREQUENCY OF THE HIGHEST MODE YOU WANT
TYPE*, ' PLOTTED. FREQUENCY (IN HERTZ) = ?'
ACCEPT*, ANS
FREQMAX = ANS*6.2832
C
C READ IN THE EIGENVALUES OF THE SYSTEM
CALL READ
C PLOT THE MODE SHAPES
CALL PLOT1 (FREQMAX,MTERM,WNAT,EVECT)
END

SUBROUTINE PRINT1
C THIS SUBROUTINE PRINTS FOR THE USER'S INFORMATION
C THE SET OF DEFAULT PARAMETERS
WRITE(6,701)
FORMAT(1X,////, '----- STANDARD PARAMETERS -----',/)
TYPE*, ' TOTAL LENGTH = 228.6 m
TYPE*, ' NUMBER OF SPANS = 3
TYPE*, ' NUMBER OF DROPPERS = 18
TYPE*, ' STIFFNESS OF THE TOWERS = 17,506 kN/m
TYPE*, ' STIFFNESS OF THE DROPPERS = 43,766 kN/m
TYPE*, ' TENSION OF THE UPPER WIRE = 24,012 N

```

```

215 SIGMA(IM,IM) = SIGMA(IM,IM)+BETA
CONTINUE
C SIGMA IS NOW THE COMPLETE MATRIX ( DENOTED
C SIGMA + XI IN THE TEXT)
C
C FIND THE EIGENVALUES AND EIGENVECTORS OF THE SYSTEM
C SET THE PARAMETERS FOR THE EIGENVALUE SUBROUTINE
NMAX=41
IBALAN=1
IFORT=1
IVAL=1111
IVEC=1111
ISNGL=0
NAME=' '
NPRINT=0
CALL EISPAC (NMAX,MTERM2,IBALAN,IFORT,SIGMA,WR,WI,EVECT
1 ,IER,IVAL,IVEC,ISNGL,NAME,NPRINT,LU)
CALL ORDER(WR,WI,EVECT,MTERM2,NMA..)
C
C CALCULATE THE NATURAL FREQUENCIES: THE SQUARE
C ROOT OF THE EIGENVALUES
C DO 216 I=1,MTERM2
WNAT(I) = SQRT(WR(I))
CONTINUE
216
C
C PRINT OUT THE EIGENVALUES AND EIGENVECTORS OF THE SYSTEM
C I.E. THE FREQUENCY AND THE AMPLITUDES OF THE SINE TERMS
C FOR EACH NATURAL MODE
OPEN (6, NAME ='EVAL.DAT', STATUS='NEW')
CALL PRINT2
CLOSE (6)
C
C CONTINUE
100

```



```

210 CONTINUE
    SIGMA(I,J)=(-2./ (RHOB*ALEN))*SUM
209 CONTINUE
208 CONTINUE
    C
    C
    FILL THE LOWER RIGHT HAND QUADRANT OF THE SIGMA MATRIX
    DO 211 I=(MTERM+1), (2*MTERM)
    DO 212 J=(MTERM+1), (2*MTERM)
    IM=I-MTERM
    JR=J-MTERM
    SUM=0.0
    DO 213 JDROP=1,NDROP
    SUM = SUM + DSPRING*SIN((IM*PI*DSPACE(JDROP))/ALEN)
    1 *SIN((JR*PI*DSPACE(JDROP))/ALEN)
213 CONTINUE
    SIGMA(I,J)=(2./ (RHOB*ALEN))*SUM
212 CONTINUE
211 CONTINUE
    C
    C
    ADD THE DIAGONAL COMPONENTS (THE XI MATRIX IN THE TEXT)
    TO THE SIGMA MATRIX
    DO 214 IM = 1,MTERM
    FIM = FLOAT (IM)
    DUM1 = (TENSA/RHOA)*(PI*FIM/ALEN)**2
    DUM2 = (EIA/RHOA)*(PI*FIM/ALEN)**4
    ALPHA= DUM1 + DUM2
    SIGMA(IM,IM)=SIGMA(IM,IM) + ALPHA
    CONTINUE
214 DO 215 IM = (MTERM+1), (2*MTERM)
    FIM = FLOAT(IM - MTERM)
    DUM1 = (TENSB/RHOB)*(PI*FIM/ALEN)**2
    DUM2 = (EIB/RHOB)*(PI*FIM/ALEN)**4
    BETA = DUM1 + DUM2

```

```

TYPE*, TENSION OF THE LOWER WIRE = 28,014 N
TYPE*, LINEAR DENSITY OF THE UPPER WIRE = 1.7851 kg/m
TYPE*, LINEAR DENSITY OF THE LOWER WIRE = 2.3778 kg/m
TYPE*, BENDING STIFFNESS OF THE UPPER WIRE = 861.2 N m**2
TYPE*, BENDING STIFFNESS OF THE LOWER WIRE = 2,583.6 N m**2
WRITE(6,702)
FORMAT(1X,////)
RETURN
END

```

702

```

SUBROUTINE STDPAR
THIS SUBROUTINE SETS THE STANDARD, DEFAULT VALUES
FOR THE PARAMETERS OF THE CATENARY SYSTEM

```

C  
C  
C

```

REAL*8 WNAT,WR,WI,EVECT
COMMON ALEN,NSPAN,NTOW,NDROP,TSPRING,DSPRING,TENSA,TENSB,
1RHOA,RHOB,EIA,EIB,MTERM,MTERM2,TSPACE(5),DSPACE(30),
2WNAT(41),WR(41),WI(41),EVECT(41,42)

```

C

```

ALEN = 228.6
NSPAN =3
NTOW =2
NDROP =18
TSPRING = 17506300.
DSPRING = 43765750.
TENSA = 24012.
TENSB = 28014.
RHOA = 1.7851
RHOB = 2.3778
EIA = 861.2
EIB = 2583.6
RETURN

```

END

SUBROUTINE INPUT

C THIS SUBROUTINE IS CALLED FOR THE INPUT OF THE CATENARY  
C PARAMETERS UNLESS THE USER OPTS FOR THE STANDARD PARAMETERS  
C

REAL\*8 WNAT,WR, WI,EVECT  
COMMON ALEN,NSPAN,NTOW,NDROP,TSPRING,DSPRING,TENSA,TENSB,  
LRHOA,RHOB,EIA,EIB,MTERM,MTERM2,TSPACE(5),DSPACE(30),  
2WNAT(41),WR(41),WI(41),EVECT(41,42)

C

WRITE(6,701)

FORMAT(1X,///)

701

TYPE\*, TOTAL LENGTH (m) = ?

ACCEPT\*, ALEN = ?

TYPE\*, NUMBER OF SPANS = ?

ACCEPT\*, NSPAN = NSPAN - 1 = ?

TYPE\*, NUMBER OF DROPS = ?

ACCEPT\*, NDROP = ?

TYPE\*, STIFFNESS OF THE TOWERS (kN/m) = ?

ACCEPT\*, ANS = ?

TSPRING = ANS \* 1000.

TYPE\*, STIFFNESS OF THE DROPS (kN/m) = ?

ACCEPT\*, ANS = ?

DSPRING = ANS \* 1000.

TYPE\*, TENSION OF THE UPPER WIRE (N) = ?

ACCEPT\*, TENSA = ?

TYPE\*, TENSION OF THE LOWER WIRE (N) = ?

ACCEPT\*, TENS3 = ?

TYPE\*, LINEAR DENSITY OF THE UPPER WIRE (kg/m) = ?

ACCEPT\*, RHOA = ?

```

TYPE*, ' LINEAR DENSITY OF THE LOWER WIRE (kg/m) = ?'
ACCEPT*, RHOB
TYPE*, ' BENDING STIFFNESS OF THE UPPER WIRE (Nmm) = ?'
ACCEPT*, EIA
TYPE*, ' BENDING STIFFNESS OF THE LOWER WIRE (Nmm) = ?'
ACCEPT*, EIB
RETURN
END

```

```

SUBROUTINE PRINT2
C THIS SUBROUTINE PRINTS OUT THE RESULTS
C IT PRINTS OUT THE PARAMETERS OF THE CATENARY USED
C AND THEN THE SET OF NATURAL FREQUENCIES AND AMPLITUDES
C OF THE SINE TERMS (EIGENVALUES & EIGENVECTORS)

```

```

REAL*8 WNAT,WR, WI,EVECT
COMMON ALEN,NSPAN,NTOW,NDROP,TSPRING,DSPRING,TENSA,TENSB,
IRHOA,RHOB,EIA,EIB,MTERM,MTERM2,TSPACE(5),DSPACE(30),
2WNAT(41),WR(41),WI(41),EVECT(41,42)

```

```

C
C PRINT OUT THE PARAMETERS
WRITE(6,701) MTERM, ALEN, NSPAN, NDROP
701 FORMAT(' MTERM = ',I2,T25,'ALEN = ',1PE11.4,/,
1,' NSPAN = ',I2,T25,'NDROP = ',I2)
WRITE(6,702) TSPRING, DSPRING, TENSA, TENSB
702 FORMAT(' TSPRING = ',1PE11.4,T25'DSPRING = ',1PE11.4,/,
1,' TENSA = ',1PE11.4,T25,'TENSB = ',1PE11.4)
WRITE(6,703) RHOA, RHOB, EIA, EIB
703 FORMAT(' RHOA = ',1PE11.4,T25,'RHOB = ',1PE11.4,/,
1,' EIA = ',1PE11.4,T25,'EIB = ',1PE11.4)

```

```

C
C PRINT OUT THE NATURAL FREQUENCIES AND EIGENVALUES

```

```

704 WRITE(6,704)
    FORMAT(///~ THE NATURAL FREQUENCIES:~, T35,
1~ IN HERTZ:~, T70, ~ THE EIGENVALUES:~/)
    DO 201 J=1,MTERM2
    HRFREQ = WNAT(J)/6.283185308
    WRITE(6,705) WNAT(J),HRFREQ,WK(J)
705 FORMAT(1X,1PE16.8,T35,1PE16.8,T70,1PE16.8)
201 CONTINUE
    C
    C PRINT OUT THE EIGENVECTOR ASSOCIATED WITH EACH NATURAL
    C FREQUENCY. PRINT IN ROWS OF 6 TO CONSERVE SPACE.
    C I THE SINE TERM NUMBER
    C J = THE MODE NUMBER
    C
    DO 202 J=1,MTERM2,6
    WRITE(6,706)
    FORMAT(///~ NAT FREQ~,T20,~ NAT FREQ~,T40,~ NAT FREQ~,
1 T60,~ NAT FREQ~,T80,~ NAT FREQ~,T100,~ NAT FREQ~)
    WRITE(6,707) WNAT(J), WNAT(J+1), WNAT(J+2), WNAT(J+3),
1 WNAT(J+4), WNAT(J+5)
707 FORMAT(1X,1PE12.5,T20,1PE12.5,T40,1PE12.5,T60,1PE12.5,
1T80,1PE12.5,T100,1PE12.5)
    WRITE(6,708)
    FORMAT(/~ EIGENVECTOR~,T20,~ EIGENVECTOR~,T40,~ EIGENVECTOR~,
1T60,~ EIGENVECTOR~,T80,~ EIGENVECTOR~,T100,~ EIGENVECTOR~)
    DO 203 I=1,MTERM2
    WRITE(6,707) EVECT(I,J), EVECT(I,(J+1)), EVECT(I,(J+2))
    1,EVECT(I,(J+3)),EVECT(I,(J+4)), EVECT(I,(J+5))
203 CONTINUE
202 CONTINUE
    RETURN
    END
    C

```

```

SUBROUTINE READ
C THIS SUBROUTINE READS IN THE PARAMETERS AND EIGENVALUES
C OF A PREVIOUSLY COMPUTED CATENARY SYSTEM, AND IS CALLED
C WHEN THE MODE SHAPES ARE PLOTTED
C
REAL*8 WNAT,WR,WI,EVECT
COMMON ALEN,NSPAN,NTOW,NDROP,TSPRING,DSPRING,TENSA,TENSB,
1RHOA,RHOB,EIA,EIB,MTERM,MTERM2,TSPACE(5),DSPACE(30),
2WNAT(41),WR(41),WI(41),EVECT(41,42)
C
C FIRST READ IN PARAMETERS
OPEN (5, NAME='EVAL.DAT', STATUS='OLD')
READ (5,710) MTERM, ALEN
710 FORMAT (T11,I2,T34,1PE11.4)
READ (5,711) NSPAN,NDROP
711 FORMAT (T11,I2,T35,I2)
READ (5,712) TSPRING,DSPRING
712 FORMAT (T11,1PE11.4,T34,1PE11.4)
READ (5,712) TENSA, TENSB
READ (5,712) RHOA, RHOB
READ (5,712) EIA, EIB
MTERM2 = 2*MTERM
READ (5,713)
713 FORMAT (////)
C
C READ IN NATURAL FREQUENCIES
DO 216 J=1,MTERM2
READ (5,714) WNAT(J)
714 FORMAT(1X,1PE16.8)
216 CONTINUE
C
C READ IN EIGENVECTORS
DO 217 J=1,MTERM2,6

```

```

715 READ (5,715)
    FORMAT (////////)
    DO 218 I=1,MTERM2
716 READ (5,716) ERECT(I,J), ERECT(I,(J+1)), ERECT(I,(J+2))
    1,EVERT(I,(J+3)),EVERT(I,(J+4)), ERECT(I,(J+5))
    FORMAT (1X,1PE12.5,T20,1PE12.5,T40,1PE12.5,T60,1PE12.5,
    1 T80,1PE12.5,T100,1PE12.5)
218 CONTINUE
217 CONTINUE
    CLOSE (5)
    RETURN
    END
C
C SUBROUTINE PLOT1 (FREQMAX,MTERM,WNAT,EVERT)
C THIS SUBROUTINE PLOTS THE MODE SHAPES
C
    REAL*8 WNAT(41), ERECT(41,42)
    DIMENSION ARRAY(4,101), XSCL(4)
    INTEGER*4 LTYPE
    CHARACTER*40 XLABEL
    CHARACTER*7 HR
    CHARACTER*2 MNUM
    PI = 3.14159265359
C
C CCCCCCCCCCCCCCCCCCCCCCCCCCCCCCCCCCCCCCCCCCCCCCCCCCCCCCCCC
C ARRAY(I,J) CONTAINS THE POINTS TO BE PLOTTED. I IS
C THE CURVE NUMBER, J IS THE DISTANCE ALONG
C THE CURVE.
C I = 1 FOR THE TOP WIRE MODE SHAPE
C I = 2 FOR THE BOTTOM WIRE MODE SHAPE
C I = 3,4 FOR THE REFERENCE LINES
C XSCL SCALING FACTORS FOR THE PLOTTING SUBROUTINE

```

```

C   CCCCCCCCCCCCCCCCCCCCCCCCCCCCCCCCCCCCCCCCCCCCCCCCCCCCCCCCCCC
C   C   C   C   C   C   C   C   C   C   C   C   C   C   C   C   C   C   C   C   C   C   C   C
C   C   C   C   C   C   C   C   C   C   C   C   C   C   C   C   C   C   C   C   C   C   C   C
C   LOCATE THE HIGHEST MODE NUMBER CORRESPONDING TO THE
C   FREQUENCY RANGE OF INTEREST
C   DO 205 I=1,(2*MTERM)
C   IF (WNAT(I).GT.FREQMAX) GO TO 101
C   CONTINUE
205  I=I+1
C   CONTINUE
101  MODEMAX=I-1
C
C   DO 206 MODENUM = 1, MODEMAX
C   DO 207 ICLEAR =1,101
C   ARRAY(1,ICLEAR) = 0.0
C   ARRAY(2,ICLEAR) = 0.0
C   ARRAY(3,ICLEAR) = 0.0
C   ARRAY(4,ICLEAR) = 0.0
C   CONTINUE
207  ASCALE = .3
C   BSCALE = .3
C   OFFSET = 2.
C   DO 208 M = 1, MTERM
C   DO 209 I = 1, 101
C   II=I-1
C   MB = M + MTERM
C   ARRAY(1,I) = ARRAY(1,I) + ASCALE*EVECT(M,MODENUM)
C   1*SIN((M*PI*II)/100.)
C   ARRAY(2,I) = ARRAY(2,I) + BSCALE*EVECT(MB,MODENUM)
C   1*SIN((M*PI*II)/100.)
C   CONTINUE
209  CONTINUE
208  CONTINUE

```



```

C      DO 210 I=1,101
      ARRAY(1,I) = ARRAY(1,I) + OFFSET
      ARRAY(3,I) = OFFSET
      CONTINUE

      XSCL(1) = 0
      XSCL(2) = 1
      XSCL(3) = -1
      XSCL(4) = 4
      ISCL = -2
      LTYPE = 0
      CALL LINE(LTYPE)
      WRITE(MNUM,705) MODENUM
      FORMAT(I2)
705    HRTZ = WNAT(MODENUM)/6.2832
      WRITE(HR,706) HRTZ
      FORMAT(F7.3)
      XLABEL = 'MODE NUMBER '//MNUM//': '//HR//' HERTZ'
      MOVE = 01
      LABEL = 14
      CALL QPICTR(ARRAY, 4, 101, QY(1,2), QXLAB(XLABEL),
1,QMOVE(MOVE), QLABEL(LABEL), QISCL(ISCL), QXSCL(XSCL))
      LTYPE = 7
      CALL LINE(LTYPE)
      MOVE = 10
      LABEL = 10
      CALL QPICTR(ARRAY, 4, 101, QY(3,4), QMOVE(MOVE), QLABEL(LABEL)
1,QISCL(ISCL), QXSCL(XSCL))
      CONTINUE
      RETURN
      END

210
C
206

```

```

SUBROUTINE SPACE
C THIS SUBROUTINE READS IN THE LOCATION OF THE TOWERS (TSPACE)
C AND THE DROPPERS (DSPACE)
COMMON ALEN,NSPAN,NTOW,NDROP,TSPRING,DSPRING,TENSA,TENSB,
1RHOA,RHOB,EIA,EIB,MTERM,MTERM2,TSPACE(5),DSPACE(30),
2WNAT(41),WR(41),WI(41),EVECT(41,42)
C
OPEN (5, NAME='CAT.DAT', STATUS = 'OLD')
READ (5,700)
FORMAT (//)
DO 201 I =1,NTOW
700 READ(5,701) TSPACE(I)
701 FORMAT (F11.4)
201 CONTINUE
C
READ(5,702)
702 FORMAT(/)
DO 202 I=1,NDROP
202 READ (5,701) DSPACE(I)
CONTINUE
CLOSE (5)
RETURN
END

```

```

C
C KURT ARMBRUSTER
C MASTERS THESIS PROGRAM
C COPYRIGHT 1983, MASSACHUSETTS INSTITUTE OF TECHNOLOGY
C PROGRAM FOR THE DYNAMIC RESPONSE OF A CATENARY AND PANTOGRAPH
C
C
C REAL*8 WNAT, ERECT
C CHARACTER*40 HEADER
C COMMON /BLOCK1/ ALEN, NSPAN, NTOW, NDROP, TSPRING, DSPRING, TENSA, TENSB,
1 RHOA, RHOB, EIA, EIB, MTERM, MTERM2, WNAT(41), ERECT(41, 42)
C COMMON /BLOCK2/ T, DT, Z(50), DZ(50), NEWDT, NSYS
C COMMON /BLOCK3/ AMASS(41)
C COMMON /BLOCK4/ SHAPE(6, 101), RESP(5, 201), XPANT(5)
C COMMON /BLOCK5/ MODMAX
C COMMON /BLOCK6/ HEADER, YMIN, YMAX, FTIME, TINT2, VELOC, FUP, ZETA
1, STOPHI, STOPLO, AK1, AK2, B1, BIWAY, B2, B2WAY, AM1, AM2
C
C CCCCCCCCCCCCCCCCCCCCCCCCCCCCCCCCCCCCCCCCCCCCCCCCCCCCCCCCCCCCC
C AK1 = THE SPRING CONSTANT MODELING THE STIFFNESS
C OF THE SHOE, I.E. THE SPRING BETWEEN THE
C HEAD AND THE CATENARY WIRE
C AK2 = THE SPRING CONSTANT BETWEEN THE HEAD AND THE
C FRAME
C AK3 = THE SPRING CONSTANT BETWEEN THE FRAME AND THE
C TRAIN
C ALEN = THE TOTAL LENGTH OF THE CATENARY
C AM1 = THE HEAD MASS
C AM2 = THE FRAME MASS
C AMASS(J) = THE MODAL MASS OF THE JTH MODE
C B1 = THE DAMPING BETWEEN THE HEAD AND THE FRAME
C BIWAY = THE ONE WAY DAMPING BETWEEN THE HEAD AND THE
C FRAME. PROVIDES RESISTANCE ONLY TO DOWNWARDS
C MOVEMENT.
C

```

C B2 = THE DAMPING BETWEEN THE FRAME AND GROUND  
C B2WAY = THE ONE WAY DAMPING BETWEEN THE FRAME AND  
C GROUND. PROVIDES RESISTANCE ONLY TO DOWNWARDS  
C MOTION.  
C DSPRING = THE SPRING CONSTANT OF THE DROPPERS \*  
C DT = THE TIME STEP FOR THE SIMULATION  
C DZ = THE DERIVATIVE OF THE VARIABLE Z,  
C USED IN THE RUNGE KUTTA SIMULATION  
C EIA = THE BENDING STIFFNESS OF WIRE A \*  
C EVECT(I,J) = THE AMPLITUDE OF THE SINE TERMS IN THE  
C FOURIER SUM FOR THE NATURAL MODE SHAPES  
C J = THE MODE NUMBER  
C I = THE HARMONIC NUMBER  
C FTIME = THE FINAL TIME OF THE SIMULATION  
C FUP = THE NOMINAL UPLIFT FORCE  
C IRESP = THE DATA POINT NUMBER FOR THE RESPONSE  
C PLOTS. RANGES FROM 1 TO 201  
C ISHAPE = THE CURVE NUMBER FOR THE SHAPE PLOTS  
C RANGES FROM 1 TO 5. WHEN IT REACHES 5  
C SUBROUTINE PLOT1 IS CALLED AND THE 5  
C CURVES ARE PLOTTED AT ONCE  
C HEADER = LABEL FOR THE PLOTS  
C MODMAX = THE MAXIMUM NUMBER OF MODES TO BE CONSIDERED  
C IN THE SIMULATION  
C MTERM = THE MAXIMUM NUMBER OF SINE TERMS  
C CONSIDERED  
C MTERM2 = TWICE MTERM  
C NDROP = THE TOTAL NUMBER OF DROPPERS \*  
C NEWDT = THE VARIABLE SIGNIFYING A NEW TIME STEP.  
C EQUALS -1 ON THE INITIAL CALL; USED FOR  
C INITIALIZING PARAMETERS IN EQSIM.  
C EQUALS 1 FOR A NEW TIME STEP; ALLOWS  
C PARAMETERS TO BE CHANGE IN EQSIM.

C                   EQUALS 0 AT ALL OTHER TIMES.  
 C                   = THE NUMBER OF SPANS OF THE CATENARY  
 C                   EQUALS NTOW + 1 \*  
 C                   = THE TOTAL NUMBER OF TOWERS \*  
 C                   = THE ARRAY CONTAINING THE VARIABLES  
 C                   OF INTEREST FOR PLOTTING  
 C                   = THE LINEAL DENSITY OF THE UPPER WIRE \*  
 C                   = THE SHAPE OF THE CATENARY AT SPECIFIC  
 C                   INSTANTS IN TIME. I GIVES THE CURVE NUMBER  
 C                   (FROM 1 TO 5), J GIVES THE DISTANCE ALONG  
 C                   THE LENGTH OF THE CATENARY (FROM 1 TO 101)  
 C                   I = 6 GIVES THE TIME SCALE FOR THE PLOTS.  
 C                   = THE POSITION OF THE LOWER PANTOGRAPH HEAD STOP  
 C                   = THE POSITION OF THE UPPER PANTOGRAPH HEAD STOP  
 C                   = THE TIME IN THE SIMULATION. RANGES FROM  
 C                   0 TO FTIME  
 C                   = THE TENSION IN THE UPPER WIRE, WIRE A \*  
 C                   = TIME INTERVAL 1. GIVES THE TIME INTERVAL  
 C                   FOR THE RESPONSE PLOTS  
 C                   = TIME INTERVAL 2. GIVES THE TIME INTERVAL  
 C                   FOR THE SHAPE PLOTS  
 C                   = THE TIME SINCE THE LAST RESPONSE DATA POINT  
 C                   = THE TIME SINCE THE LAST SHAPE CALCULATION  
 C                   = THE SPRING CONSTANT OF THE TOWERS \*  
 C                   = THE VELOCITY OF THE TRAIN  
 C                   = THE NATURAL FREQUENCY OF MODE NUMBER  
 C                   J.  
 C                   = THE MAXIMUM Y VALUE FOR USE IN THE PLOTS  
 C                   = THE MINIMUM Y VALUE FOR USE IN THE PLOTS  
 C                   = THE VARIABLE USED FOR SOLVING THE DYNAMIC  
 C                   EQUATIONS: GIVES THE TIME RESPONSE OF THE MODAL  
 C                   AMPLITUDES AND THE DISPLACEMENT AND VELOCITY  
 C                   OF THE PANTOGRAPH MASSES.

```

C      ZETA      = THE DAMPING IN THE CATENARY. ASSUMED TO
C      BE THE SAME FOR EACH MODE.
C
C      NOTE: VARIABLES WITH AN ASTERISK (*) FOLLOWING THE DESCRIPTION
C      ARE NOT USED DIRECTLY IN THE PROGRAM, BUT ARE PARAMETERS OF THE
C      CATENARY USED. THEY ARE READ IN SO THEY ARE AVAILABLE IF NEEDED
C      FOR PRINTING HEADERS, ETC.
C      CCCCCCCCCCCCCCCCCCCCCCCCCCCCCCCCCCCCCCCCCCCCCCCCCCCCCCCCCC
C
C      READ IN THE PARAMETERS AND THE NATURAL MODES OF THE CATENARY
C      CALL READ1
C      READ IN THE PARAMETERS OF THE PANTOGRAPH
C      CALL READ2(DT)
C
C      IREF = 2*MODMAX
C      TINT1 = FTIME/201.
C      IRESP = 0
C      ISHAPE = 0
C
C      CALCULATE THE MODAL MASSES
C      CALL MASS
C
C      INITIALIZE EQSIM
C      NEWDT=-1
C      T=0.0
C      CALL EQSIM
C      T=0.0
C
C      CONTINUE
C      CALL RUNGEK
C      TRESP = TRESP + DT

```

```

C
C
C
C
C
C
C
C
C
C
C
TSHAPE = TSHAPE+DT
STORE THE VARIABLES OF INTEREST FOR PLOTTING
RESP(1, ) = THE TIME SCALE
RESP(2, ) = THE WIRE DISPLACEMENT
RESP(3, ) = THE PANT HEAD DISPLACEMENT
RESP(4, ) = THE PANT FRAME DISPLACEMENT
RESP(5, ) = THE CONTACT FORCE
IF (TRESP.GE.TINT1) THEN
  TRESP=TRESP-TINT1
  IRESP=IRESP+1
  RESP(1,IRESP) = T
  RESP(2,IRESP) = Z(IREF+1)
  RESP(3,IRESP) = Z(IREF+2)
  RESP(4,IRESP) = Z(IREF+4)
  RESP(5,IRESP) = Z(IREF+6)
ENDIF
CALCULATE THE POINTS FOR THE SHAPE OF THE CATENARY
IF (TSHAPE.GE.TINT2) THEN
  TSHAPE= TSHAPE - TINT2
  ISHAPE = ISHAPE +1
  CALL CSHAPE(ISHAPE)
  XPANT(ISHAPE) = VELOC*T
ENDIF
IF (T.GT.FTIME) GO TO 110
IF (ISHAPE.LT.5) GO TO 100
IF YOU HAVE MORE THAN 5 SHAPE CURVES PLOT THEM
CALL PLOT1(ISHAPE)

```

```

ISHAPE = 0
GO TO 100

110 CONTINUE
    CALL PLOT1(ISHAPE)
    CALL PLOT2(DT)
    END

C SUBROUTINE READ1
C THIS SUBROUTINE READS IN THE PARAMETERS AND NATURAL MODES
C OF THE CATENARY FROM THE DATA FILE 'EVAL.DAT'
REAL*8 WNAT, ETECT
COMMON /BLOCK1/ ALEN, NSPAN, NTOW, NDROP, TSPRING, DSPRING, TENSA, TENSBB,
1 RHOA, RHOB, EIA, EIB, MTERM, MTERM2, WNAT(41), ETECT(41, 42)
C
C OPEN (5, NAME='EVAL.DAT', STATUS='OLD')
C READ (5,710) MTERM, ALEN
710 FORMAT (T11, I2, T34, 1PE11.4)
C READ (5,711) NSPAN, NDROP
711 FORMAT (T11, I2, T34, I2)
C READ (5,712) TSPRING, DSPRING
712 FORMAT (T11, 1PE11.4, T34, 1PE11.4)
C READ (5,712) TENSA, TENSBB
C READ (5,712) RHOA, RHOB
C READ (5,712) EIA, EIB
C MTERM2 = 2*MTERM
C READ (5,713)
713 FORMAT (////)
C
C DO 216 J=1, MTERM2

```



```

714 READ (5,714) WNAT(J)
216 FORMAT(1X,1PE16.8)
CONTINUE
DO 217 J=1,MTERM2,6
READ (5,715)
FORMAT (////////)
DO 218 I=1,MTERM2
READ (5,716) EVECT(I,J), EVECT(I,(J+1)), EVECT(I,(J+2)),
1 EVECT(I,(J+3)), EVECT(I,(J+4)), EVECT(I,(J+5))
716 FORMAT (1X,1PE12.5,T20,1PE12.5,T40,1PE12.5,T60,1PE12.5,
1 T80,1PE12.5,T100,1PE12.5)
CONTINUE
218 CONTINUE
217 CONTINUE
CLOSE (5)
RETURN
END

SUBROUTINE READ2(DT)
CHARACTER *40 HEADER
COMMON /BLOCK5/ MODMAX
COMMON /BLOCK6/ HEADER, YMIN, YMAX, FTIME, TINT2, VELOC, FUP, ZETA
1, STOPHI, STOPLO, AK1, AK2, B1, BIWAY, B2, B2WAY, AM1, AM2
OPEN (5, NAME='PANT.DAT', STATUS='OLD')
READ (5,700)
FORMAT(/)
700 READ(5,701) HEADER
701 FORMAT (A40)
READ(5,702) YMIN
702 READ(5,702) YMAX
FORMAT(T18,F13.6)
703 READ(5,703) MODMAX
FORMAT(T18,I2)

```

```

READ(5,702) FTIME
READ(5,702) DT
READ(5,702) TINT2
READ(5,702) VELOC
READ(5,702) FUP
READ(5,702) ZETA
READ(5,702) STOPHI
READ(5,702) STOPLO
READ(5,702) AK1
READ(5,702) AK2
READ(5,702) AK3
READ(5,702) B1
READ(5,702) B1WAY
READ(5,702) B2
READ(5,702) B2WAY
READ(5,702) AM1
READ(5,702) AM2
CLOSE(5)
RETURN
END

```

```

SUBROUTINE MASS
SUBROUTINE TO CALCULATE THE MODAL MASSES

```

C C

```

REAL*8 WNAT, ETECT
COMMON /BLOCK1/ ALEN,NSPAN,NTOW,NDROP,TSRING,DSPRING,TENSA,TENSB,
1 RHOA,RHOB,EIA,EIB,MTERM,MTERM2,WNAT(41),ETECT(41,42)
COMMON /BLOCK3/ AMASS(41)
COMMON /BLOCK5/ MODMAX

```

C

```

DO 201 J = 1,MODMAX
SUM1 = 0.0

```

```

SUM2 = 0.0
DO 202 I= 1, MTERM
  IB = I + MTERM
  SUM1 = SUM1 + (EVECT(I, J))**2
  SUM2 = SUM2 + (EVECT(IB, J))**2
CONTINUE
202
AMASS(J) = (ALEN/2.0)*(RHOA*SUM1 + RHOB*SUM2)
CONTINUE
201
RETURN
END

SUBROUTINE EQSIM
EQUATION SIMULATOR SUBROUTINE
C
C
REAL*8 WNAT, EVECT
CHARACTER *40 HEADER
COMMON /BLOCK1/ ALEN, NSPAN, NTOW, NDROP, TSPRING, DSPRING, TENSA, TENSB,
1 RHOA, RHOB, EIA, EIB, MTERM, MTERM2, WNAT(41), EVECT(41, 42)
COMMON /BLOCK2/ T, DT, Z(50), DZ(50), NEWDT, NSYS
COMMON /BLOCK3/ AMASS(41)
COMMON /BLOCK5/ MODMAX
COMMON /BLOCK6/ HEADER, YMIN, YMAX, FTIME, TINT2, VELOC, FUP, ZETA
1, STOPHI, STOPLO, AK1, AK2, B1, B1WAY, B2, B2WAY, AM1, AM2
DIMENSION DISPL(41)
PI = 3.14159265359
CCCCCCCCCCCCCCCCCCCCCCCCCCCCCCCCCCCCCCCCCCCCCCCCCCCCCCCCCCCC
C
DISPL(J) = THE DISPLACEMENT DUE TO MODE J
IREF = THE TOTAL NUMBER OF TERMS USED FOR THE MODAL RESPONSE
YB = THE FULL DISPLACEMENT OF THE LOWER WIRE
Z(IREF+1) = DISPLACEMENT OF THE LOWER WIRE (AVAILABLE TO THE
C MAIN PROGRAM)
C

```

```

C      Z(IREF+2) = DISPLACEMENT OF THE PANTOGRAPH HEAD MASS
C      Z(IREF+3) = VELOCITY OF THE PANTOGRAPH HEAD
C      Z(IREF+4) = DISPLACEMENT OF THE PANTOGRAPH FRAME MASS
C      Z(IREF+5) = VELOCITY OF THE PANTOGRAPH FRAME
C      Z(IREF+6) = THE CONTACT FORCE
C
C      CCCCCCCCCCCCCCCCCCCCCCCCCCCCCCCCCCCCCCCCCCCCCCCCCCCCCCCCC
C
C      IF(NEWDT) 101, 102, 103
C
C      GOES HERE ON INITIALIZATION, NEWDT = -1
101    CONTINUE
        FORCE = FUP
C
C      GOES HERE AT EACH NEW TIME STEP, NEWDT = 1
103    CONTINUE
C
C      GOES HERE ALWAYS, NEWDT = 0
102    CONTINUE
C      CALCULATE THE DISPLACEMENT OF THE LOWER WIRE FOR EACH MODE
        DO 201 J = 1, MODMAX
          DISPL(J) = 0.0
          CONTINUE
        DO 202 J = 1,MODMAX
        DO 203 I = 1,MTERM
          IB = I+ MTERM
          DISPL(J) = DISPL(J) + ERECT(IB,J)*SIN((I*PI*VELOC*T)/ALEN)
          CONTINUE
        CONTINUE
201
203
202
C      FIND MODAL AMPLITUDES, Z(J)
C      YB = 0.0

```

```

DO 210 J=1,MODMAX
JA = J*2 - 1
JB = J*2
DZ(JA) = Z(JB)
DZ(JB) = FORCE*(DISPL(J)/AMASS(J)) - 2*ZETA*WNAT(J)*Z(JB) -
1      (WNAT(J)**2)*Z(JA)
C
C THE DISPLACEMENT OF THE LOWER WIRE EQUALS THE DISPLACEMENT
C OF EACH MODE TIMES THE AMPLITUDE OF THAT MODE
YB = YB + Z(JA)*DISPL(J)
C
CONTINUE
210
C CALCULATE THE PANTOGRAPH STATE VARIABLES
IREF = 2*MODMAX
FORCE = AK1*(Z(IREF+2) - YB) + FUP
IF (FORCE.LT.0.0) FORCE = 0.0
C
C FIRST CHECK IF THE HEAD HAS HIT THE STOPS
IF ((Z(IREF+2)-Z(IREF+4)).GT.STOPHI)
1   Z(IREF+2) = STOPHI + Z(IREF+4)
IF ((Z(IREF+2)-Z(IREF+4)).LT.STOPLO)
1   Z(IREF+2) = STOPLO + Z(IREF+4)
C
C BLOCK FOR ALL MOTION
Z(IREF+1) = YB
DZ(IREF+2) = Z(IREF+3)
DZ(IREF+3) = -(B1*(Z(IREF+3) - Z(IREF+5)) + FORCE - FUP
1   + AK2*(Z(IREF+2)-Z(IREF+4)))/AM1
DZ(IREF+4) = Z(IREF+5)
DZ(IREF+5) = -( B1*(Z(IREF+5)-Z(IREF+3)) + B2*(IREF+5)
1   + AK2*(Z(IREF+4)-Z(IREF+2))
2   + AK3*(Z(IREF+4))/AM2
Z(IREF+6) = FORCE

```

```

C
C IF HEAD TO FRAME VELOCITY IS NEGATIVE (DOWNWARDS)
C ADD ONE-WAY HEAD DAMPING
C IF ((Z(IREF+3) - Z(IREF+5)).LT. 0.0) THEN
DZ(IREF+3) = -((B1+B1WAY)*Z(IREF+3) - Z(IREF+5)) + FORCE
1 - FUP + AK2*(Z(IREF+2)-Z(IREF+4))/AM1
DZ(IREF+5) = -( (B1+B1WAY)*(Z(IREF+5)-Z(IREF+3)) + B2*Z(IREF+5)
1 + AK2*(Z(IREF+4)-Z(IREF+2))
2 + AK3*Z(IREF+4))/AM2
ENDIF
C
C IF FRAME VELOCITY IS NEGATIVE ADD ONE-WAY FRAME DAMPING
C IF (Z(IREF+5).LT. 0.0) THEN
DZ(IREF+5) = -( (B1+B1WAY)*(Z(IREF+5)-Z(IREF+3)) + (B2+B2WAY)
1 *Z(IREF+5) + AK2*(Z(IREF+4)-Z(IREF+2))
2 + AK3*Z(IREF+4))/AM2
ENDIF
C
C RETURN
C END
C
C SUBROUTINE RUNGEK
C THIS SUBROUTINE IS A STANDARD FOURTH ORDER RUNGE
C KUTTA INTEGRATION SUBROUTINE
C
COMMON /BLOCK2/ T,DT,Z(50),DZ(50),NEWDT,NSYS
COMMON /BLOCK5/ MODMAX
DIMENSION Z0(50), DZ0(50), DZ1(50), DZ2(50)
NEWDT =0
DIT = DT/2.0
NSYS = 2*MODMAX+6
C

```

```

DO 10 I =1, NSYS
Z0(I) = Z(I)
DZ0(I) = DZ(I)
Z(I) = Z(I) + DZ(I)*DIT
CONTINUE
10
C
T=T+DIT
CALL EQSIM
DO 20 I=1, NSYS
DZ1(I) = DZ(I)
Z(I) = Z0(I) + DZ(I)*DIT
CONTINUE
20
C
CALL EQSIM
DO 30 I=1, NSYS
DZ2(I)=DZ(I)
Z(I)=Z0(I) + DZ(I)*DT
CONTINUE
30
C
T= T +DT
CALL EQSIM
DO 40 I=1, NSYS
Z(I)=Z0(I)+((DZ0(I)+2.*DZ1(I)+2.*DZ2(I)+DZ(I))/6.0)*DT
CONTINUE
NEWDT = 1
CALL EQSIM
RETURN
END
40

```

```

SUBROUTINE CSHAPE(ISHAPE)
THIS SUBROUTINE CALCULATES THE SHAPE OF THE ENTIRE CATENARY
AT A SPECIFIC INSTANT IN TIME
C
C

```

```

C
REAL*8 WNAT, EVECT
COMMON /BLOCK1/ ALEN, NSPAN, NTOW, NDRUP, TSPRING, DSPRING, TENSA, TENSB,
1  RHOA, RHOB, EIA, EIB, MTERM, MTERM2, WNAT(41), EVECT(41, 42)
COMMON /BLOCK2/ T, DT, Z(50), DZ(50), NEWDT, NSYS
COMMON /BLOCK4/ SHAPE(6, 101), RESP(5, 201), XPANT(5)
COMMON /BLOCK5/ MODMAX
PI = 3.1415926536
C
CCCCCCCCCCCCCCCCCCCCCCCCCCCCCCCCCCCCCCCCCCCCCCCCCCCCCCCCCCCC
C
C   AMODE = THE DISPLACEMENT OF THE CATENARY AT EACH MODE
C   IDIST = THE DISTANCE ALONG THE CATENARY
C
CCCCCCCCCCCCCCCCCCCCCCCCCCCCCCCCCCCCCCCCCCCCCCCCCCCCCCCCCCCC
C
DO 201 IDIST = 1, 101
DO 202 J = 1, MODMAX
JA = 2*J - 1
AMODE = 0.0
DO 203 I = 1, MTERM
IB = I + MTERM
AMODE = AMODE + EVECT(IB, J)*SIN((I*PI*(IDIST-1))/100.)
CONTINUE
SHAPE(ISHAPE, IDIST) = SHAPE(ISHAPE, IDIST) + Z(JA)*AMODE
CONTINUE
CONTINUE
RETURN
END
203
202
201
SUBROUTINE PLOT1 (ISHAPE)
REAL*8 WNAT, EVECT

```



```

CHARACTER *40 HEADER
COMMON /BLOCK1/ ALEN, NSPAN, NTOW, NDROP, TSPRING, DSPRING, TENSA, TENS,
1   RHOA, RHOB, EIA, EIB, MTERM, MTERM2, WNAT(41), ERECT(41, 42)
COMMON /BLOCK4/ SHAPE(6, 101), RESP(5, 201), XPANT(5)
COMMON /BLOCK6/ HEADER, YMIN, YMAX, FTIME, TINT2, VELOC, FUP, ZETA
1, STOPHI, STOPLO, AK1, AK2, B1, B1WAY, B2, B2WAY, AM1, AM2

CHARACTER*40 XLABEL
CHARACTER*40 YLABEL
CHARACTER*6 WORD1
CHARACTER*5 WORD2
DIMENSION XSCL(4)
DIMENSION YLINES(10, 2)
INTEGER*2 IXPLOTT(16)

DO 201 I = 1, 101
SHAPE(6, I) = FLOAT(I-1)*(ALEN/100.)
CONTINUE
201
C
C
CONVERT FORM METERS TO CENTIMETERS
DO 202 J = 1, 5
DO 203 I = 1, 101
SHAPE(J, I) = SHAPE(J, I)*100.
CONTINUE
202
C
WRITE(WORD1, 710) VELOC
WRITE(WORD2, 711) TINT2
FORMAT(F6.1)
FORMAT(F5.3)
XLABEL = 'CATENARY SHAPE'
YLABEL = '//WORD1//' DELTA T = '//WORD2
710
711

```

```

MOVE = 01
LABEL = 14
ISCL = -2
XSCL(1) = 0
XSCL(2) = ALEN

XSCL(3) = YMIN
XSCL(4) = YMAX

C
CALL QPICTR(SHAPE,6,100,QY(1,2,3,4,5),QX(6),QMOVE(MOVE),QLABEL(LABEL),
1QISCL(ISCL),QXSCL(XSCL),QXLAB(XLAB),QYLAB(YLAB))

C
DO 225 I = 1,5
IM = I + 5
YLINES(I,1) = -2.
YLINES(I,2) = -.5
YLINES(IM,1) = XPANT(I)
YLINES(IM,2) = XPANT(I)
CONTINUE
225
C
NROW = 10
NVAR = 5
NPTS = 2
NX = -1
MOVE = 10
LABEL = 10
IXPLOT(1) = 6
IXPLOT(2) = 7
IXPLOT(3) = 8
IXPLOT(4) = 9
IXPLOT(5) = 10

C
CALL PICTR (YLINES,NROW,XLAB,XSCL,NVAR,NPTS,NX,MOVE,

```

```

1 LABEL, ISCL, FTIME, LOOK, IXPLOTT)
C
DO 204 JCLEAR = 1,5
XPANT(JCLEAR) = 0.0
DO 205 ICLEAR= 1,101
SHAPE(JCLEAR, ICLEAR) = 0.0
CONTINUE
CONTINUE
205
204
C
RETURN
END
SUBROUTINE PLOT2(DT)
REAL*8 WNAT, ETECT
CHARACTER *40 HEADER
COMMON /BLOCK1/ ALEN, NSPAN, NTOW, NDROP, TSPRING, DSPRING, TENSA, TENSBB,
1 RHOA, RHOB, EIA, EIB, MTERM, MTERM2, WNAT(41), ETECT(41, 42)
COMMON /BLOCK4/ SHAPE(6, 101), RESP(5, 201), XPANT(5)
COMMON /BLOCK6/ HEADER, YMIN, YMAX, FTIME, TINT2, VELOC, FUP, ZETA
1, STOPHI, STOPLO, AK1, AK2, B1, BIWAY, B2, B2WAY, AM1, AM2
C
CHARACTER*40 XLABEL
CHARACTER*40 YLABEL
DIMENSION XSCL(4)
710 FORMAT(F7.0)
711 FORMAT(F7.4)
YLABEL = HEADER
C
CHANGE FROM METERS TO CENTIMETERS AND ADD OFFSET
OFFSET = 1.0
DO 202 I = 1,201
RESP(2,I) = RESP(2,I)*100.

```

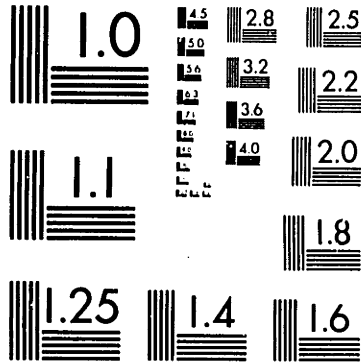
```
RESP(3,I) = RESP(3,I)*100. - OFFSET
RESP(4,I) = RESP(4,I)*100. - 2*OFFSET
CONTINUE
```

202  
C

```
MOVE = 0
ISCL = -2
XSCL(1) = 1
XSCL(2) = 0
XSCL(3) = YMIN
XSCL(4) = YMAX
LABEL = 14
NPTS = IFIX(FTIME/DT)
IF(NPTS.GT.200) NPTS = 200
XLABEL = 'CATENARY, PANTOGRAPH, FRAME DISPLACEMENT'
CALL QPICTR (RESP,5,NPTS,QY(2,3,4),QX(1),QMOVE(MOVE),QLABEL
```

```
(4) = 200.
LABEL = 14
XLABEL = 'CONTACT FORCE'
CALL QPICTR (RESP,5,NPTS,QY(5),QX(1),QMOVE(MOVE),QLABEL(LABEL),
1QISCL(ISCL),QXSCL(XSCL),QXLAB(XLABEL),QYLAB(YLABEL))
RETURN
END
```

C



MICROCOPY RESOLUTION TEST CHART  
NATIONAL BUREAU OF STANDARDS-1963-A

20X

NOTICE - THIS MATERIAL MAY BE  
PROTECTED BY COPYRIGHT LAW  
(TITLE 17 U.S. CODE )

